Arterial pulse wave analysis

Millasseau, Sandrine Celine

Arterial pulse wave analysis

Sandrine Millasseau

Thesis submitted for the Degree of Doctor of Philosophy (PhD)
of the University of London

Department of Clinical Pharmacology

Centre for Cardiovascular Biology and Medicine

King's College London

St. Thomas' Hospital

London, SE1 7EH

Abstract

There is currently much interest in the use of pulse contour analysis in studying vascular structure and function. The usual approach is to record the radial pressure pulse non-invasively, to apply a transfer function to estimate the aortic pressure pulse, and then to derive the aortic augmentation index (AIx), an index of arterial tone and stiffness. Whereas the transfer function allows a good estimation of aortic systolic blood pressure, this thesis shows that its accuracy in estimating AIx remains questionable. Furthermore, transforming the radial pulse to the aortic pulse may not be necessary, as similar information is present in the peripheral pulse. Measurement of infra-red light transmission through the finger pulp to obtain a digital volume pulse (DVP) provides a particularly simple means of obtaining a peripheral pulse. The contour of the DVP has hitherto been analysed in terms of 2nd derivative indices. These are influenced by ageing and vasoactive drugs but their physical meaning is not clear. This thesis shows that the contour of the DVP (in contrast to its amplitude which is influenced by local perfusion) is closely related to that of the pressure pulse, and can be interpreted as the summation of a direct and reflected wave. A reflection index (RI) has been defined to quantify the degree of wave reflection sensitive to drug induced change in arterial tone. Timing of the reflected wave relative to the direct wave is determined by pulse wave velocity in the large arteries and allows an index of large artery stiffness (SI) to be estimated from the DVP. Comparison of RI and SI with 2nd derivative indices suggests that, at least in healthy subjects, RI performs better in tracking effects of vasoactive drugs on arterial tone, and SI correlates better with age and blood pressure, and is thus likely to be a better index of vascular ageing. Clinical studies show that contour analysis of the DVP can be used to assess endothelial function and to study vascular structure and function in pregnancy and in relation to birth weight.

Table of contents

Table of figures

Table of tables

List of abbreviations

AIx	:	Augmentation Index
AIx-C	:	Carotid Augmentation Index
AIx-R	:	Radial Augmentation Index
AIx_{TFC}	:	Augmentation Index derived from the aortic pulse estimated from the Carotid pulse with the use of a transfer function
AIx_{TFR}	:	Augmentation Index derived from the aortic pulse estimated from the Radial pulse with the use of a transfer function
BP	:	Blood Pressure
d^2DVP/dt^2	:	Second derivative of the DVP (acceleration plethysmogram)
DBP	:	Diastolic Blood Pressure
DVP	:	Digital Volume Pulse
FFT	:	Fast Fourier Transform
GTF	:	Generalised Transfer Function
GTN	:	Glyceryl trinitrate
HR	:	Heart Rate
ITF	:	Individual Transfer Function
MAP	:	Mean Arterial Pressure
RMS	:	Root Mean Square

SBP	:	Systolic Blood Pressure
SBP_{TFC}	:	Central Systolic Blood Pressure obtained from the Carotid pulse using a transfer function
SBP_{TFR}	:	Central Systolic Blood Pressure obtained from the Radial pulse using a transfer function
SD	:	Standard Deviation
SE	:	Standard Error
WCV	:	Within subject Coefficient of Variation
WSD	:	Within subject Standard Deviation

Publications from this thesis

Chapter 3:

Millasseau SC, Patel SJ, Redwood SR, Ritter JM, Chowienczyk PJ. Pressure wave reflection assessed from the peripheral pulse: Is a transfer function necessary ?. Hypertension. 2003; 41(5):1016-1020.

Chapter 4:

Millasseau SC, Guigui FG, Kelly RP, Prasad K, Cockcroft JR, Ritter JM, Chowienczyk PJ. Noninvasive assessment of the digital volume pulse. Comparison with the peripheral pressure pulse. Hypertension. 2000; 36(6):952-956.

Chapter 5, section 5.4 and chapter 8, section 8.1:

Chowienczyk PJ, Kelly RP, MacCallum H, Millasseau SC, Andersson TLG, Gosling RG, Ritter JM, Anggård EE. Photoplethysmographic Assessment of Pulse Wave Reflection. JACC. 1999; 34:2007-2014.

Chapter 6:

Millasseau SC, Kelly RP, Ritter JM, Chowienczyk PJ. Determination of age related increases in large artery stiffness by digital pulse contour analysis. Clinical Science. 2002; 103:371-377.

Chapter 7:

Millasseau SC, Kelly RP, Ritter JM, Chowienczyk PJ. The vascular impact of aging and vasoactive drugs: Comparison of two digital volume pulse measurements. American Journal of Hypertension. 2003; 16(6): 467-472.

Statement of conjoint work

The clinical work of this thesis was performed in conjunction with my supervisor, Dr. Phil Chowienczyk.

Dr Ronan Kelly helped with the clinical aspect and the data acquisition for chapter 4, 5, 6 and 7.

Dr Sundip Patel assisted with the data acquisition for chapter 3.

Dr Louise Melson did the data acquisition on pregnant women (section 8.2).

Chris Broyd did the data acquisition relative to birth weight (section 8.3).

Acknowledgements

The work described in this thesis was sponsored by Micro Medical Ltd, and would not have been possible without the help and support of many individuals.

I am most grateful to Dr Phil Chowienczyk, my supervisor, for his invaluable advice, guidance and lasting enthusiasm during the fulfilment of this thesis. He always had time and dedication in supervising this thesis.

I am very grateful to the clinical team without which data acquisition would not have been possible and for the great help they gave me in the understanding of the clinical and physiological aspect of this thesis. In alphabetical order, they are Dr. Sally Brett, Dr. Lorenita de Angelis, Dr. Ronan Kelly, Dr. Louise Melson, Dr. Sundip Patel, Prof. Jim Ritter, Dr. Andrew Stewart and obviously Dr. Phil Chowienczyk. I would like to thank the rest of the past and present members of the Department of Clinical Pharmacology for their support and encouragement and in particular my "office-mate", Katrina de Saram.

Finally, I would like to thank Marc Touret for all his support and invaluable advice and reassurance on the mathematical and technical aspect of this work.

CHAPTER 1: Introduction

Interest in the mechanical properties of arteries commenced with clinical examination of the arterial pulse, which has been used as a diagnostic aid since ancient times. Quantitative attempts to measure the form of the arterial pulse were made as long ago as 1860. In the early 1900s, it was appreciated that the elasticity of the arterial wall governs the speed of pressure wave propagation (PWV) providing a method for measuring arterial compliance. In the mid-twentieth century, photoelectric techniques based on the absorption of infra-red light by red-blood cells were used to recorded a simple volume pulse. With modern instrumentation, and the appreciation of the clinical importance of physical properties of arteries there has been a resurgence of interest in the application of non-invasive techniques based on pulse wave analysis to assess arterial structure and function.

1.1 Arterial pressure pulse

For a long time, the only way to assess the pulse was by feeling it and there was no way of measuring it quantitatively. It was only in 1860 that the first quantitative recording of the arterial pulse was made. Etienne Jules Marey developed a mechanical "sphygmogram", which reproduced the arterial pulse waveform on a paper display.

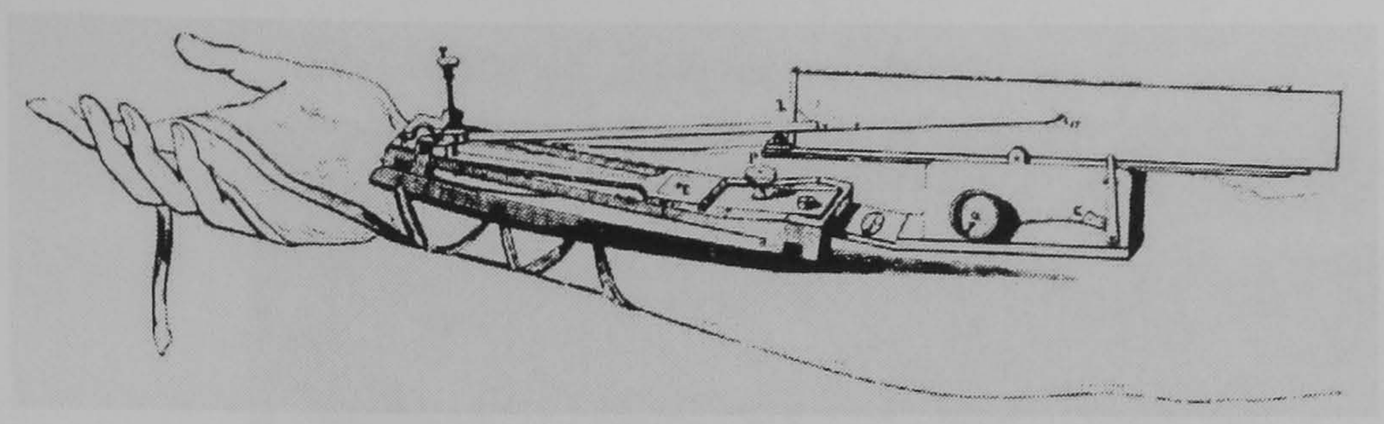

figure 1: Mechanical sphygmogram developed by E.J. Marey.
The waveform is directly plotted onto smoked paper, moved by a clock-work mechanism.

The sphygmogram was used by English clinicians such as Mahomed[82-84], Broadbent[22] and Mackensie[79] at the turn of the nineteenth century. They wrote articles about the interpretation of the shape of the pulse for diagnosing clinical hypertension. Mahomed, for example, accurately described how the pulse waveform changes with age[83] and blood pressure [82]. At a time when ECGs and X-rays were not in clinical use, Mackensie was using the sphygmogram as a standard tool in assessing diseases and studying the response to treatment. In 1879, in studies published in the Lancet, Murrell used the sphygmogram to describe the alterations of the radial pressure pulse after amyl nitrite and glyceryl trinnitrate[98-101] (see figure 2).

However, the technique remained difficult to implement and the interpretation of the pulse shape was far from easy. With the introduction of sphygmomanometer by Riva-Rocci and Korotkov in the early 1900s, which enabled systolic and diastolic pressure to be measured, interest in the shape of the pulse disappeared. A renewed interest came with the introduction of new technology, recording apparatus and signal processing. It is now possible to measure the arterial pulse accurately and easily and to use all the information contained within the pressure pulse.

Influence of Nitrite of Amyl on the Pulse.

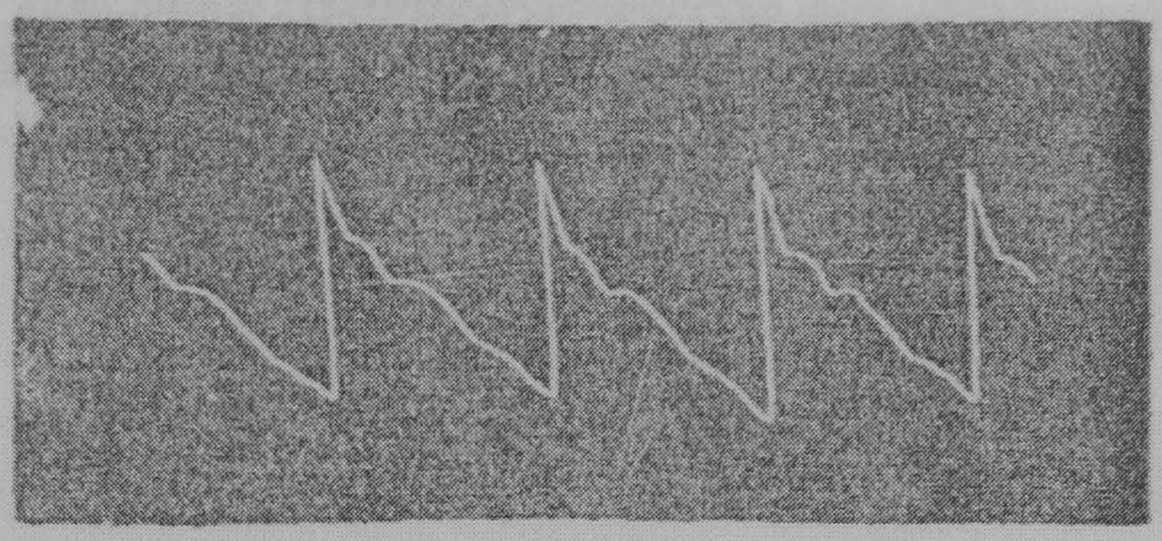

No. 1.—Before inhalation.

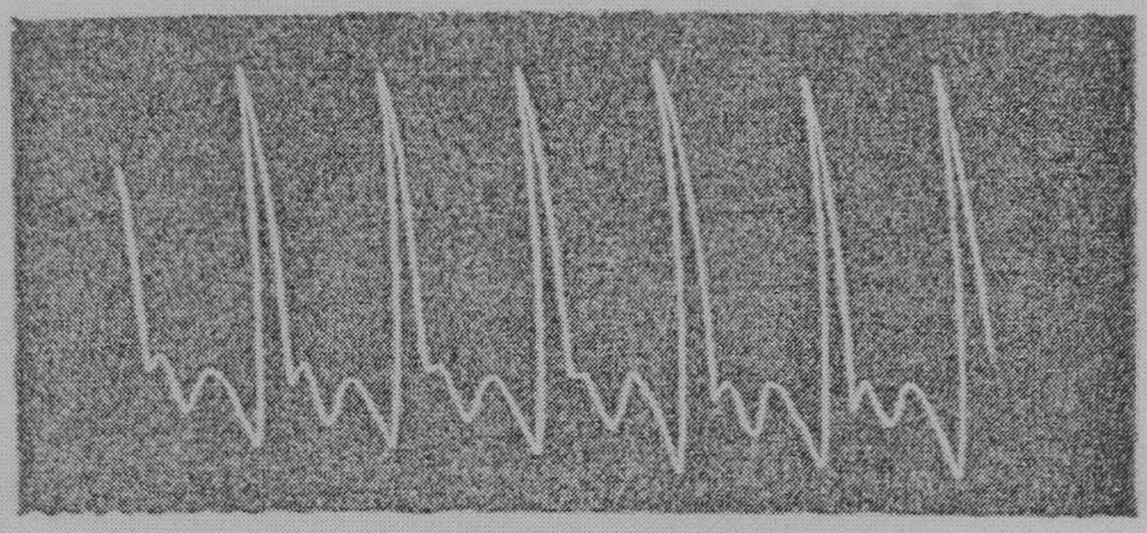

No. 2.—One minute after inhalation.

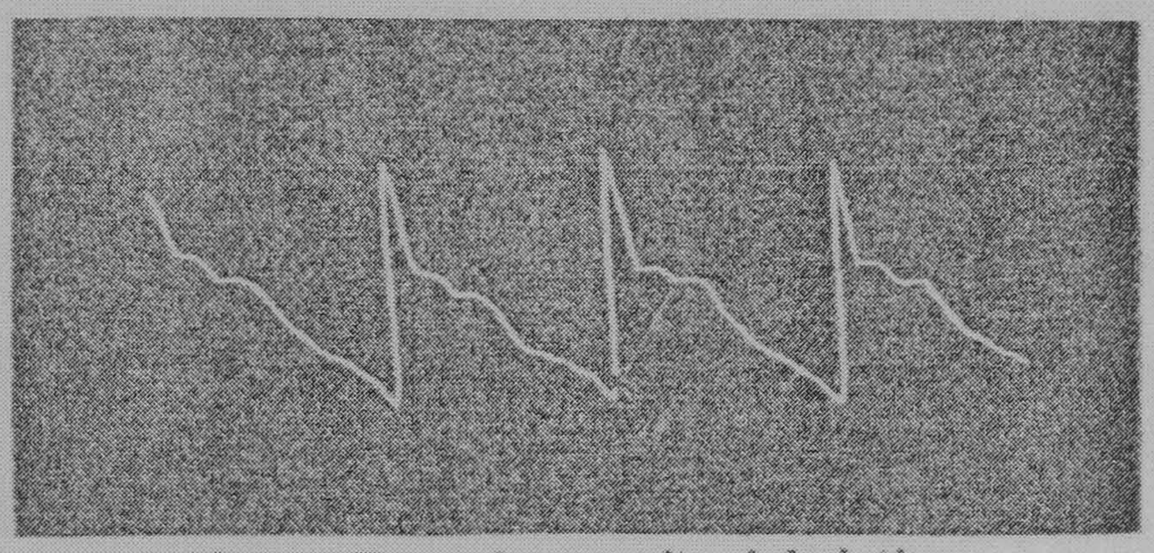

No. 3.—Two minutes after inhalation.

figure 2: Changes of the radial pressure pulse after inhalation of amyl nitrite from the Lancet 1879[99]

Independently of the sphygmograph, much work was done in the early 20th century to interpret the arterial pulse. Otto Franck[40] in 1899 introduced the Windkessel model to explain the pattern of the pressure pulse. It assumes that flow from a pump (the heart) enters an elastic chamber (arteries) through a one

way valve (the aortic valve), entering more rapidly than it can leave by way of a narrow exit tube (representing resistance vessels) that impedes outflow.

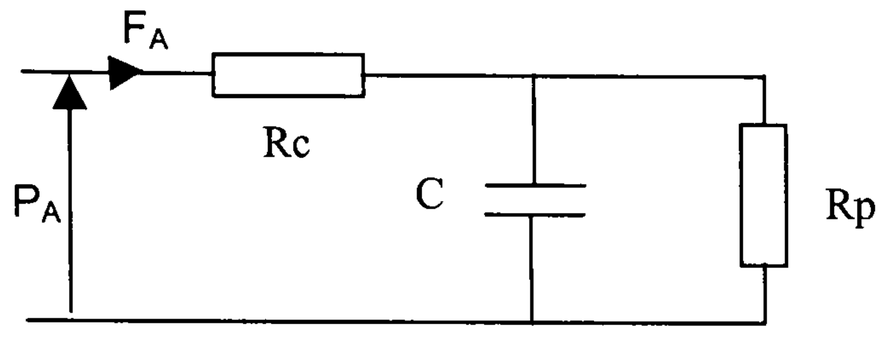

figure 3: Windkessel model
Rc is the characteristic resistance of the arterial tree.
C is its compliance and Rp its peripheral resistance.
PA is the aortic pressure and FA the aortic flow.

The Windkessel model is still used as a simple model to explain the basic shape of the pressure pulse and the damping process of the pressure waves within the arterial tree[31;39;88;154]. However, it fails to take into account the reflection phenomena explained by McDonald[104], Womersley[152] and Taylor[87]. Womersley showed that the arterial system behaves as a linear system[152] in which Fourier decomposition can be used to separate pressure and flow waveforms into their constituent harmonics. This work permitted the study of pressure waves and the input impedance of the arterial tree. The study of the Fourier decomposition of pressure waves at difference sites along the aorta animals such as rabbits, dogs and wombats (figure 4) and in humans, shows a progressive increase in the amplitude of the harmonics towards peripheral vessels suggesting the presence of a reflection site[104;109]. Fluctuations of the input impedance agree with the presence of a reflection site in the lower body.

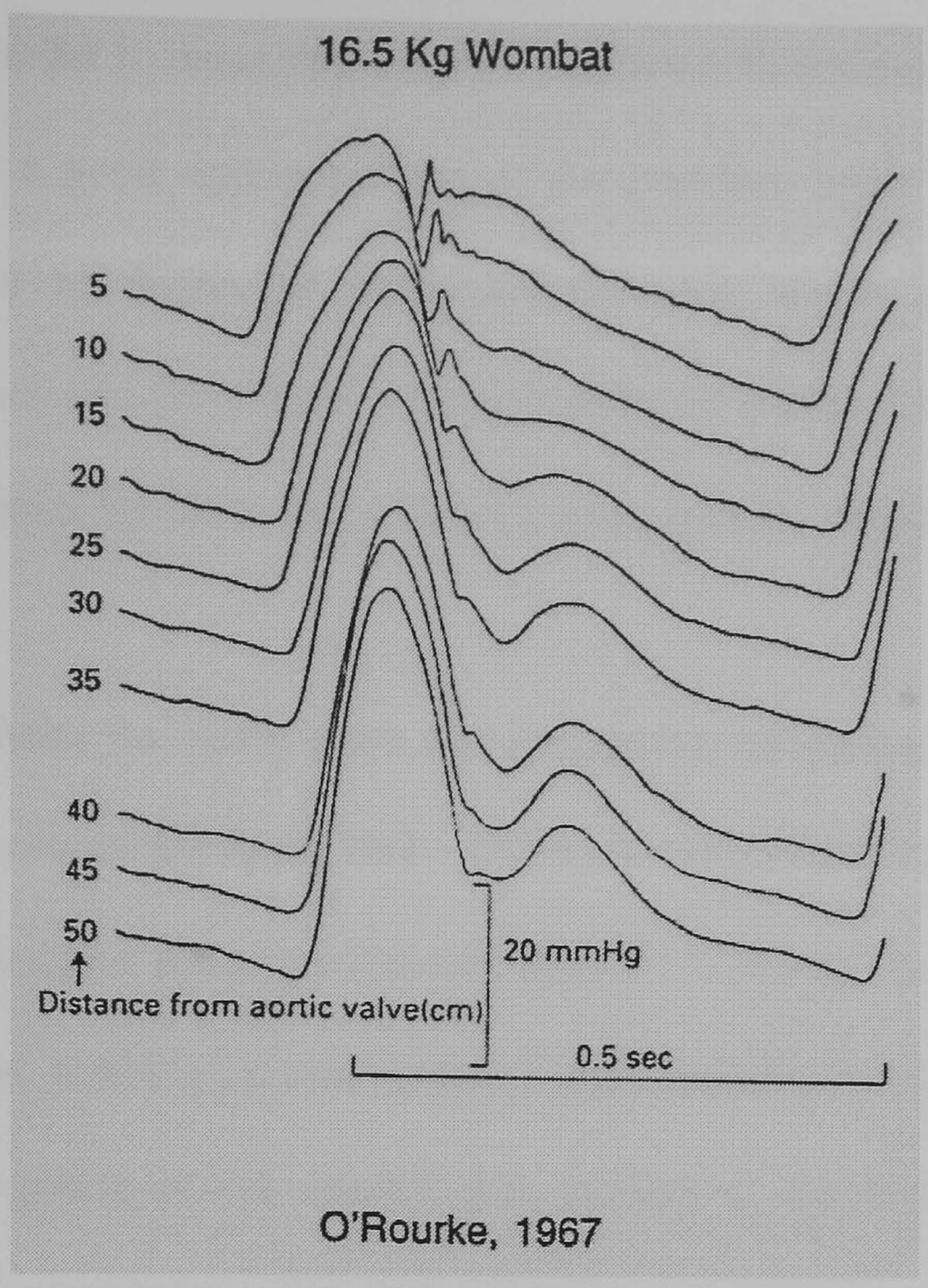

figure 4: Aortic pressure in a wombat aorta[109]

recorded at increasing distances from the aortic valve.

There is a progressive delay of the foot of the waveform due to the finite speed of pressure propagation in the elastic aorta. The diastolic reflected component of the waveform (at distances greater than 25cm from the aortic valve where it is clearly separated from the systolic component) can be observed travelling in the opposite direction.

These data are in favour of propagation and reflection of pressure waves in the arterial tree forming the arterial pulse. Using the theory of wave propagation in elastic tubes, Avolio[6], inspired by the work of Taylor[135], designed a computer model of the systemic circulation consisting of multiple branching elastic tubes. In models proposed by Avolio[6], and later by Karamanoglu et al.[56;57], the arterial tree was divided into tubes each defined by its length, its Young's modulus (which is its elasticity), its attenuation coefficient and reflection coefficient. Their computer models give an aortic impedance

approximation similar to measured values[6;56]. When a flow wave is used as input, the models give a good approximation of the pressure pulse[56]. These models provide evidence in favour of numerous reflected waves generated at the termination of each arterial branch. All these reflected waves summate and, when viewed from a point far from the reflective sites, can be interpreted as a single reflected wave.

Viewed from the heart, there are 2 apparent reflection sites, one in the lower body, and one in the upper body. O'Rourke introduced the asymmetric T-tube model to describe these 2 reflection sites[109;110] (figure 5). When the heart beats, it generates a direct pressure pulse, which travels forward in the arterial tree. At various points in the arterial tree, resistance and capacitance vary to create points of impedance mismatch. These points produce reflected waves, which travel back in the arterial tree and summate with the direct wave. The pressure pulse at any point of the arterial tree is hence the summation of a direct wave and reflected waves from the periphery.

Differences in the timing and amplitude of reflected waves will alter the pressure pulse contour, and explain the difference in the pressure pulse contour measured at different site. The shape of pressure pulse can hence be used to improve the understanding of the arterial system. Indices have been derived from the pressure pulse, such as the augmentation index described in further detail in section 3.1.1, to quantify changes in the arterial pulse associated with ageing, vascular disease and to study the influence of vasoactive drugs[104;111].

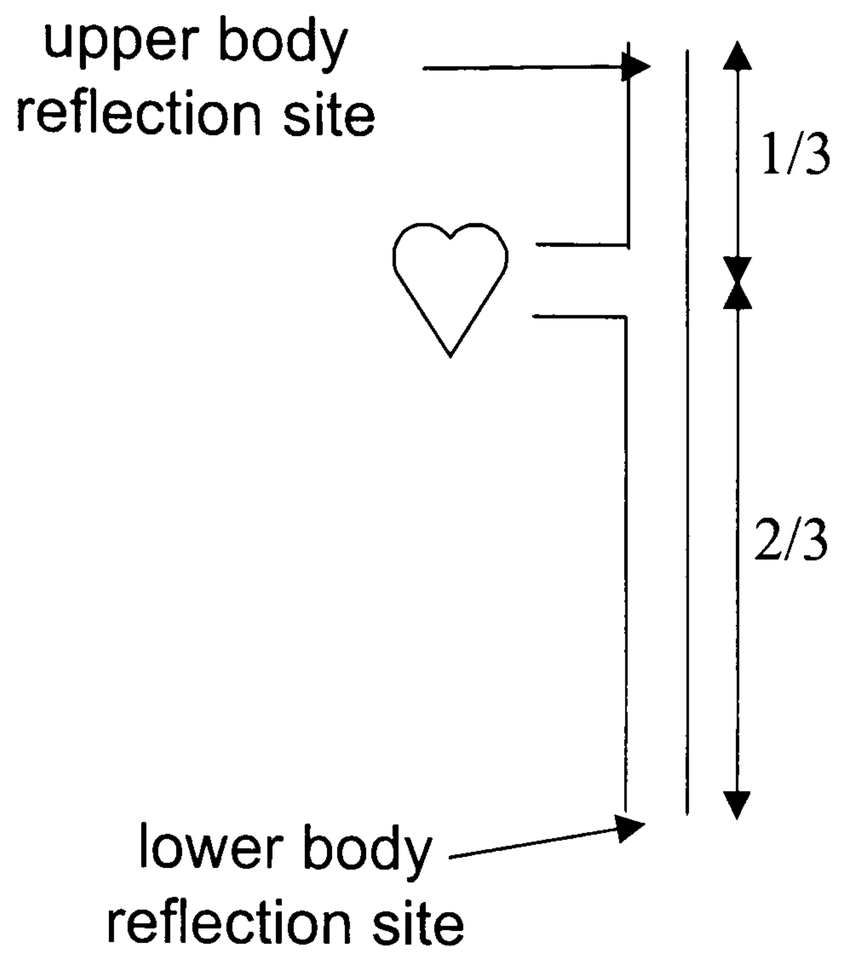

figure 5: T-tube model

1.2 Vascular function and the arterial wall

The arterial pulse is created by the heart ejecting blood into the arterial tree. This discontinuous ejection of blood is transformed into a pulsatile but continuous flow in the peripheral arteries and in the capillaries where gas and nutrient exchange can occur. The aorta and other large conduit arteries act as a transporting and cushioning system of the arterial pulse (described as the Windkessel effect in section 1.1).

The arterial wall consists of a layer of endothelial cells lining the lumen surrounded by smooth muscle cells arranged circularly and embedded in elastin and collagen fibres. The endothelial cells act as a barrier to plasma proteins and secretes numerous chemical mediators, which control the vasodilation/

contraction of the smooth muscle cells. The aorta, iliac arteries and other major branches are referred to as elastic arteries. They perform most of the cushioning function (the Windkessel effect) and hence are very distensible and rich in elastin fibres. Degenerative changes in elastin occur with age leading to a stiffening of elastic arteries, a process that may be accelerated by hypertension and other risk factors for vascular diseases. These alterations causes the arterial pulse waveform to change with ageing[62]. The wall of the muscular arteries (such as the radial and tibial arteries) contains more smooth muscle cells and is much thicker than the elastic arteries compared to their lumen. Together with the resistance vessels, the muscular arteries have a rich autonomic nerve supply and can contract or relax to regulate downstream blood flow. These changes in vascular tone alter wave reflections influencing the shape of the arterial pulse[59].

Over the last two decades it has been realised that the release of mediators from endothelial cells plays an important role in the relaxation/contraction of the underlying smooth muscles. Nitric oxide (NO) is probably the most important endothelium derived vasodilator[51;114]. It has received particular attention as, in addition to the regulation of vascular tone, it has anti-atherogenic actions. These include inhibition of adhesion molecules, inhibition of platelet adhesion and aggregation and inhibition of vascular smooth muscle proliferation[93]. A decrease in the availability of NO is thought to underlie much cardiovascular disease[102]. There has thus been much interest in the idea that endothelium dependent vasodilation mediated by NO can be used to test for endothelial dysfunction predisposing to development of cardiovascular disease. An alteration in endothelium dependent vascular tone will influence the shape of the pulse wave. Pulse wave contour analysis coupled with an

appropriate endothelium dependent stimulus could therefore be used to test endothelium function. This idea is explored in section 8.1.

1.3 Pulse wave velocity

As shown in figure 4, the pressure pulse takes a finite time to propagate along the aorta. The velocity of propagation (PWV) was shown to be determined by the elastic modulus of the arterial wall by Moens[92] and Korteweg[66] at the end of the nineteen century.

Moens-Korteweg equation:

$$PWV = \sqrt{\frac{E.h}{2r.\rho}}$$

E : elastic modulus

h : arterial wall thickness

r : arterial radius

ρ : blood viscosity

In 1922, Bramwell and Hill modified this equation and expressed it as a change in arterial volume (ΔV) to variation of pressure (ΔP) as expressed by the Bramwell-Hill equation[21]: $PWV = \sqrt{\frac{\Delta P.V}{\rho.\Delta V}}$

An increase in aortic PWV with age and blood pressure (BP) was recognised as early as 1934-1936 by Hallock[43] and Haynes et al.[46]. This has been confirmed by several authors and in particularly in a large rural and urban Chinese population where the presence of high salt diet and hypertension increased aortic PWV[8;9]. Aortic PWV has received much recent interest because it has been found to be an independent predictor of cardiovascular events and/or

mortality. In 1999, Blacher et al.[17] reported that, in patients with end-stage renal disease, aortic PWV is a strong independent predictor of cardiovascular mortality and a better predictor of mortality than BP. In hypertensive patients, PWV was found to be significantly associated with the occurrence of coronary events and to predict these better than conventional Framingham risk factors[20]. PWV was significantly associated in hypertensive patients with all-cause and cardiovascular mortality, independently of previous cardiovascular disease, age and diabetes[69]. Meaume et al.[90] showed that aortic PWV is a strong independent predictor of cardiovascular death in patients aged more than 70 years of age with or without heart failure or history of stroke. In a 10 year follow up study, Cruickshank et al.[32] found aortic PWV to be a powerful independent predictor of mortality in patients with diabetes and glucose intolerance. Because PWV is an independent predictor of cardiovascular risk, there is great interest in drugs that may improve aortic PWV. Conventional anti-hypertensive treatment may have a modest BP independent effect on PWV[2]. Among the different classes of anti-hypertensive drugs, ACE-inhibitors seems to produce the best improvement in PWV independently of BP[4].

1.4 History and use of the Digital Volume Pulse

In the 1930s, Alrick Hertzman[48] described a "photoelectric plethysmograph", a device which "takes advantage of the fact that the absorption of light by a transilluminated tissue varies with its blood contents". He described a device, which illuminated the skin and back-scattered light was measured by a

photocell (see figure 6, left panel). Robert Goetz[41] described a device measuring light transmitted through the finger (see figure 6, right panel).

John Dillon and Alrick Hertzman[36] later described characteristics of the digital volume pulse (DVP) in normal subjects and patients with arterial disease. They described the shape of the DVP in terms of "crest time, the duration of the ascent of the primary wave" and "height of the incisura on the catacrotic limb" (figure 7). They observed a tendency of the incisura to rise with vasoconstriction (caused by immersing the opposite hand in water at 4°C) and an increase in the dicrotism (a decrease of the height of the incisura) during and shortly after amyl nitrite inhalation[36]. They described similar changes in the DVP to those observed by Murell in the radial pressure pulse after GTN[98-101]. They also compared the traces of normal subjects with those from subjects with hypertension or arteriosclerosis and found "an increase in the crest time, loss of the rebound wave and triangulation of the DVP"[36]. However they did not quantify these changes, mainly because of the absence of signal processing facilities at that time.

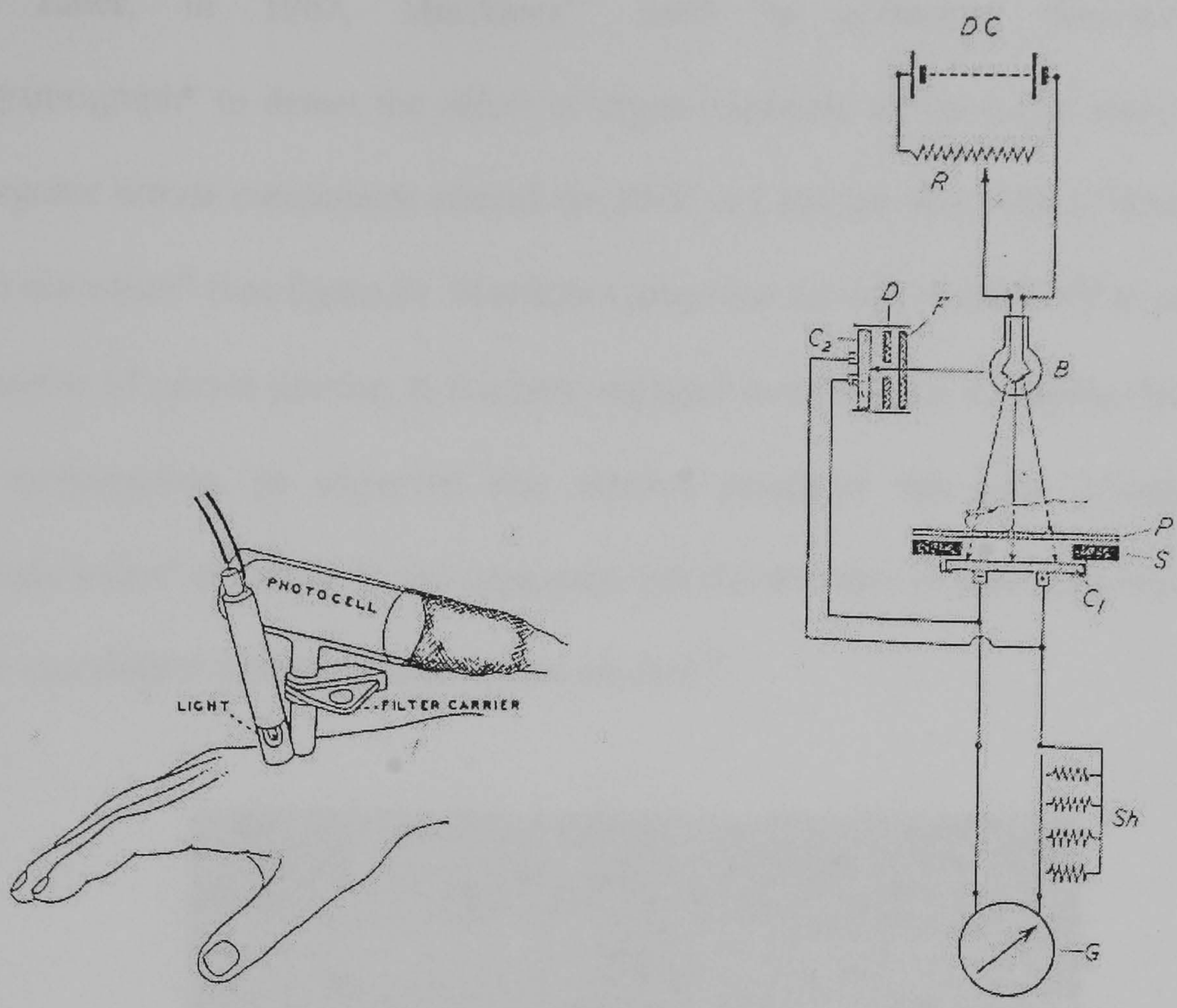

figure 6: Mid-20th century photoplethysmograph

Left panel: Hertzman's reflection photoplethysmograph[48]

Right panel: Goetz's transmission photoplthysmograph[41]

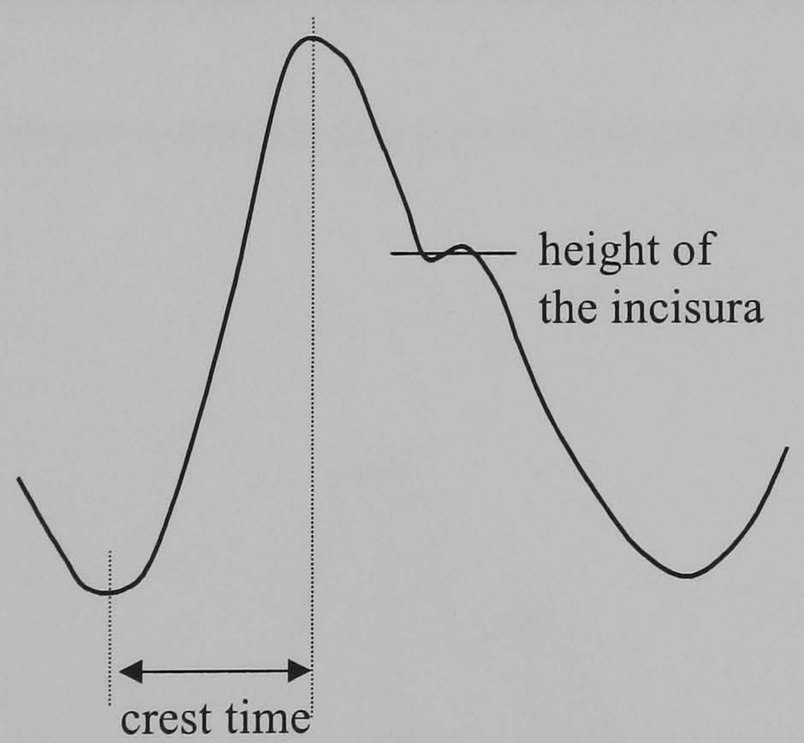

figure 7: Features of the DVP described by Hertzman and Dillon

Later, in 1967, Morikawa[94] used "a reflection photoelectric plethysmograph" to detect the effect of organic nitrates on the pulse wave. All the organic nitrate compounds altered the DVP in a similar way with a "decrease in the dicrotism" (see figure 8). Morikawa proposed the use of the DVP to detect the degree of nitrate poising in workers engaged in producing dynamite. During this investigation, he observed that alcohol produced the same change in "dicrotic index" of the DVP and suggested that the decrease in dicrotism was due to the vasodilator effects of nitrates and alcohol[95].

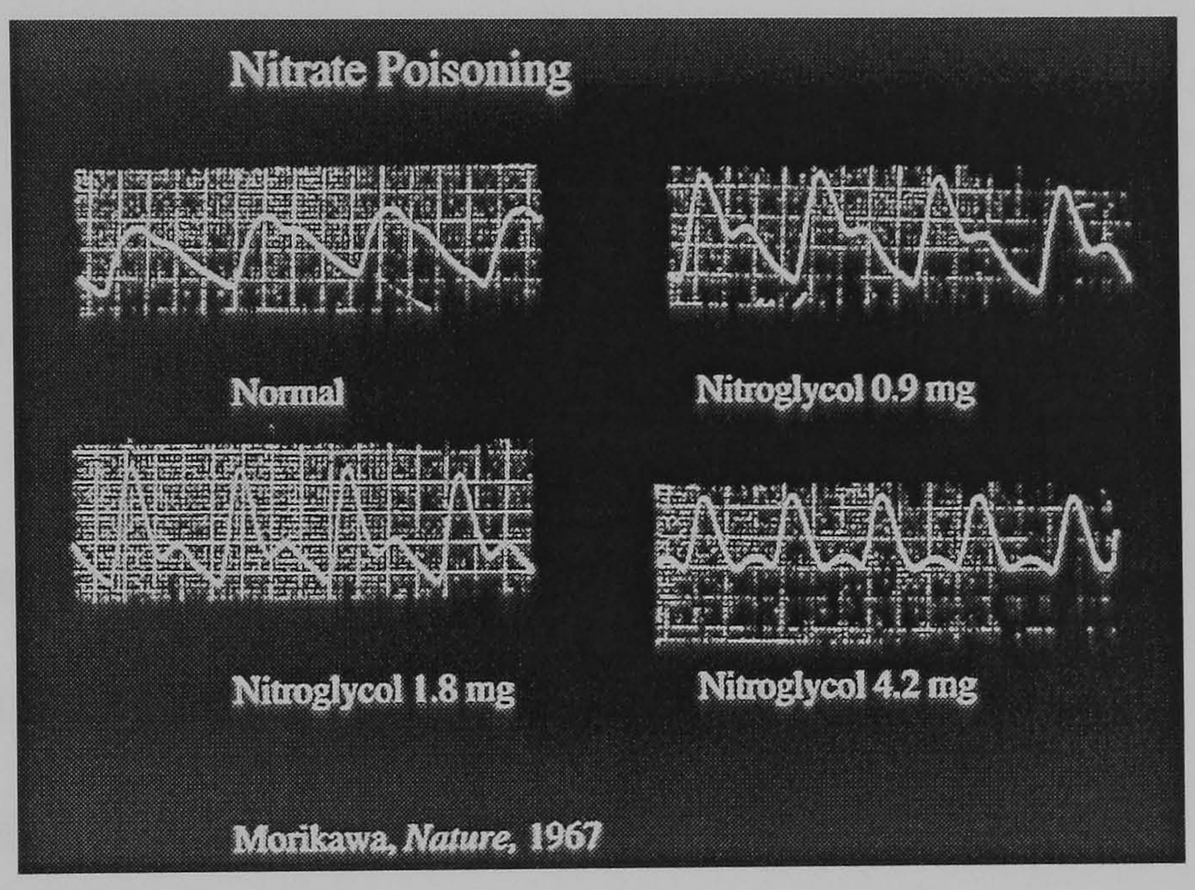

figure 8: Measure of nitrate poising with photoplethysmography[94]

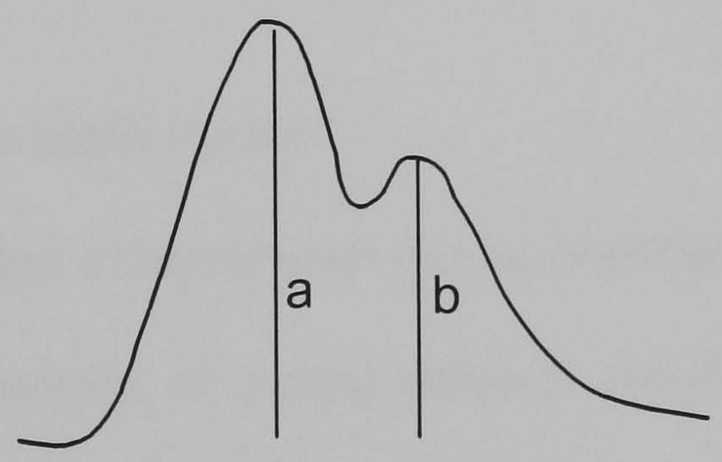

figure 9: Morikawa's dicrotic index = b/a

Later, in Europe, the previously described "dicrotic index" was used as a sensitive index of vasomotor effects of drugs particularly nitrates[14;23;44;78;123;128;139;140] and also other vasodilators such as isoprenaline, sodium nitroprusside[89;151] and nifedipine[65;128].

The early observations of Hertzman and Dillon about the alteration of the DVP in hypertensive subjects and patients with arteriosclerosis were confirmed in a sub-study of the Framingham cohort. Lax et al.[71] introduced a device they called a "vasculograph". This device measured pressure in a sensitive rubber cuff inside an inelastic backing applied around the finger, effectively providing a DVP[71]. They observed the presence of a "well-defined dicrotic wave" in healthy volunteers, whereas 98% of patients with clinical evidences of arteriosclerosis had a "diminution or disappearance of the dicrotic wave" [71]. Using the same technique, Dawber et al.[34] obtained the DVP in 1778 subjects recruited for the Framingham study during the period from 1965 to 1966. The DVP was characterised into 4 classes[34]:

Class 1 : "A distinct incisura is inscribed on the downward slope of the pulse wave"

Class 2 : "No incisura develops but the line of descent becomes horizontal"

Class 3 : "No notch is present but a well-defined change in the angle of the descent is observed"

Class 4 : "No evidence of a notch is seen"

Like previous authors, they characterised the down-slope of the DVP. They found that a higher proportion of young subjects exhibited a class 1 DVP whereas class 4 DVP was mainly observed in older subjects[34]. Patients diagnosed with coronary heart disease were more likely to exhibit a class 4 trace.

Multivariate logistic regression analysis for cardiovascular end-points occurring within 6 years, with age, systolic blood pressure and DVP classification as independent variables, showed the "level of dicrotism" to be related to cardiovascular outcome[54].

The DVP has also received much interest in Japan. Analysis there has centred on the second derivative of the DVP called the "acceleration photoplethysmograph". According to Takazawa et al.[133], Takada et al.[131] and Imanaga et al.[52], the acceleration photoplethysmogram has been employed instead of the DVP to facilitate the distinction of various components in the waveform. The acceleration photoplethysmogram (d^2DVP/dt^2) typically comprises of 5 sequential waves called the a, b, c, d and e waves. The relative heights of these waves (b/a, c/a, d/a and e/a ratios), particularly the d/a ratio, have been related to age[19;131;133], BP[19;131], PWV[45] and vasoactive drug effects[132]. The b/a ratio has been related to ageing and carotid distensibility[52]. Following the results of the correlation of the b/a, c/a, d/a and e/a ratios with age, an ageing index has been defined as (b-c-d-e)/a[133]. Although the ageing index shows a strong correlation with age[45;133] and BP, it is only weakly correlated with PWV[45]. The second derivative of the DVP has been recently used to study arterial distensibility in adolescents and the d/a was proposed to identify individuals at an increase risk of developing atherosclerosis[91].

1.5 Purpose of this thesis

Despite the interest in measurements derived from the contour of the arterial pulse, the interpretation of these remains controversial. This is particularly true for the DVP, the simplest and potentially most widely used test of vascular health. The purpose of this thesis is to examine the potential value of pulse contour analysis in the assessment of vascular function and structure both with respect to age, disease related changes and to pharmacological actions of vasoactive drugs. Following a discussion of methodology, the relationship between the peripheral pulse and the central aortic pulse is examined, as is the validity of the transfer function approach in estimating central aortic pressure from peripheral pressure. The relationship between the pressure pulse and the DVP is investigated. Indices characterising wave propagation and reflection derived from contour of the DVP are presented and compared with existing measurements derived from the second derivative of the DVP. Finally, clinical applications of the new DVP indices are discussed.

CHAPTER 2: Methods

2.1 Pressure pulse

2.1.1 Applanation tonometry

Applanation tonometry is a non-invasive technique for measuring arterial pressure. A piezo-resistive transducer is applied over an artery. When the piezo-electric crystal is deformed by arterial pressure transmitted through the overlying superficial tissue and skin, its resistance changes. This change in resistance is directly related to the pressure applied on the crystal. The piezoelectric transducer can be mounted on the tip of pen-type probe (Millar micro-manometer, Texas, US, figure 10 and figure 11) or an array of transducers can be strapped around the wrist (Colin wrist probe, Japan, figure 12). Applanation tonometry requires the artery to be flattened against a hard surface such as the head of the radial bone (radial artery) or the vertebral column and ligaments in the neck (carotid artery). It takes a little training to obtain optimal traces and, in obese patients when the artery is deep, it can be difficult to obtain satisfactory waveforms. Applanation tonometry has been validated and the radial artery pressure waveform obtained is very close to that obtained using invasive intra-arterial measurements of the radial artery pressure waveform[61]. Tonometer pressure and invasive pressure, when calibrated to shygmomanometric measurements of systolic and diastolic pressure, agree closely. When the spectrum of the waveform is examined, a small systemic difference is seen. The tonometer tends to overestimate the 1st harmonic by 0.6mmHg and underestimate higher harmonics by no more than 0.4mmHg[61].

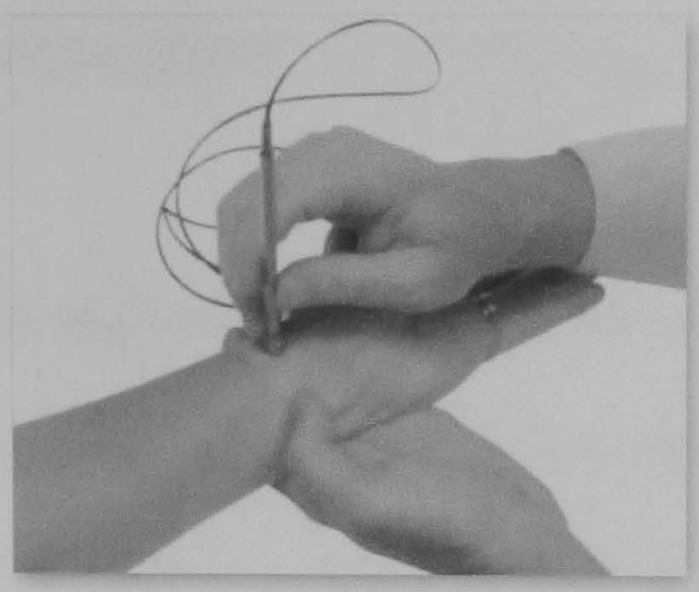

figure 10: Tonometer (from Atcor website)

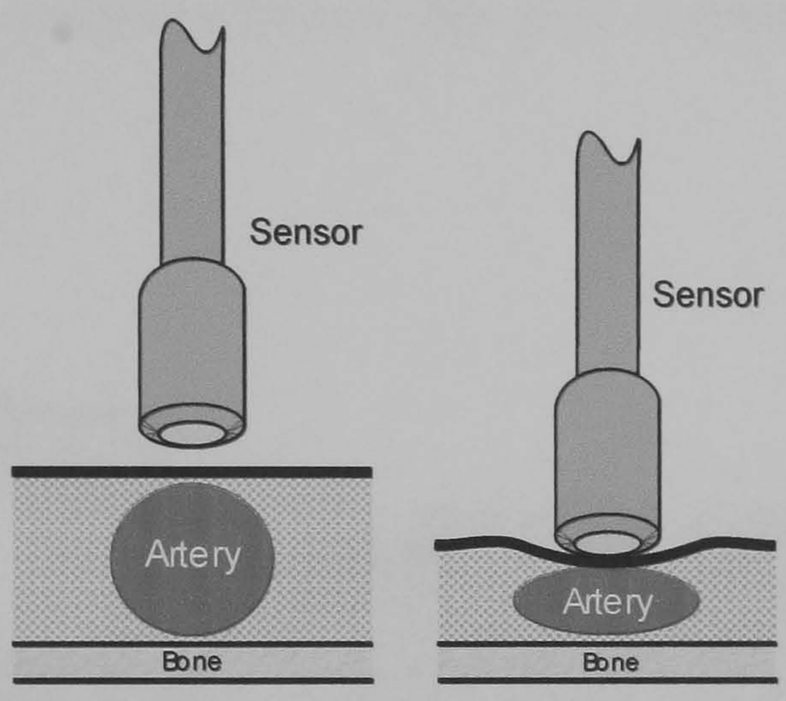

figure 11: Tonometry technique (from Atcor website)

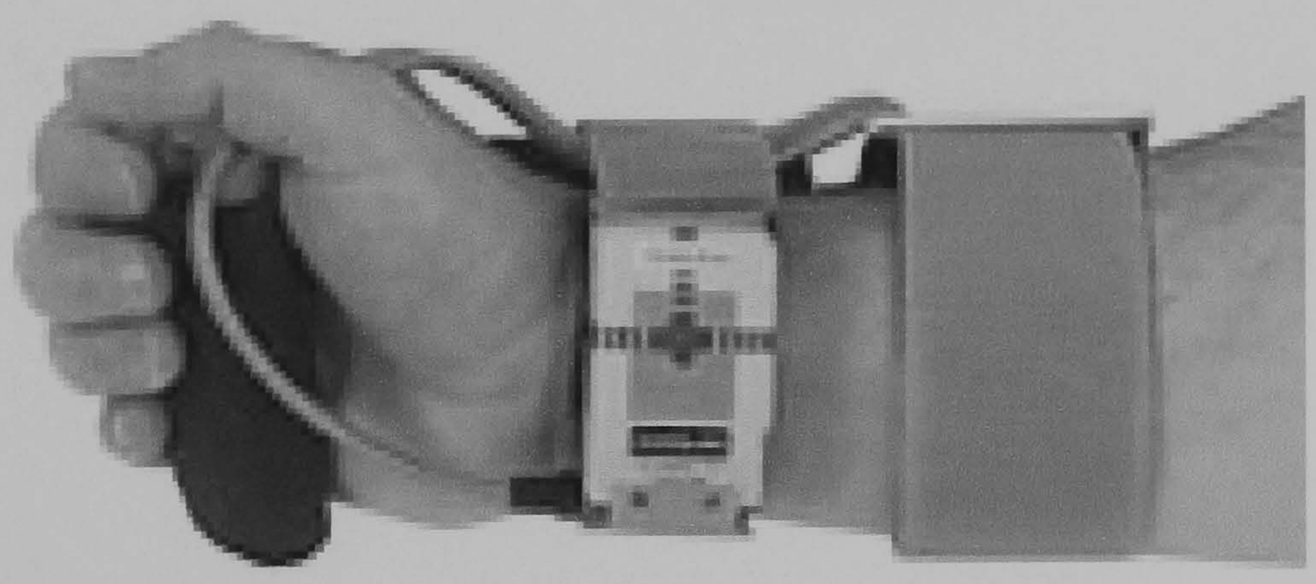

figure 12: Colin wrist tonometer probe (from Colin website)

2.1.2 The digital pressure pulse

A method to record the digital pressure pulse was introduced by Peñaz[116] and commercialised under the name of Finapres or Finometer (Finapres Medical system, Holland, figure 13). A cuff is inflated around the middle finger and a servo-controlled pump used to change the pressure inside the cuff to keep the amount of light passing through the finger constant. This method measures digital pressure waveform continuously and has been validated against invasive measurements[53].

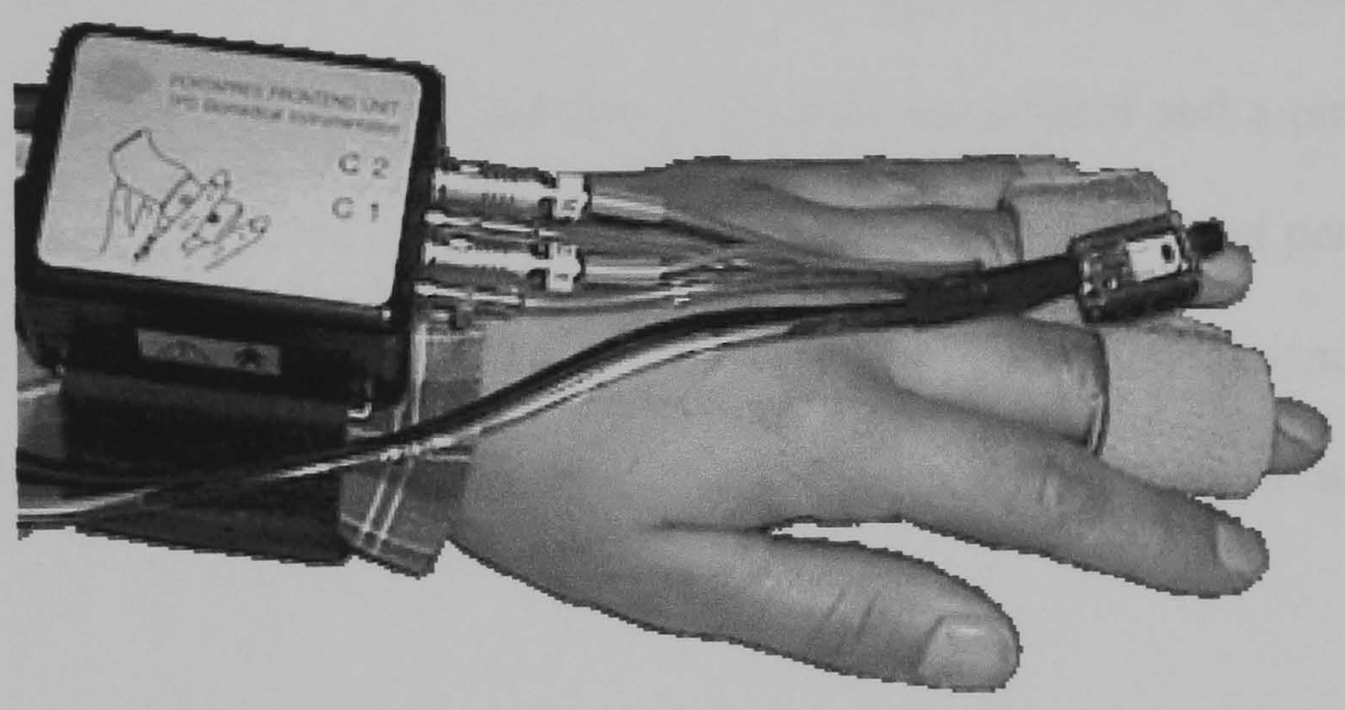

figure 13: Finapres (from Finapres website)

2.2 Digital Volume Pulse

2.2.1 Oxymetry technique

By transillumimating tissue in the finger, one can measure the light absorption in the finger. This technique is widely used in oxymeter devices to determine oxygen saturation in the arterial blood. Oxygen saturation is measured from the ratio of absorbance of the red (usually 660 nm) and infra-red (usually 940 nm) light, the red light being mainly absorbed by deoxyhemoglobin and the infra-red light by oxyhemoglobin. In the finger, blood from veins, venules, capillaries, arterioles, arteries and tissues absorbs light as shown in figure 14. The light absorbance can be divided into a constant component and a pulsating component, which gives the arterial volume pulse. Reduction in blood perfusion in the finger tip (for example in subjects with cold hands or Raynaud syndrome) results in a smaller constant and pulsatile components but pulse contour remains similar[41].

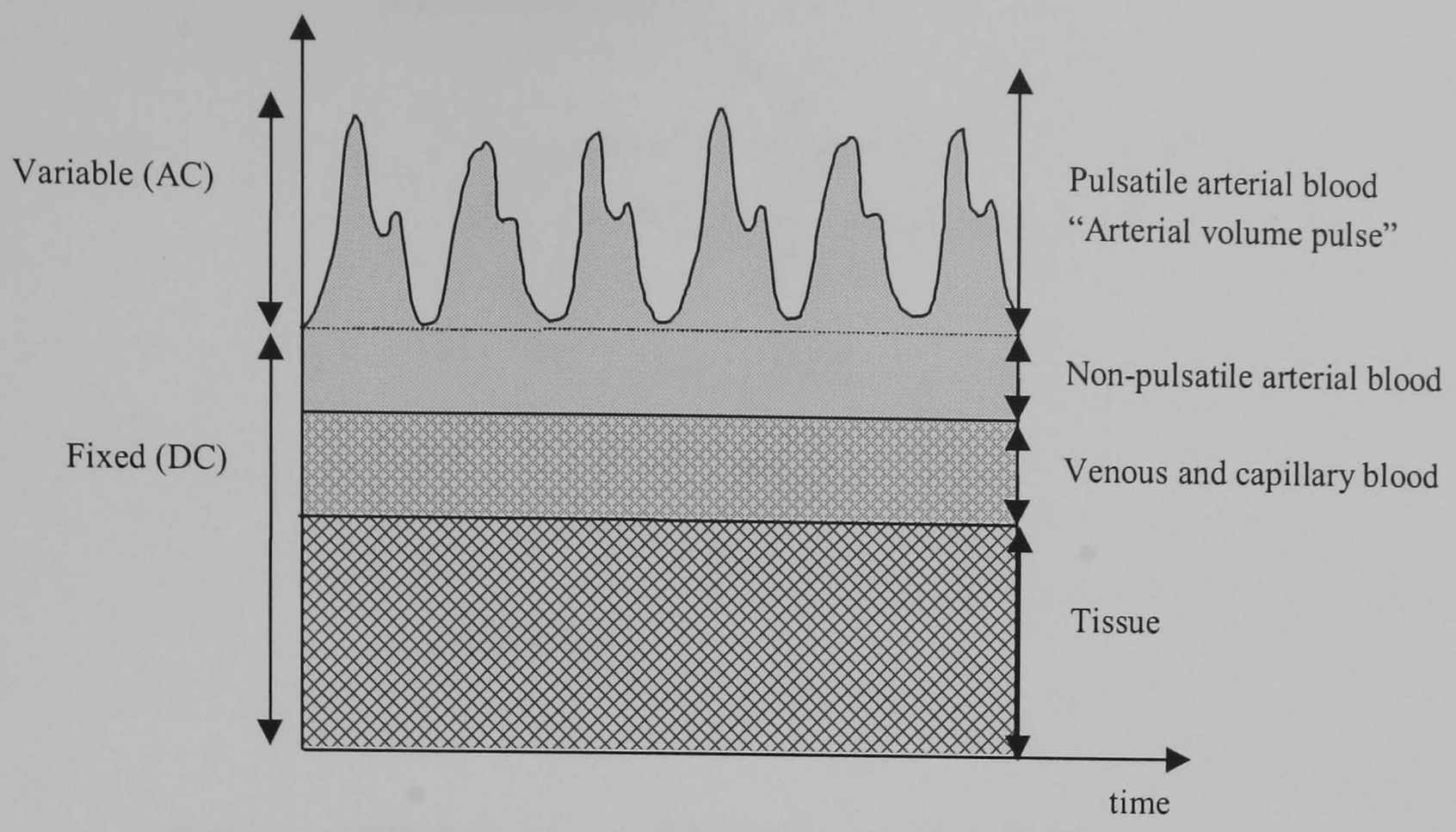

figure 14: Principle of photoplethysmography

2.2.2 DVP probe

Of the 2 wavelengths used in pulse oxymetry, infra-red light is absorbed most by the finger pulp, and provides the pulsatile signal of the greatest amplitude. For this reason the DVP was measured using a modified pulse oxymetry probe (Nellcor, California, US). It consists of an infra-red light emitting diode and a photodiode mounted on a finger clip as shown in figure 15. The pulsatile (AC component) part of the signal measured by the photodiode is the DVP. The signal from the photodiode was filtered and amplified and the DC component removed by an electronic circuit (Micro Medical Ltd, Gillingham, UK).

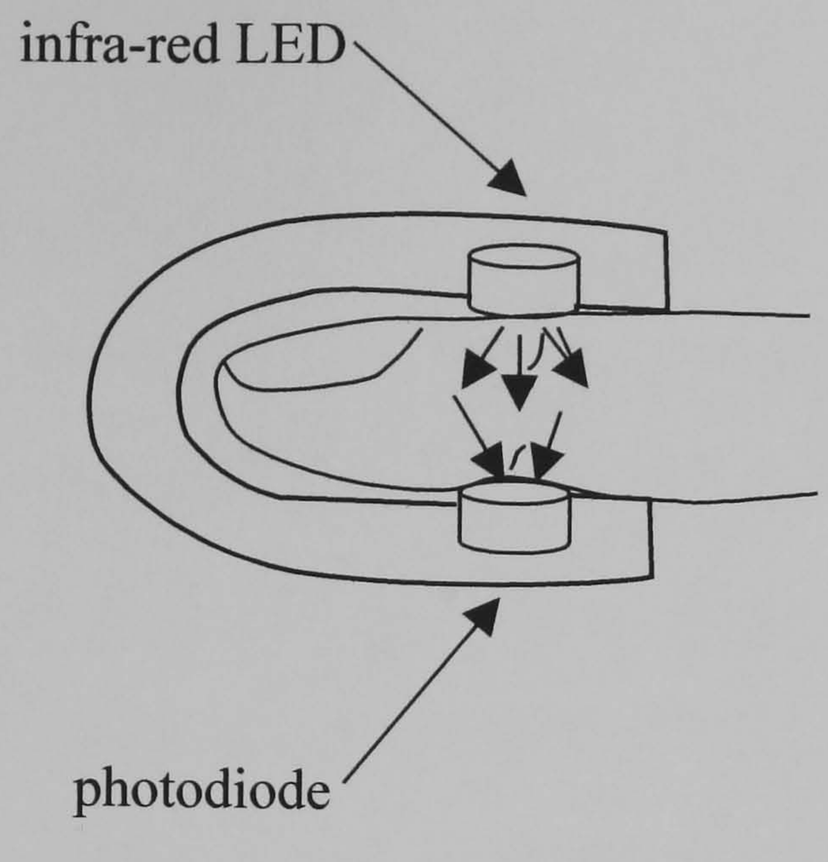

figure 15: Schematic of a modified pulse oxymeter probe
The photodiode measures the transmitted infra-red light emitted by the light emitting diode (LED).

figure 16: Digital volume pulse probe

2.2.3 DVP signal conditioning

For studies in chapter 4, 5 and 7, the signal from the modified Nellcor probe was sampled at 100Hz using a 12-bit analogue to digital acquisition board (PC30F Series Board of Eagle Technology) and stored on a PC using custom-built software. The software allowed continuous recording of the DVP waveform

for further analysis such as the calculation of the second derivative (chapter 7), transfer function (chapter 4) or indices characterising the contour of the pulse (see appendices). The algorithms described in appendix 10.1 to calculate the average pulse and the contour indices were first developed with Matlab (Mathworks, US) and then implemented as embedded software in a microprocessor based desktop unit (PulseTrace, Micro Medical Ltd, UK). In this unit, the signal is digitalised at 100 Hz and sampled with 8-bit resolution. Pulses are ensemble averaged and contour indices are derived from the averaged DVP. The algorithm used is described in the appendix section 10. The PulseTrace device was used to measure DVP in the studies described in chapters 6 and 8.

2.3 Pulse wave velocity

Pulse wave velocity (PWV) is a measure of arterial distensibility as explained in section 1.3. PWV can be measured using the Bramwell-Hill equation from the relative change of volume and pressure[21]. But a more practical approach is to measure transit time, the time the arterial wave takes to travel from one point to another point. The assessment of PWV then relies on the determination of the pulse transit time (TT) over an arterial segment of length (L):

$$PWV = \frac{L}{TT}$$

Determination of pulse transit time involves the measurement of the arterial pulse at 2 different sites. The pressure wave itself may be used (measured by tonometer) or, alternatively, another signal such as blood velocity (Doppler

probe) or wall movement (mechano-transducer) that bears a constant relationship with the pressure pulse. Measurements at the 2 different sites can be done simultaneously, or successively using the R-wave of an ECG as a time reference. Arterial length is estimated from surface markings between the 2 sites of measurement.

The Sphygmocor (AtCor, Australia) device uses successive measurements of pressure waveforms and a simultaneous ECG. The pressure pulse is obtained with a high-fidelity applanation tonometer (Millar, Texas, US) as explained in section 2.1.1. For each measurement site, the delay from the R-wave of the ECG to the foot of the pressure pulse is determined. Subtraction of the R-wave to pulse foot time at the proximal and distal sites provides the transit time. PWV is then calculated from the arterial length and transit time.

2.4 Vasoactive drugs

In this thesis, 4 different vasoactive drugs have been used to probe vascular function: glyceryl trinitrate (GTN), a non-endothelium dependent vasodilator, salbutamol, an endothelium-dependent vasodilator and the vasoconstrictors angiotensin II and noradrenaline.

2.4.1 GTN

GTN is routinely used to treat stable and unstable angina. As a powerful vasodilator, it vasodilates the coronary arteries, the resistance vessels (reducing peripheral vascular resistance and hence blood pressure) and causes veno-relaxation (hence reduces pre-load). In addition to these classical actions it is now recognised that GTN has an important effect on conduit arteries and muscular arteries proximal to resistance vessels. It is metabolised within smooth muscle cells to NO. NO stimulates cyclic guanosine monophosphate (cGMP) formation, which activates protein kinases, resulting in the dephosphorylation of myosin light chains of the smooth muscle hence producing muscle relaxation[120].

2.4.2 Salbutamol

Salbutamol is a β_2-agonist, primarily used in the treatment of asthma when administered by the inhaled route. Salbutamol acts on β_2 receptors in bronchial smooth muscles to cause bronchodilation via an increase in cyclic adenosine monophosphate (cAMP). Salbutamol also causes vasodilation. This was thought to be mediated mainly through the activation of β_2 receptors on vascular smooth muscle (increasing cAMP as in the bronchial smooth muscle). However, β_2 receptors are present on the vascular endothelium and it now acknowledged that much of the vasodilator action of salbutamol is due to activation of these receptors and subsequent release of endothelium derived NO[35]. Salbutamol, therefore, falls into the class of endothelium dependent

vasodilator drugs. These rely on the integrity of the endothelium and may be used to probe endothelium-dependent vascular function.

2.4.3 Angiotensin II

Angiotensin II is a powerful circulating hormone regulated by the renin-angiotensin system. It has a direct vasoconstrictor action on vascular smooth muscle cells and increases noradrenaline release from sympathetic nerves. Both angiotensin II and noradrenaline act on the G-protein-coupled receptors of the smooth muscle cell to increase calcium ion concentration leading to muscle contraction[120]. Antagonism of angiotensin II by the use of an angiotensin receptor blocker (ARB) or by inhibition of its synthesis using an angiotensin converting enzyme inhibitor (ACEI, which inhibits conversion angiotensin I to angiotensin II) is a common treatment for hypertension. In sections 5.5 and 7.6, angiotensin II will be used for its vasoconstricting properties.

2.4.4 Noradrenaline

Noradrenaline is released from sympathetic nerves and plays a major role in the regulation of vascular tone by the autonomic nervous system. Noradrenaline acts on G-protein-coupled receptors of the smooth muscle cell and increase calcium ion concentration leading to muscle contraction[120]. This drug has been used in chapter 3 to increase vascular tone.

2.5 Statistics

Unless otherwise is stated, subject characteristics are presented as means ± SD and results as means ± SE. Comparison of results between groups was performed by analysis of variance (ANOVA). The relationship between indices derived from the DVP and potential explanatory variables were explored using univariate and multivariate regression analysis.

Repeatability was assessed as the mean within subject standard deviation (WSD) of measurements obtained on the same day and reproducibility as the WSD of measurements made on different days:

$$WSD = \sqrt{mean\_variance}$$

Repeatability and reproducibility were also expressed as the within coefficient of variation (WCV)[119]:

$$WCV = \frac{\sqrt{mean\_variance}}{overall\_mean} \times 100$$

Correlation coefficients refer to Pearson correlation coefficients.

Agreement between measurements was examined using with Bland-Altman plots[18] in which the difference between two measurements is plotted against the mean of the two measurements.. The mean difference between measurements was used to quantitate the systemic error and the standard deviation of the differences the variation in agreement.

CHAPTER 3: Relationship between the peripheral and central pressure pulse

3.1 Background

3.1.1 The augmentation index

Since the introduction of cardiac catherisation in medical care, physicians have had the opportunity to observe characteristics of the aortic pressure waveform. The aortic pressure waveform is the result of an interaction between the heart and the arterial system and, as described in section 1.1, is generally accepted to be determined by the summation of a direct wave and one or several reflected waves[104]. During systole, the heart generates a direct wave, which propagates along the arterial tree. The direct wave is reflected at arterial bifurcations and at points where arterial diameter and distensibility change. Waves generated by these reflections can be seen as a single reflected wave, which travels backwards in the arterial tree and adds to the direct wave to form the observed aortic pulse[104;111].

Indices to characterise the pressure pulse can be derived from the contour of the pulse. The feature of the pulse contour, which has received the most interest, is the peak (or shoulder) that occurs in systole due to reflected waves. Murgo et al.[97] studied the contour of the pressure pulse in detail and were the first to define the augmentation index (AIx) as in figure 17. AIx is a measure of the increase in BP caused by the return of the reflected wave during systole. AIx will depend on the characteristics of the reflected wave such as its timing (large artery stiffness) and its amplitude (related to peripheral vascular tone).

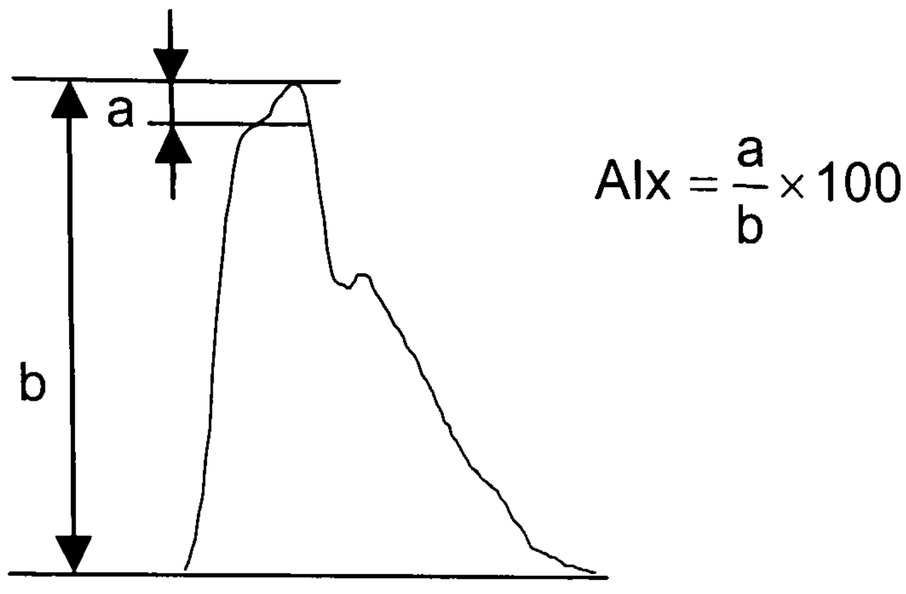

figure 17: Definition of the Augmentation Index on the aortic pulse

Aortic AIx has been widely studied and found to vary with age[7;62;143;153], BP[143;149;153], gender[153], body height[153] ,HR[148;153], aortic pulse wave velocity[153] and to be influenced by vasoactive drugs including caffeine[81;138]. Aortic AIx has been found to be higher in subjects with diabetes than in control subjects[136] and higher in subjects with hypercholesterolemia than in controls[145]. Vasodilator drugs such as GTN and salbutamol decrease AIx[144]. AIx also decreases during a hyperinsulhaemic euglycaemic clamp[141].

The contour of the pulse pressure waveform differs according to the site of measurement[68;109] due to the propagation and reflection of pressure waves throughout the vasculature[110]. There is, however, little difference between the carotid pulse and the aortic pulse because the distance between the two arteries is relatively small. The carotid pulse is easily accessible and can be measured non-invasively with applanation tonometry. A carotid augmentation index (AIx-C) has been derived following the same definition (figure 17). AIx-C has been shown to be correlated with the aortic AIx[28;63], age[5;15;60;62;76], BP[15;76;136], gender[15;76], body height[76], left ventricle ejection time[76], aortic PWV[76] and

tabacco consumption[15]. The AIx-C has been found higher in hypertensive than in normotensive subjects[136] and has been reported higher in patients with end-stage renal disease compared with matched control subjects[77]. AIx-C decreases after treatment with nitrendipine or perindopril + indapamide, but not after atenolol[3;15;42;136]. In a recent study, AIx-C predicted cardiovascular survival in patients with end-stage renal disease[76].

Whilst the carotid pulse is easily accessible it can be difficult to obtain high quality waveforms due to the variability of underlying structures in the neck. By contrast, the radial pulse is easily accessible and the artery can be applanated against the radial bone without difficulty. The shape of the radial pulse is very different from the aortic pulse (figure 18). The propagation, timing and reflection of pressure waves in the vasculature[110] cause the peripheral pressure pulse to differ from the central pressure pulse. Mechanical and elastic properties of the arterial tree distort the direct and reflected waves during their propagation and, especially in young subjects, the peripheral SBP is increased compared to central SBP [30;80;108].

figure 18: Radial and aortic pulses

Radial pressure pulse (left panel) and aortic pressure pulse (right panel) decomposed in schematic manner into direct wave and reflected waves

In the radial waveform, the reflected wave usually causes a shoulder on the down-slope of the systolic part of the radial pressure pulse. A radial augmentation (AIx-R) can be defined using this shoulder (see figure 19).

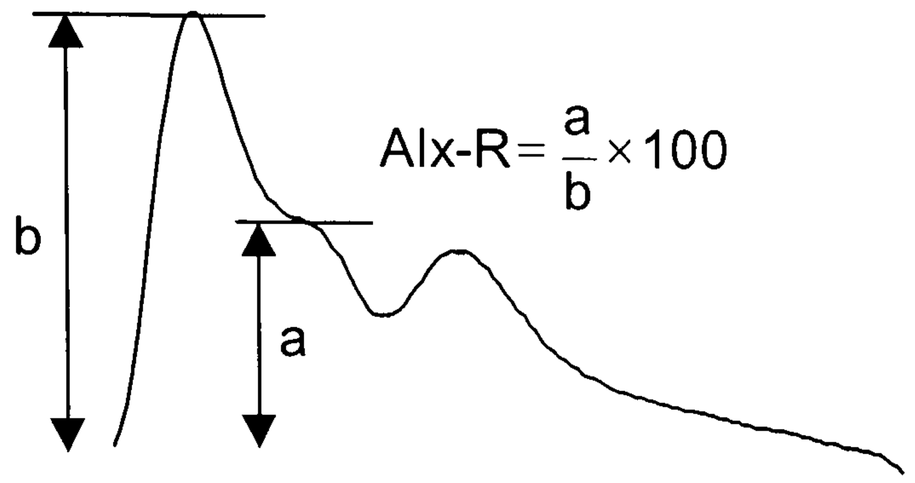

figure 19: AIx-R definition

The radial augmentation index has received much less attention than the aortic AIx. It has, however, recently been used to assess endothelium function by looking at the vasodilator response to salbutamol[47;75]. The radial waveform is extensively use to estimate the central pressure pulse with the use of a transfer function.

3.1.2 Notion of a transfer function

Taylor[134] followed by Avolio et al.[6] and Karamanoglu et al.[56;57] showed that the arterial tree could be successfully represented by a multi-branched model of elastic tubes. Applying the propagation theory of pressure waves in elastic tubes, a transfer function should exist relating the input pressure (aortic pressure) to the output pressure (peripheral pressure such as the radial pressure) of such a system.

A transfer function (TF) is a mathematical statement that describes the relationship between 2 variables in a system, S_1 and S_2, which are functions of time (t) and can also be represented in the frequency domain (f).

The transfer function of a system is:

$$TF(f) = \frac{S_1(f)}{S_2(f)} = \frac{FFT(S_1(t))}{FFT(S_2(t))}$$

where FFT stands for Fast Fourier Transform. The Fourier transform is a mathematical way of expressing a temporal signal in the frequency domain. A temporal signal can be decomposed into a summation of several sinusoids of different frequency (Fourier's Theorem). Each sinusoid is characterised by its amplitude and phase. A signal may be represented in the frequency domain by a graph of the amplitude and phase of each sinusoid versus the frequency of the sinusoids. The transfer function between two signals S_1 and S_2 may be represented by the ratio of their amplitude and their phase difference plotted versus frequency.

Karamanoglu et al.[58] first reported the existence of a generalised transfer function between radial and brachial pressure and aortic pressure waveforms. They showed that TFs calculated for individual patients undergoing diagnostic cardiac catheterisation were similar and little influenced by administration of sublingual GTN. They averaged these "individual" transfer functions to produce a generalised transfer function that could be applied to calculate aortic pressure from peripheral pressure in any patient. This was later confirmed by Chen et al.[27] using a TF in the frequency domain on patients undergoing diagnostic cardiac catheterisation, by Sugimachi et al.[129] on patients with arrhythmias and by Fetics et al.[38] using a TF in the time domain. A generalised transfer function (GTF) has

been implemented in a commercially available device (Sphygmocor, AtCor, Sydney, Australia).

3.1.3 Validation of the use of the transfer function

Both radial and carotid waveforms can be used to synthesise the central pulse. However the most widely used approach is to perform radial artery tonometry, as it is simpler and better tolerated by the patient. Carotid tonometry, on the other hand, requires a high degree of technical expertise[28;107].

The validation of the commercially available radial to aorta TF has been assessed by several investigators. However, most assessments of the accuracy of the TF in synthesising the aortic pressure pulse from the radial pulse have focused on the estimation of aortic SBP and not on features of the contour of the aortic waveform such as the AIx. Pauca et al.[115] recruited 62 patients undergoing cardiac surgery and simultaneously recorded invasive radial and aortic pressure waveforms before and during GTN infusion. The difference in aortic SBP between the measured and the synthesised aortic pulse was 0.1 ± 4.3 mmHg (mean ± SD). Segers et al.[125] compared invasive aortic and radial pressure waveforms in 45 patients before cardiac procedures and after GTN infusion (n=40). AIx from the reconstructed aortic pulse underestimated measured aortic AIx by 4 ± 16% at baseline and by 2 ± 15% after GTN (errors in AIx are given in percentage units and not as a percentage of the measured value). Söderström et al.[127] measured the true aortic pressure waveforms on 12 patients with angina pectoris and compared them to the estimated aortic pressure from the radial pulse

measured by tonometry. The patients were studied at rest, following midazolam, sublingual GTN and during Valsava manoeuvres. They concluded that aortic SBP was underestimated by 6 to 8 mmHg. The difference in measured aortic AIx and estimated aortic AIx was 6 ± 9.5% (estimated from their Bland-Altman graph)[127]. Results from studies in which the accuracy of the TF for predicting central SBP and aortic AIx has been examined and shown in table 1.

Investigator	Method	Error in SBP	Error in AIx §
Chen et al.[27] *†	non-invasive radial invasive aortic pulse	0 ± 3.7 mmHg	-7 ± 9 %
Fetics et al.[38] †	non-invasive radial invasive aortic pulse	0.4 ± 2.9 mmHg	-54 ± 232 % % (% error in AIx)
Karamanoglu et al.[58] *†	invasive radial invasive aortic pulse	2.4 ± 1.0 mmHg	-
Pauca et al.[115]	invasive radial invasive aortic pulse	0.1 ± 4.3 mmHg	-
Segers et al.[125]	invasive radial invasive aortic pulse	-	3 ± 16 %
Söderström et al.[127]	non-invasive radial invasive aortic pulse	6 to 8 mmHg	6 ± 9.5 %

table 1: Validation studies of the radial-aortic transfer function

** denotes authors who use the same data to generate a TF and validate it*

† denotes authors who have used their own TF and not the commercially available one

§ errors in AIx are expressed in % units not in % of the measured value unless stated otherwise

An important difference between these studies was the method used to measure the radial pressure pulse. Pauca et al.[115] and Segers et al.[124] measured it invasively and validated the use of the commercially available TF to estimate central BP. Söderström et al.[127], Chen et al.[27] and Fetics et al.[38] used the tonometry technique to assess the radial pulse. Although tonometry has been shown to provide similar waveforms to those obtained by direct intra-arterial pressure monitoring[61], non-invasive recording might add some additional error in the estimation of the aortic pulse. This could also explain why Söderström et al. observed an underestimation of the SBP. Calculated values for SBP fall broadly within the range specified for the AAMI and BHS requirements[106] at least for directly recorded radial waveforms. The error between the measured and estimated AIx is substantial (≈5% units) compared to average AIx values (about 20%) and to the changes expected after biological effects. The second important point relates to the spread of this error around the mean, which is expressed by the standard deviation (SD). The SD of the error ranges from 9 to 16%, which is considerable compared to biological effects. For example, five years of vascular ageing is associated with an increase in AIx of 6.3%[60]. The difference between control and diabetic subjects is 6.3%[150] and between control and hypercholesterolemic patients 9.2%[145]. Compared to these values, an error of 5% between measured and estimated AIx is considerable.

3.1.4 Reproducibility of the estimated central waveform

The reproducibility of measurements obtained with the Sphygmocor has been studied by several authors[126;147] (table 2). Wilkinson et al.[147] looked at the reproducibility of the aortic AIx estimated by transformation from the radial artery. They found a within-observer difference of 0.5% ± 5.4% (mean ± SD) and a between observer difference of 0.2% ± 3.8%. Siebenhofer et al.[126] studied the inter-operator variability of aortic SBP and aortic AIx obtained from the radial pulse. Intra-operator difference was 0.1 ± 1.7 mmHg for aortic SBP and 0.4 ± 6.4% for AIx.

Investigators	Index	
Benetos et al.[15]	Carotid AIx	reproducibility: 8.1 ± 4.4 %
Wilkinson et al.[147]	AIx_{TFR}	within observer variability: 0.5 ± 5.4 % between observer variability: 0.2 ± 3.8 %
Yasmin et al.[153]	AIx_{TFR}	difference between repeated measures: 0.18 ± 4.7 %
Siebenhofer [126]	AIx_{TFR}	mean difference (±SD): 0.4 ± 6.4%
Westerbacka et al. [141]	AIx_{TFR}	coefficient of variation: 5 ± 1%

table 2: Results of reproducibility studies on AIx

AIx_{TFR} : aortic AIx estimated from the radial pulse with a transfer function

From these data the fact that the SD of the difference between measured and estimated aortic AIx is up to 16% (see section 3.1.3) and the SD of the variability up to 6.4 % is worrying. An error of 10% in the determination of AIx represents an error of 8 years of vascular ageing, or a change of 25 bpm in HR. However the difference between measured and estimated aortic SBP is of a smaller scale (up to 8 mmHg).

The transfer function has been established and validated with invasive measurements of aortic pressure waveforms, which have been obtained during catherisation. For ethical reasons, subjects undergoing aortic catherisation are usually unhealthy and generally of an older age. The generalised TF may thus be less suitable for a younger healthy population.

The accuracy of the TF for estimating aortic SBP but inaccuracy in estimating AIx may be explained by the variability of individual TFs at high frequencies[27;38;57]. Figure 20 shows that individual TFs are similar at frequencies up to 4Hz but from 4Hz to 10Hz the 95% confidence interval (representing the variation between individuals) becomes wider.

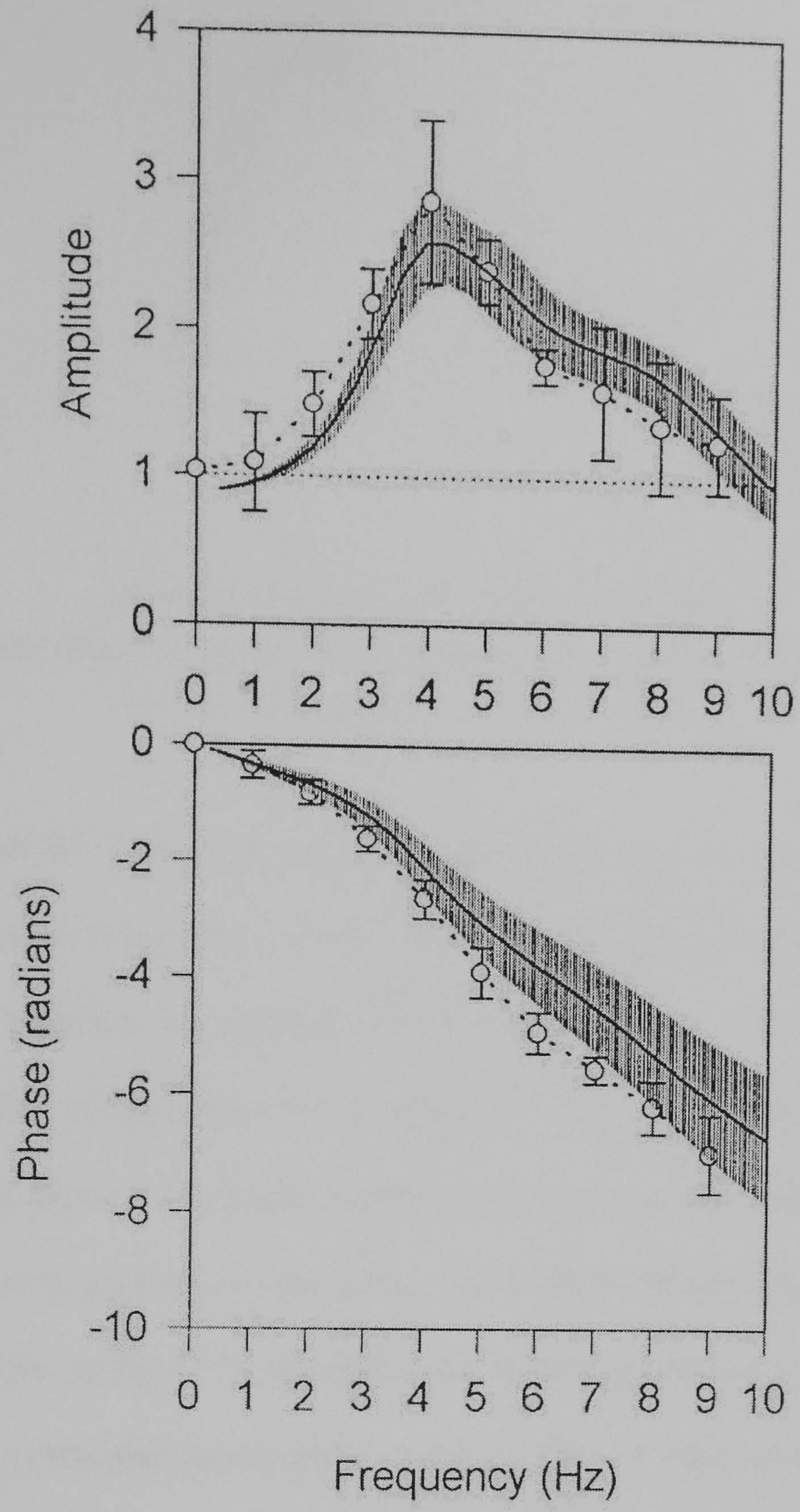

figure 20: Radial-aortic transfer function

Transfer function with 95% confidence intervals (representing the variation between individuals TFs). Open circles with errors bars from Karamanoglu et al.[58], solid line with shaded area from Chen et al.[27] (reproduced from Chen et al.[27])

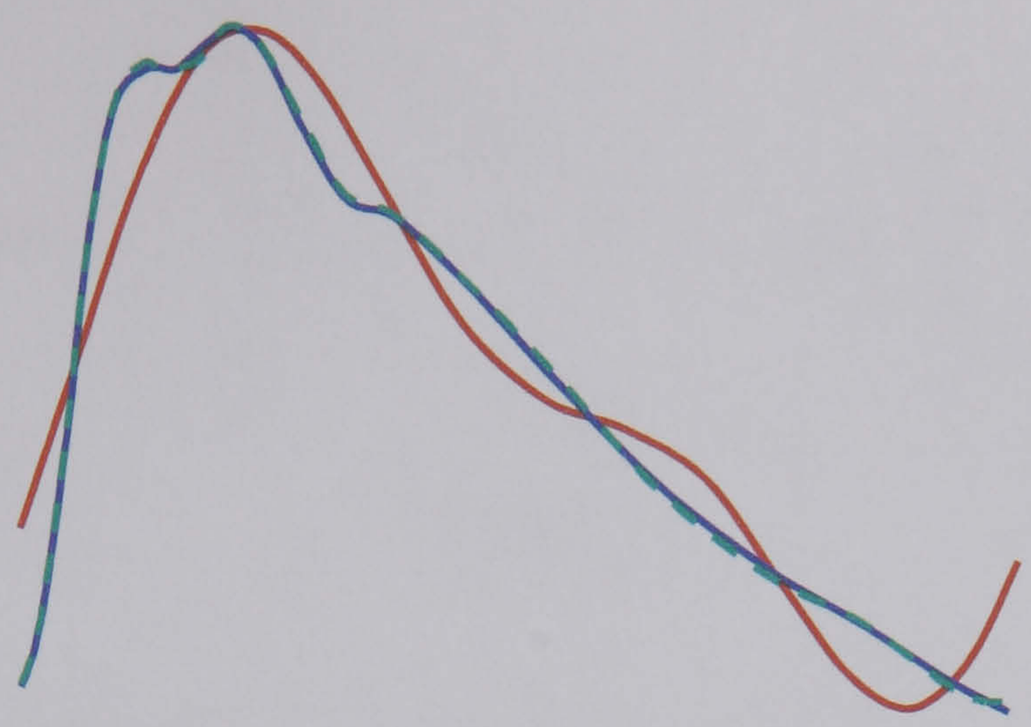

figure 21: Importance of the various harmonics
The original pulse (blue), the pulse constructed from the first 3 harmonics (red) and the pulse constructed from the first 10 harmonics (green).

In figure 21, the relative influence of high frequency harmonics is shown. With 3 harmonics (equivalent of 4Hz for a subject with HR=60bpm), systolic and diastolic pressure are properly determined. However AIx depends upon higher frequency components of the waveform. The discrepancy between the individual TFs above 4 Hz might explain why the generalised transfer function (GTF) is relatively accurate in estimating central SBP whereas estimation of AIx is less acceptable. In figure 22, the influence of the high frequency variability of the TF on the synthesised aortic pulse is shown. The TF used is as described by Chen et al.[27] with the upper and lower 95% confidence limits of the individual TFs (dotted lines). Change in the TF had little effect on SBP but a greater effect on AIx.

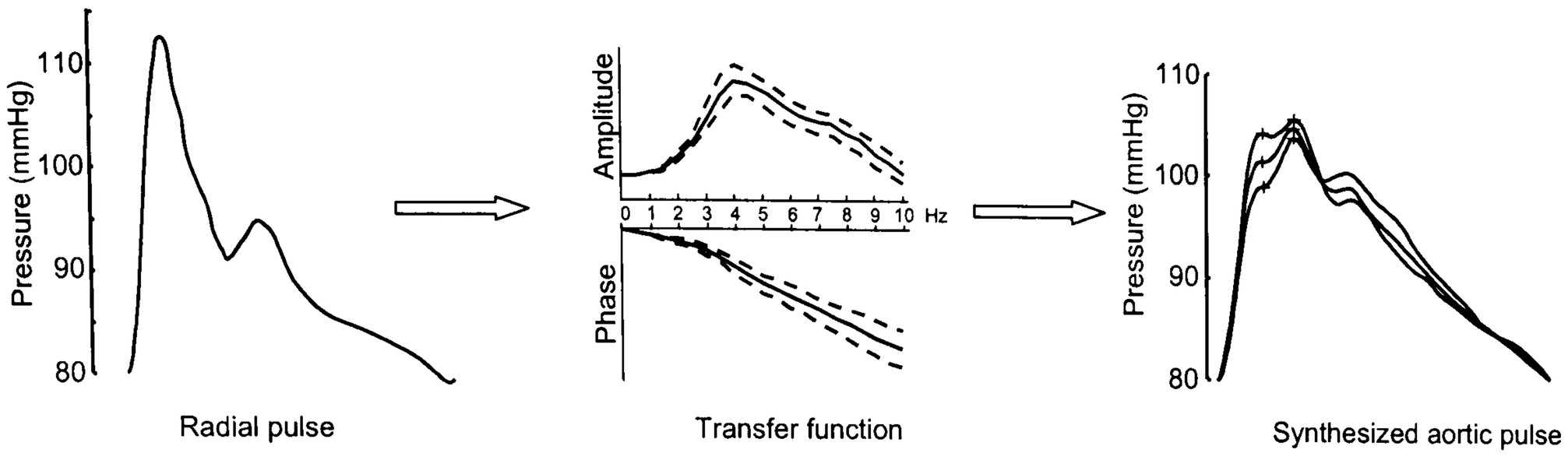

figure 22: Influence of the TF on the synthesised aortic pulse

The radial to aortic transfer function described by Chen at al.[27] (middle panel) applied to a typical radial waveform(left panel) using the upper and lower 95% confidence limits for the coefficients (dotted lines). The resulting synthesised aortic waveforms (right panel) exhibit little variation in systolic pressure but marked variation in the aortic AIx.

3.2 Aims

The transfer function (TF) has been established and tested mainly with regard to estimation of central SBP in older subjects with coronary artery diseases. Reservations regarding the TF approach to derived AIx are discussed above. The aim of this study was to re-evaluate the accuracy of the TF approach especially in younger healthy subjects. For ethical reasons access to invasive aortic pressure pulse is not possible in healthy subjects, so the carotid pulse which bears strong similarities to the aortic pulse[28;63] was used.

The aims of the study were to:

1/ compare aortic SBP derived by application of a TF to the carotid (aortic SBP_{TFC}) and radial pulse (aortic SBP_{TFR})

2/ compare AIx derived by application of a TF to the carotid (AIx_{TFC}) and radial pulse (AIx_{TFR})

3/ determine the relationship between the AIx derived directly from radial pulse (AIx-R) and the aortic AIx derived after application of the TF to the radial pulse (AIx_{TFR}).

Healthy subjects and older subjects with hypertension and coronary artery disease were studied in order to obtain a high range of values of AIx. In a sub-group of healthy subjects, vasoactive drugs were administered to determine whether changes in aortic AIx tracked those in the radial AIx (AIx-R).

3.3 Methods

Studies were performed with the approval of St Thomas' Hospital Research Ethics Committee and with the written informed consent of the subjects. Three groups of subjects were studied: healthy volunteers (n=30, age: 37±8 years, BP: 119±11/69±8 mmHg, mean ± SD), subjects with uncomplicated essential hypertension (n=30, age: 51±13 years, BP: 142±22/89±14 mmHg) and patients with coronary artery disease (n=23, age: 57±8 years, BP: 131±19/79±9 mmHg). Measurements were performed with subjects supine in a quiet temperature controlled environment after at least 15 min at rest. Radial and carotid arterial pressure waveforms were obtained by applanation tonometry (Millar Instruments, Texas) as describe in section 2.1.1 with Sphygmocor software version 6.3 (AtCor, Australia). Three successive recordings were obtained from each artery and measurements were repeated if the waveform(s) did not pass the automatic quality controls specified by the Sphygmocor

software. Brachial artery BP was measured in triplicate with an oscillometric device (Omron 705CP, Omron, Japan) and the mean of 3 readings used to calibrate the radial pressure pulse. The carotid pressure pulse was calibrated using the diastolic and mean arterial pressure obtained from the calibrated radial pulse. The aortic pulse was synthesised from the radial pulse and from the carotid pulse using the transfer functions supplied by Sphygmocor.

Effects of vasoactive drugs were assessed in a subset of 12 of the healthy volunteers. A similar protocol was used to obtain carotid and radial pressure pulse recordings at baseline and during the last 10 min of a 15 min intravenous infusion of noradrenaline (50 $ng.kg^{-1}.min^{-1}$, n=8) or GTN(100 $\mu g.min^{-1}$, n=4).

Statistics

Agreement between estimates of the same measurement was assessed by Bland-Altman plots. The mean difference between measurements was used to quantitate systematic error and the standard deviation of the differences the variation in agreement[18]. Pearson correlation coefficients are also presented with the recognition that these are of limited value in the comparison of closely related measurements[18]. Different measurements (aortic and radial AIx) were compared by regression analysis. A Bland-Altman plot was used to compare aortic AIx with aortic AIx predicted from AIx-R (using the coefficients of the regression equation of radial vs. aortic AIx). $P<0.05$ was considered significant. All tests were 2-tailed.

3.4 Results

3.4.1 Central systolic blood pressure

Values of central SBP computed from the radial pulse using the radial to aortic TF were in close agreement with those computed from the carotid pulse using the carotid to aortic TF (figure 23). Correlation coefficients were 0.87, 0.99 and 0.99 in control, hypertensive and CAD groups respectively. Mean ± SD differences between values obtained from the transformed radial and carotid waveforms in the respective groups were 0.03±5.3, –2.0±4.7 and –1.0±3.4 mmHg. The overall correlation coefficient for all groups was 0.98 and the mean difference –0.9±4.6 mmHg. Two standard deviations (2SD, the Bland-Altman statistic giving the confidence limits within which, assuming a normal distribution, 95% of readings will be in agreement) of the difference between the two measures of central SBP was 9.2 mmHg.

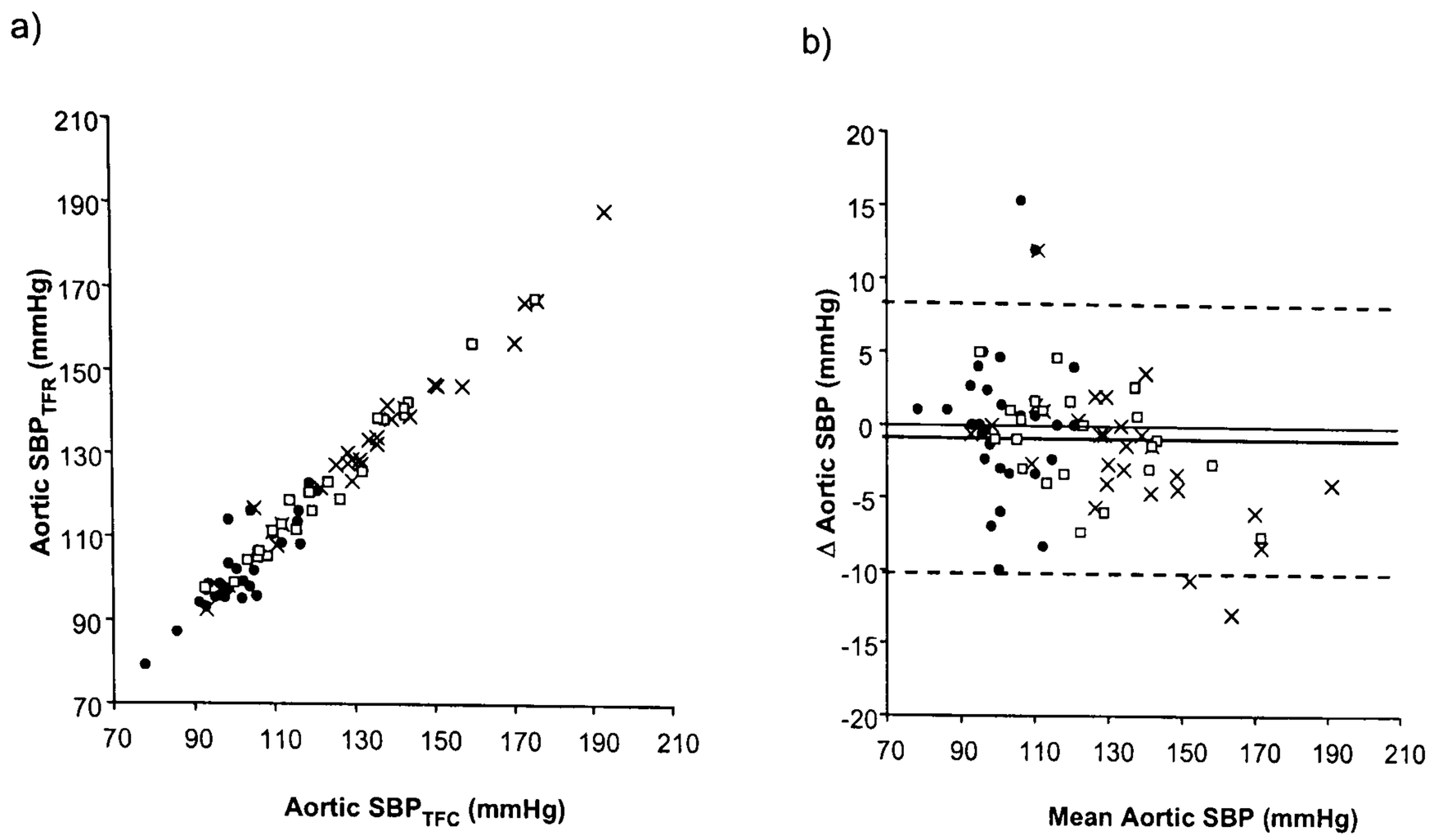

figure 23: Central systolic blood pressure

Comparison of aortic systolic blood pressure (SBP) estimated by applying transfer functions to radial (SBP_{TFR}) and carotid pulse waveforms (SBP_{TFC}) in control subjects (•), hypertensive subjects (×) and subjects with coronary artery disease (□): a) scatter plot; b) Bland-Altman plot of difference in SBP ($\Delta SBP = SBP_{TFR} - SBP_{TFC}$) versus mean SBP. The solid line represents the mean difference and the dashed lines are 2 standard deviations from the mean.

3.4.2 Aortic AIx

Mean values of aortic AIx estimated from the transformed radial waveform (AIx_{TFR}) were 8.3±8.7, 27.9±10.6 and 29.5±11.8 % in control, hypertensive and CAD patients respectively. Agreement between AIx_{TFR} and AIx_{TFC} was relatively poor with correlation coefficients 0.47, 0.83 and 0.84 and mean differences –3.8±12.4, –8.8±6.0 and –5.8±7.1 mmHg for the control, hypertensive and CAD groups respectively. The overall correlation coefficient for all groups was 0.84 and the mean difference –6.2±9.2%. The SD of the

difference (2SD = 18.4 %) was substantial in comparison with the difference of approximately 20% seen between mean values of AIx in the control and hypertensive/CAD patients. Similar results were obtained when AIx_{TFR} was compared with carotid AIx, a validated estimation of the aortic AIx[28] (overall correlation coefficient: 0.86; 2SD of the difference: 22.6 %).

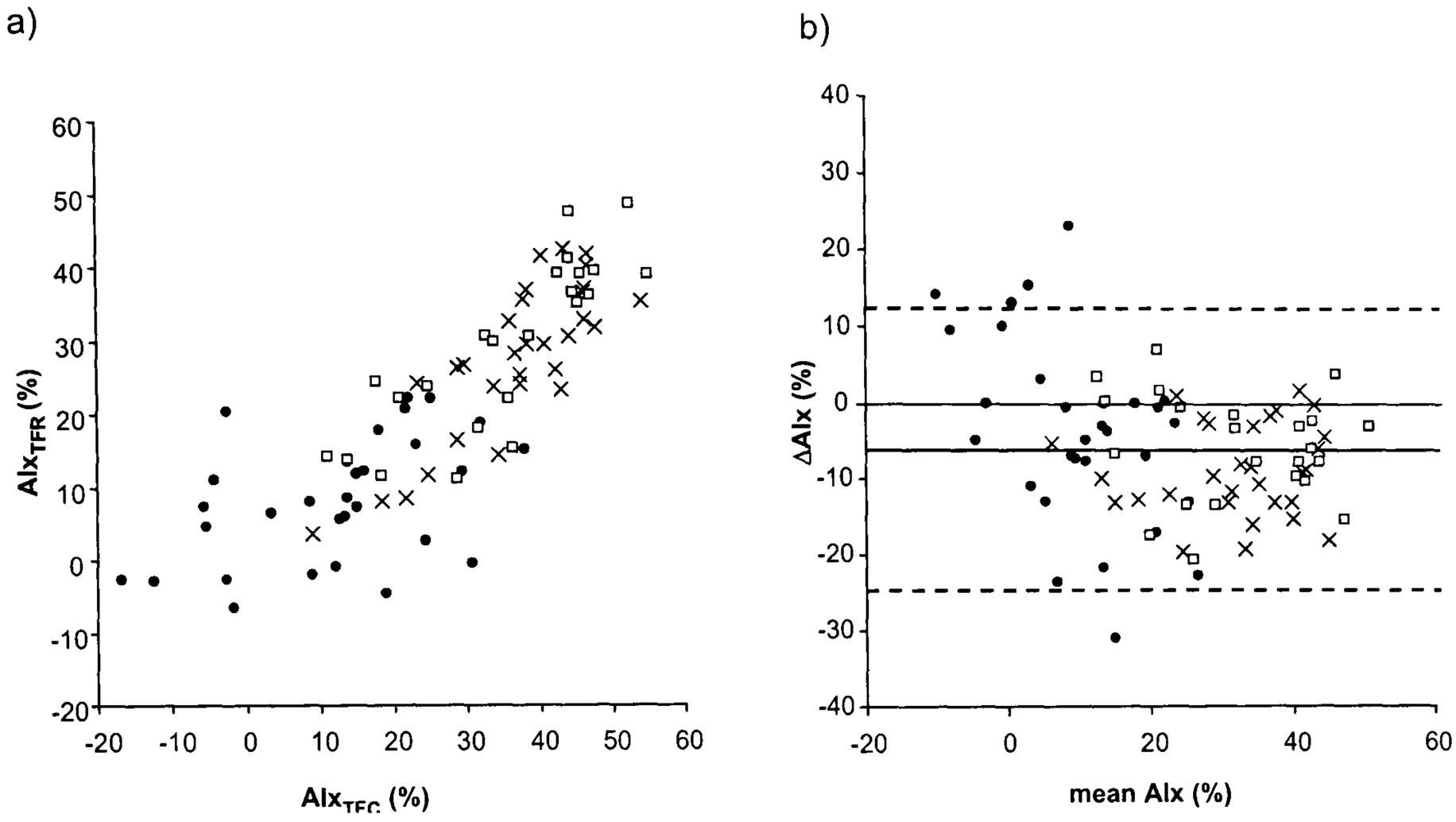

figure 24: Aortic augmentation index

Comparison of aortic augmentation index estimated by applying transfer functions to radial (AIx_{TFR}) and carotid pulse waveforms (AIx_{TFC}) in control subjects (•), hypertensive subjects (×) and subjects with coronary artery disease (□): a) scatter plot; b) Bland-Altman plot of difference in AIx ($\Delta AIx = AIx_{TFR} - AIx_{TFC}$) versus mean AIx. The solid line represents the mean difference and the dashed lines are 2 standard deviations from the mean.

3.4.3 Comparison of aortic with radial AIx

There was a close approximately linear correlation (R>0.92 within each group and R=0.96 for all groups, figure 25) between AIx_{TFR} obtained by applying a TF to the radial waveform and AIx-R obtained without use of a TF. For comparison with previous data, a Bland-Altman plot was constructed for the difference between aortic AIx and AIx estimated from the regression line relating aortic to radial AIx. 2SD of the difference was 5.4%, less than that seen for the difference between AIx_{TFR} and AIx_{TFC} obtained using transfer functions.

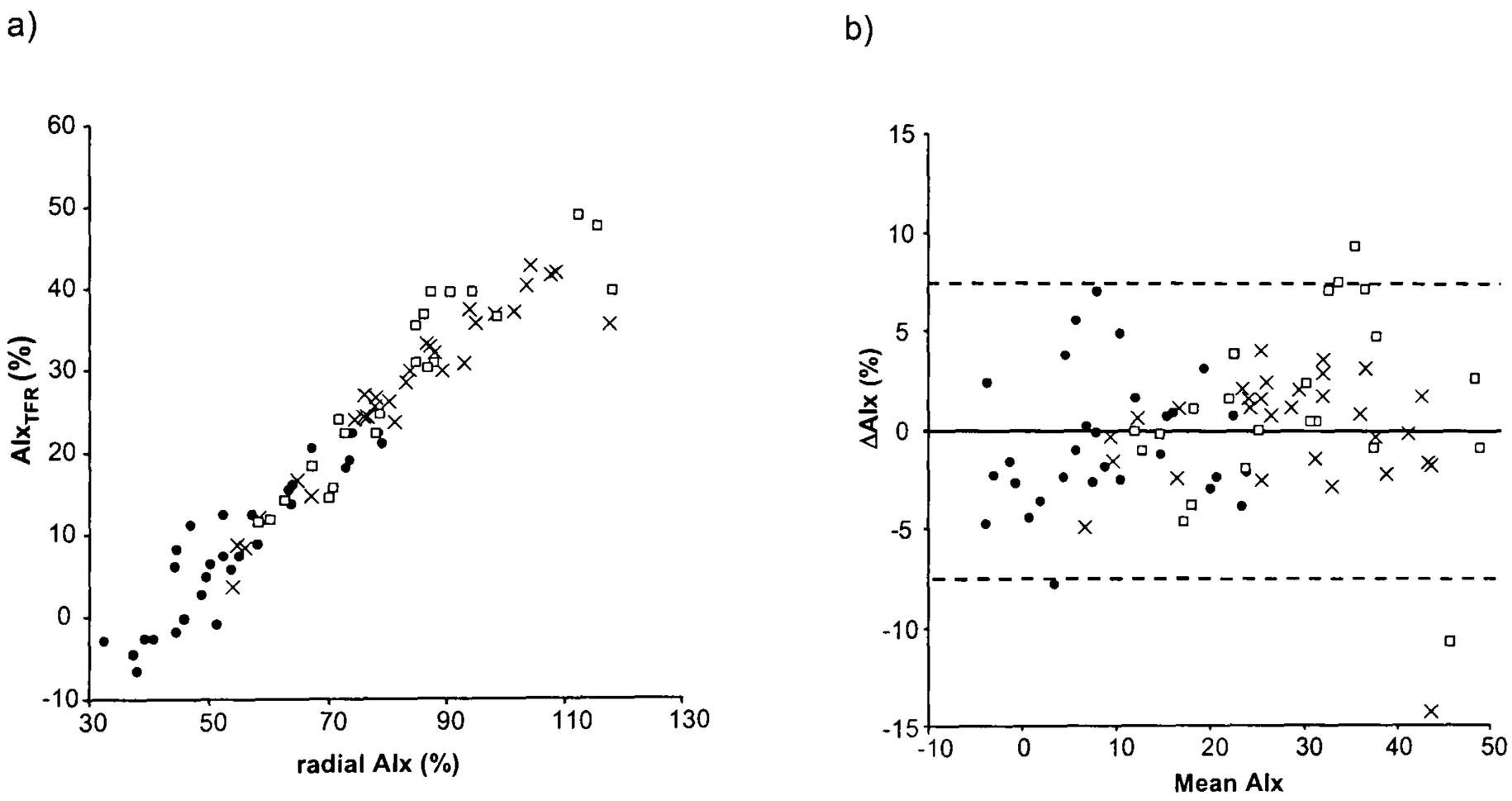

figure 25: Aortic AIx and radial AIx

Comparison of aortic augmentation index (AIx) estimated by applying a transfer function to the radial arterial waveform (AIx_{TFR}) and radial AIx obtained without a transfer function in control subjects (•), hypertensive subjects (×) and subjects with coronary artery disease (□): a) scatter plot; b) Bland-Altman plot for the difference (ΔAIx) between aortic AIx predicted from the radial AIx (using the coefficients of the regression equation of radial AIx versus AIx_{TFR}) and radial AIx versus mean AIx. The solid line represents the mean difference and the dashed lines are 2 standard deviations from the mean.

Changes in aortic AIx produced by GTN and noradrenaline correlated with those in radial AIx (R=0.93, P<0.0001, figure 26).

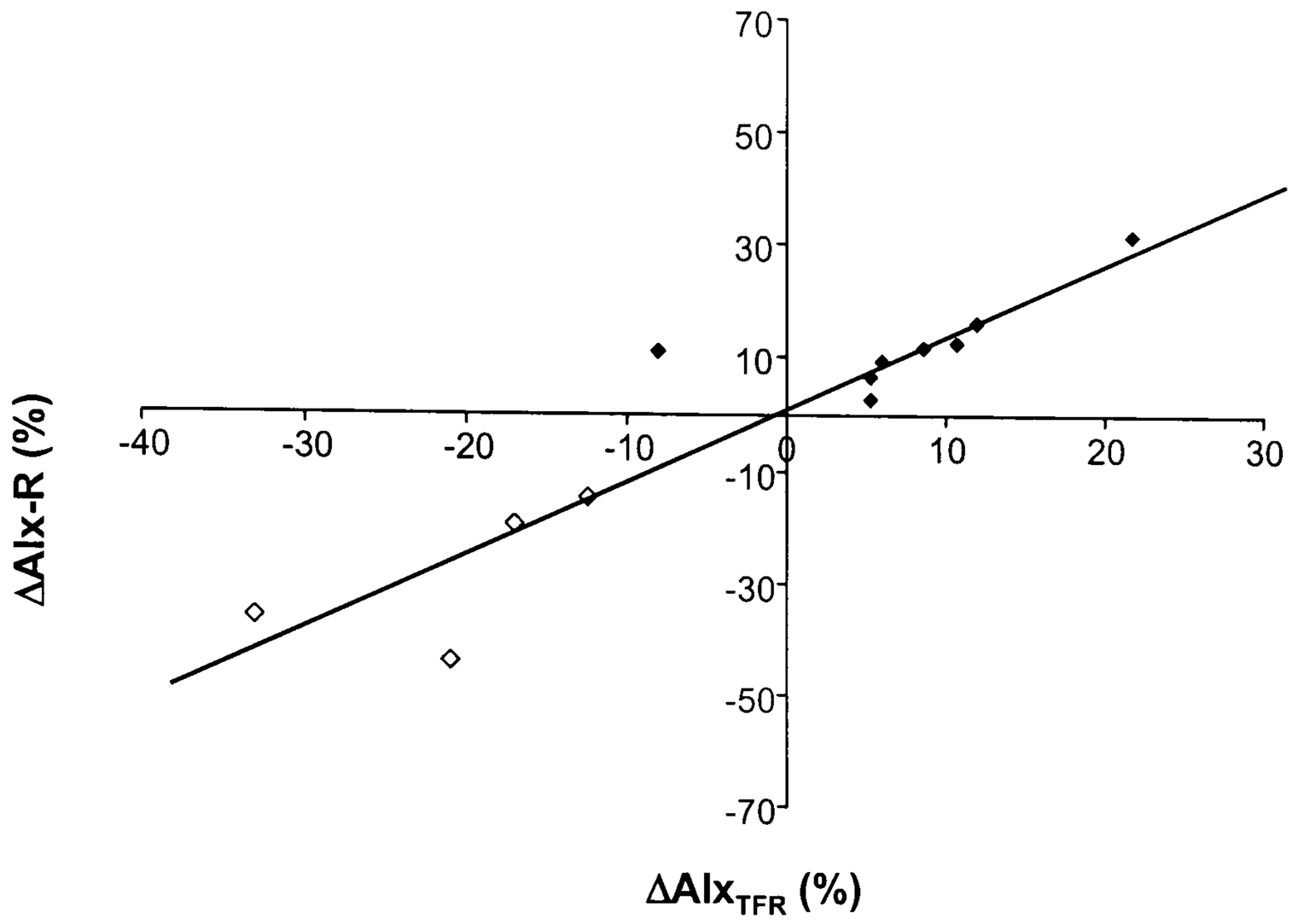

figure 26: Effects of vasoactive drugs

Change in aortic AIx(ΔAIx_{TFR} estimated by applying a transfer function to the radial artery) and change in radial AIx (ΔAIx-R, obtained without using a transfer function) during intravenous infusion of glyceryl trinitrate (open symbols) and noradrenaline (closed symbols).

3.5 Discussion

The transfer function (TF) used to estimate the central pressure pulse from the radial pulse has been calculated in patients in whom direct measurements of aortic pressure can ethically be obtained. So the TF has been established in patients undergoing cardiac catheterisation, such as patients

undergoing diagnostic angiography or post heart transplant[27;38;58]. The validation studies have focussed mainly on the accuracy of determining SBP and this falls within the range of the BHS requirements[105;106]. However, in studies in which the accuracy of the TF for determining aortic AIx has been assessed, the discrepancy between values of AIx obtained using a TF and measured values are quite high compared with patho-physiological changes[27;38].

In the present study, the agreement between measures of SBP and of aortic AIx obtained from transformed radial and carotid pressure waveforms have been compared. The agreement between estimates of central SBP were within acceptable limits in all groups of subjects with the mean difference less than 2 ± 5.3 mmHg (mean ± SD). This is consistent with validation studies in which aortic pressure estimated from the radial pulse has been compared with direct intra-aortic recordings[27;115].

In contrast to central systolic pressure, estimates of aortic AIx derived from the radial (AIx_{TFR}) and carotid (AIx_{TFC}) waveforms showed relatively poor agreement, especially in young healthy subjects. In these subjects there was no significant correlation between values of AIx_{TFR} and AIx_{TFC}. Two SDs of the difference was 18.4 % units (see Bland-Altman plot, figure 25). This difference is large in comparison with patho-physiological changes. A change of approximately 14%, for example, is seen in association with 10 years of ageing[60]. In the above data, the difference between young healthy subjects and older CAD patients was about 20%. This discrepancy between values of AIx derived by applying transfer functions to the carotid and radial arteries suggests that one, or

other, or both of the transfer functions are of limited accuracy in predicting aortic AIx especially in healthy subjects.

The validity of carotid-aortic TF has not been studied as much as the radial-aortic TF. However because the pressure waveform and the change in the wall properties with ageing are similar in the carotid artery and in the ascending aorta[63], several studies have used the carotid pulse as a direct estimation of the aortic pulse. The carotid artery is close to the aorta, and the assumptions that arterial properties (path length, impedance mismatched) determining the TF may be more justified. Indeed the aortic AIx can be estimated from the carotid without use of a TF[28] and we found similar discrepancy between AIx_{TFR} and AIx-C to that between AIx_{TFR} and AIx_{TFC}. The error could have arisen from the carotid tonometry measurements, as it can be quite difficult to obtain a consistent beat to beat carotid pressure pulse in some subjects[107]. However, great care was been taken in this study to obtain the best waveforms possible and traces of poor quality were discarded. So the majority of the error is most likely to reside in the radial to aortic TF. The transfer function used is a "generalised transfer function" (GTF) calculated from TFs from individual subjects. It assumes that the properties of the arterial tree between the radial artery and the aortic arch are the same in everybody under all conditions. This is obviously quite a generous assumption as the body size, age, presence or absence of arteriosclerosis and atherosclerosis and other parameters influence the arterial pathway. This assumption holds for the frequency components determining central SBP but not for those determining AIx. The discordance in the accuracy of the TF with central SBP and aortic AIx is consistent with the characteristics of the transfer function. SBP is determined by the coefficients for the lower frequencies and

these coefficients show much less spread than those for the higher frequencies, which influence AIx (see figure 21 and figure 22). When the GTF and the 95% confidence intervals TF are applied to the same radial pulse, a difference up to 15% can be observed for the AIx, whereas the values of SBP are equivalent (see figure 22).

The GTF is a good tool to determine central SBP from the radial artery. It may not, however, be necessary to use it to assess central pressure wave reflection. In the present study we observed a close correlation ($R > 0.92$ in all groups) between the AIx_{TFR} derived by application of a GTF to the radial waveform and the AIx-R calculated directly without use of a GTF. Furthermore when changes in AIx were induced by vasoactive drugs there was a highly significant correlation between changes in AIx_{TFR} and AIx-R. That a close relation between aortic and radial AIx should exist is not unexpected. A transfer function does not add any information, so everything contained within the transformed waveform should be possible to infer directly from the radial waveform. What is surprising is the linear relationship between AIx_{TFR} and radial AIx (AIx-R). This means that AIx-R may provide an equally good measure of central pressure wave reflection and has the advantage that it is not dependent on a relatively arbitrary manipulation of the waveform derived from observations made in a selected groups of subjects.

In conclusion, our findings suggest that transforming the radial pulse to the central pulse may be not necessary and that the peripheral pulse could be used directly to study the wave reflections.

CHAPTER 4: Relationship between the pressure pulse and the volume pulse

4.1 Background

The digital volume pulse (DVP) can be obtained by measuring infra-red light transmission through the finger by photoplethysmography[36;78;94] as described in section 2.2. Müller and Weis[96] in 1911 were the first to mention that the DVP and the pressure pulse bear some similarities. In 1939, Hertzman when studying the DVP, noted that "*the volume pulse is here* (in the digit) *indistinguishable in form from the peripheral arterial pulse*"[48]. The description of changes in the DVP occurring after GTN by Hertzman[48] and Morikawa[94] mimic the changes described in the peripheral pressure pulse[59;98]. These observed similarities make it attractive to explain the characteristics of the DVP with the same theory applied to the pressure pulse contour.

The pressure waveform has been subject to extensive analysis and it is now well accepted the pressure waveform is formed by a direct wave and several reflected waves arising mainly from the lower body as described in section 1.1. The amplitude and the velocity of the reflected waves largely determine the contour of the pressure pulse. The DVP is formed by the pulsatile component of infra-red light transmitted through the finger pulp. Infra-red light is mainly absorbed by oxyhemoglobin in the blood, so the DVP follows changes in the blood volume in the finger pulp. If it is assumed that the blood volume in capillaries and veins remains approximately constant during the cardiac cycle, the DVP would be caused by changes in blood volume in the digital artery and possibly in arterio-veinous shunts. Variations of the digital intra-arterial pressure during the cardiac cycle distend the arterial wall and so increase blood volume in

the arterial segment and downstream vessels and thus generate the DVP. Because of the elasticity and the viscosity of the arterial wall, wall displacement is not linearly related to the arterial pressure pulse[104] but a relationship should exist between the DVP and the pressure pulse.

As described in the previous chapter, the central pressure pulse can be estimated from the peripheral pressure waveform with the help of a generalised transfer function (GTF). The use of the GTF is based on the assumption that the difference between various subjects in the physical properties of the transmission path between the radial (or carotid) and aortic artery on different subjects is negligible. If the physical properties of the arterial tree in the finger that determine the DVP are reasonably similar, a GTF should exist between the DVP and the digital pressure pulse or radial pressure pulse.

4.2 Aim

The aim of this study was to establish whether a simple TF can be used to relate the DVP to the radial and digital artery pressure pulses in healthy subjects and in patients with essential hypertension. The effect of administration of the vasodilator GTN was examined to verify if TFs between the DVP and pressure pulses depend on local vasodilation.

4.3 Methods

4.3.1 Subjects

Healthy normotensive (n=40, 118±11/67±9 mmHg, mean ± SD) and hypertensive subjects (n=20, 152±14/92±12 mmHg) aged 24 to 80 years (including 10 women) were recruited from the local community in south-east London. None of the hypertensive subjects had clinical evidence of cardiovascular disease other than hypertension. Twelve were receiving anti-hypertensive therapy at the time of the study (diuretics: 7/12; beta-adrenoreceptor antagonists: 5/12; alpha-adrenoreceptor antagonists: 1/12; ACE inhibitors: 3/12; angiotensin II receptor antagonists: 2/12; calcium channel blockers: 4/12).

The study was approved by St Thomas' Hospital Research Ethics Committee and all subjects gave written informed consent.

4.3.2 Pressure and volume pulse recordings

The DVP was determined using a finger probe (as described in section 2.2.2) applied to the index finger of the right hand. A pen-like tonometer (Millar SPT 301, Millar Instruments, USA) was used to record radial artery pressure and was applied over the radial artery of the left arm (see section 2.1.1). Digital artery pressure was measured non-invasively on the middle finger of the right hand using the Finapres device (Finapres 2300, Ohmeda, USA) as described in

section 2.1.2. Signals from all transducers were recorded via a 12-bit analogue to digital converter (sampling frequency 100 Hz) on a PC. Further digital signal processing was performed off-line with Matlab^{TM} (MathWorks, USA). Brachial artery pressure (left arm) was measured using an automated oscillometric method (Dinamap, Critikon, UK).

4.3.3 Protocol

Subjects rested supine in a temperature-controlled laboratory (26±1°C) for 30 min to allow HR and BP to stabilise. Simultaneous pressure and DVP waveforms were recorded for 30 seconds at 5 minutes intervals for 15 min. In a subset of 20 of the normotensive subjects GTN (500 μg) was then administered sublingually and further simultaneous volume and pressure recordings were obtained 3 min after GTN when effects of GTN were maximal. GTN was used to induce a change in the shape of the pressure and DVP waveforms in order to examine whether the relationship between pressure and DVP pulses remains constant despite a vasodilator stimulus.

4.3.4 Data analysis

Since the purpose of the study was to compare the shape of the waveforms, the amplitude of the DVP was normalised to be equal to that of the pressure pulse. Pulses from each cardiac cycle were identified (see algorithm in appendix 10.4) and normalised in time and amplitude in order to obtain an

average pulse. Normalisation was performed using a cubic interpolation to a fixed number of samples. After normalisation, an average pulse was constructed by taking the mean of the signal at each time points. Brachial BP was used to calibrate pressure signals from the tonometer and the Finapres.

Transfer Function (TF):

For each measurement a transfer function (TF) was determined in the frequency domain from pressure and DVP pulses as shown below.

$$TF(P_{rad}/V_{dig}) = FFT(P_{rad})/FFT(V_{dig}) \qquad (1)$$

$$TF(P_{dig}/ V_{dig}) = FFT(P_{dig})/FFT(V_{dig}) \qquad (2)$$

P_{rad} = radial artery pressure

V_{dig} = digital volume

P_{dig} = digital artery pressure

FFT = Fourier Transform

A TF for each volunteer was computed at baseline (using 3 consecutive measurements at 5 minute intervals) and 3 minutes after GTN (when changes due to GTN were maximal). Each measurement was determined using a minimum of 6 consecutive stable cycles obtained simultaneously on all three transducers. Since harmonics greater than 10 do not contribute significantly[121], only the first 10 harmonics of each waveform were used for the analysis.

General Transfer Function (GTF):

A general transfer function for control waveforms (GTF_c) was derived by averaging all TFs at baseline. A general transfer function after GTN (GTF_{GTN}) was derived from TFs obtained 3 min after GTN. GTF_c and GTF_{GTN} were used to calculate a mean general transfer function (MGTF) for all subjects (weighted average). The MGTF was used to predict pressure waveforms from the DVP waveforms.

Measure of agreement:

The agreement between predicted and measured waveforms was quantified by the root mean square (RMS) difference between the two signals.

Statistical analysis:

Results are presented as means ± SD. Analysis of variance (for repeated measures where appropriate) was used to compare RMS errors between the groups and waveforms. $P<0.05$ was taken as significant.

4.4 Results

Typical DVP and pressure waveforms are shown in figure 27. Radial and digital pressure waveforms were in close agreement in all subjects. The mean RMS error for the difference between radial and digital pressure waveforms was 4.4±1.4 mmHg (mean for all subjects ± SD). The DVP signal differed from the

pressure signals (figure 10) with the main difference being in the height of the diastolic component of the waveform.

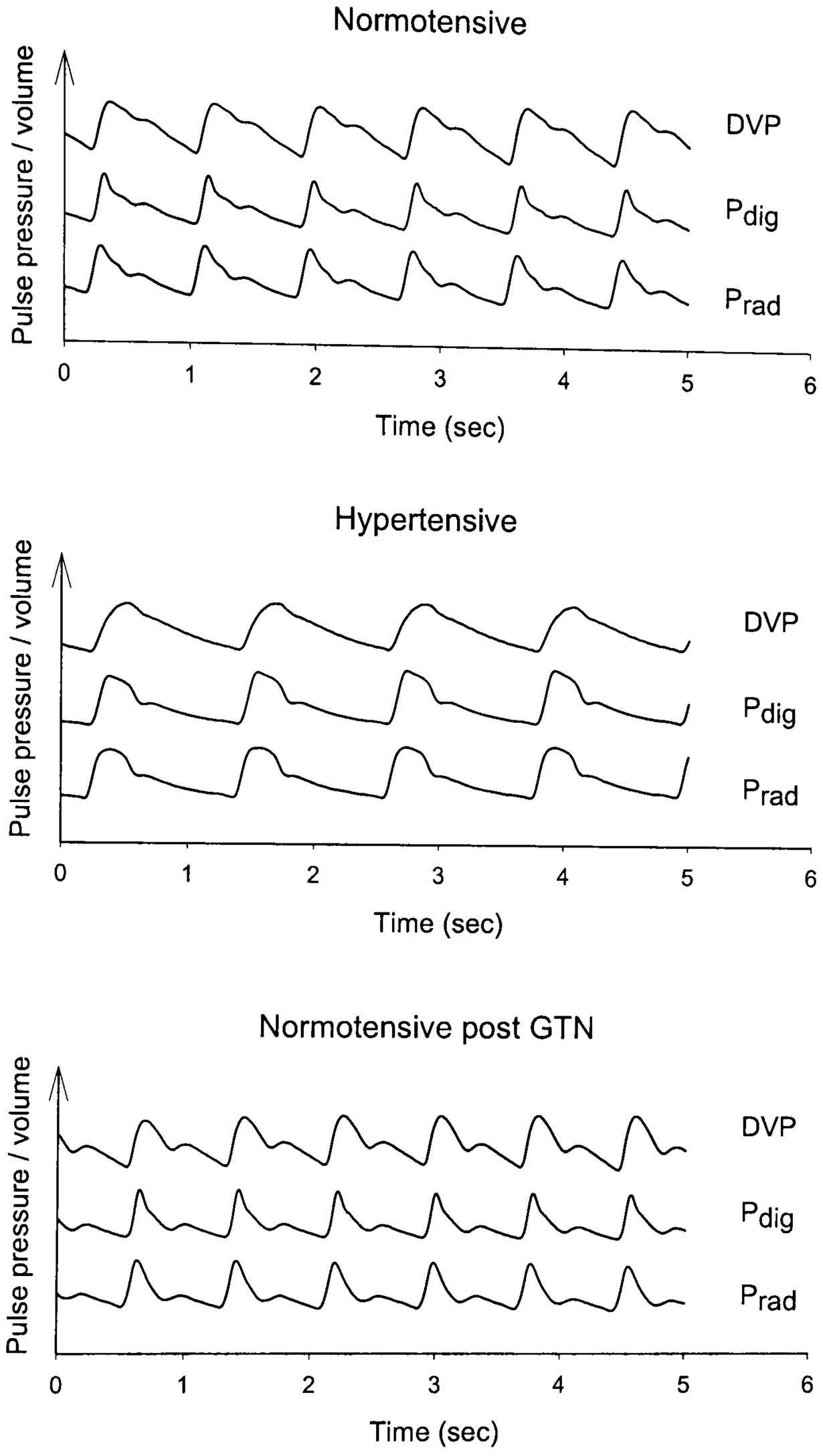

figure 27: DVP and pressure waveforms

Examples of the digital volume waveforms (DVP), digital pressure waveforms (P_{dig}) and radial pressure waveforms (P_{rad}) for normotensive and hypertensive subjects and in normotensive subjects after glyceryl trinitrate (GTN)

Following administration of GTN to a subset of the normotensive subjects, SBP fell by 1.2±6.0 mmHg (P=NS) and DBP by 5.2±3.8 mmHg (P<0.001). Figure 28 shows the GTF for normotensive subjects before and after GTN and the GTF for hypertensive subjects. As they are similar, we calculated the mean general transfer function (MGTF) from GTFs derived from all subject groups (control normotensive, GTN normotensive and hypertensive subjects).

It has to be noted that the phase of the TFs are negative for frequencies above 4Hz. This does not represent a real time shift of the highest frequencies, but this is due to the process used to calculate the TF. As explained in section 10.4, TF were determined from averaged DVP and pressure pulses, which were arbitrarily aligned in time (with respect to the foot of the pulse). This is responsible for producing negative phase values.

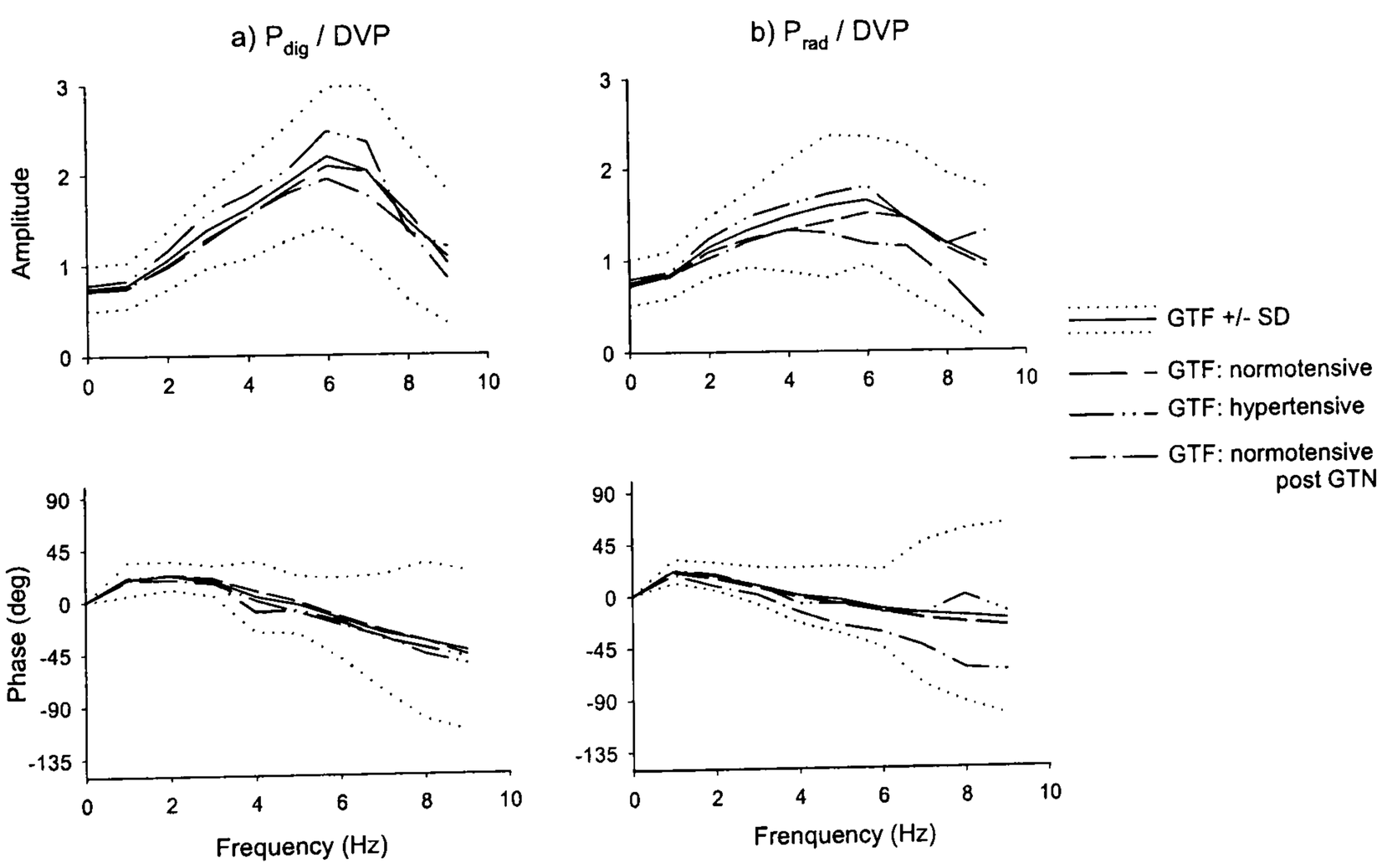

figure 28: GTF for normotensive and hypertensive subjects

Generalised transfer functions (GTF) relating a) digital artery pressure (P_{dig}) to the digital volume pulse (DVP) and b) radial artery pressure (P_{rad}) to the DVP in normotensive and hypertensive subjects and normotensive subjects after glyceryl trinitrate (GTN)

Pressure waveforms reconstructed from the DVP waveform with the MGTF are shown in figure 29. Transformed DVP waveforms were in close agreement with measured pressure waveforms in each artery. The RMS error between the transformed DVP and pressure waveforms was similar to the RMS error between the two pressure waveforms. For all subjects, the mean RMS error between transformed DVP and tonometer radial pressure signals was 4.4 ± 2.0 mmHg, and that between transformed DVP and Finapres digital artery pressure signals was 4.3 ± 1.9 mmHg. These errors did not differ significantly from the RMS error between the measured radial and digital pressure waveforms (4.4 ± 1.4 mmHg).

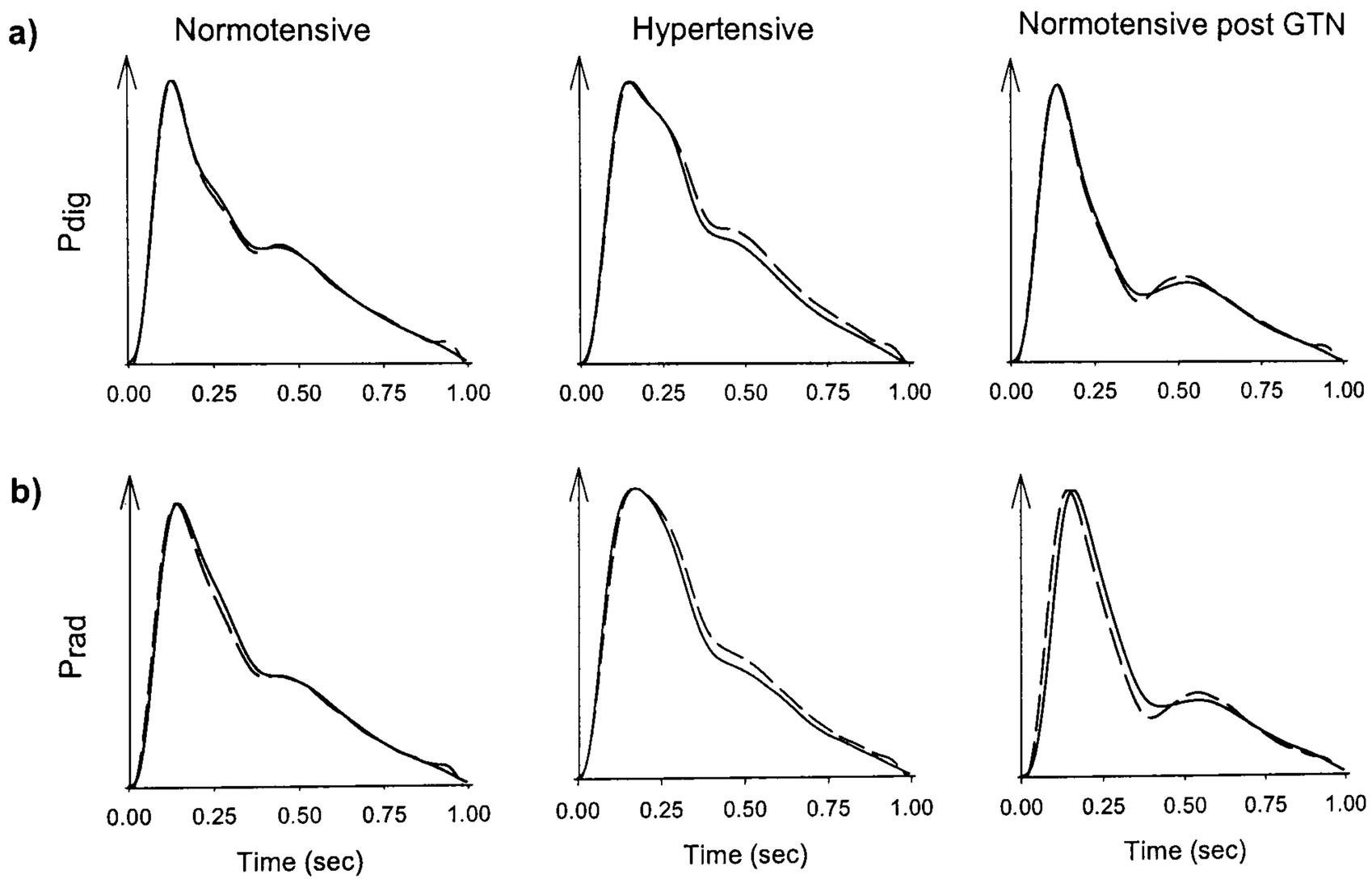

figure 29: Pressure waveforms predicted from the digital volume pulse

Averaged waveforms for a) the digital artery (P_{dig}) and b) the radial artery (P_{rad}) in normotensive, hypertensive and normotensive subjects after glyceryl trinitrate (GTN). The solid lines shows measured waveforms and the dotted lines waveforms predicted by applying a single generalised transfer function to the digital volume pulse(DVP).

4.5 Discussion

In the present study we obtained close agreement between waveforms derived from the tonometer and Finapres (RMS error = 4.4 ± 1.4 mmHg). Both instruments have been shown to provide waveforms, which closely approximate intra-arterial pressure[61;62]. The small discrepancy between the waveforms obtained from the Finapres and the tonometer reflects the limits of accuracy of these devices. Agreement between recorded pressure waveforms and waveforms reconstructed from the DVP using a single generalised transfer function (GTF) was similar to that between the tonometer and Finapres. Thus a simple TF can be used to transform the DVP into the pressure pulse. The accuracy of this TF is similar to the one obtained by Karamanoglu[55;58] and Chen[27] for the relation between peripheral and central waveforms. They found that TFs from peripheral pressure pulses to central pressure pulses are similar in different individuals and independent of effects of vasoactive drugs[27;58]. The TF from the DVP to peripheral pressure also remains constant, irrespective of the effects of hypertension or effects of vasodilation produced by GTN.

The relationship between DVP and pressure in the digital artery is determined by the impedance characteristics of vessels in the finger distal to the digital arteries. The constancy of the relationship between DVP and pressure in the presence of large changes caused by GTN suggests that effects of GTN on peripheral impedance characteristics of the finger are minor in comparison with changes in arteries in the lower body, which alter wave reflection.

In the present study, a frequency based TF approach was used. The use of a parametric TF has been shown to improve the stability and estimation in the prediction of central BP from peripheral pulse. A parametric approach to the relationship between the DVP and the pressure pulse might improve the goodness of fit but is very unlikely to alter the conclusion that the DVP and the pressure pulse contain the same information.

As the same information is contained in the pressure pulse and in the DVP, the physical properties altering the pressure pulse are very likely to produce the same effect on the DVP. The wave propagation and reflection theory should hence apply to the DVP. The following chapters will deal with the measurement of wave reflection and velocity from contour analysis of the DVP.

CHAPTER 5: Influence of vasoactive drugs on the DVP

5.1 Background

There is a wealth of data concerning the effect of vasoactive drugs, particularly organic nitrate, on the DVP[14;23;44;65;78;89;123;128;139;140;151]. Despite this, the physical properties of the arterial tree determining the change in the DVP induced by drugs is poorly understood. Effects of nitrates on the DVP, have been variously attributed to local effects, changes in pre-load[128], changes in cardiac output[128] and changes in arterial tone[65].

In the previous chapter, it has been shown that the DVP and the pressure pulse are related by a generalised transfer function (GTF) independent of individual variation and interventions. So, the DVP contains the same information as the pressure pulse and it is thus most likely that the DVP is influenced like the pressure pulse by pressure wave transmission and reflection. Like the pressure pulse, the first peak of the DVP will then correspond to a direct wave travelling from the heart to the finger and the second peak to a wave reflected from the lower body as shown in figure 30. The amplitude of the reflected wave (the 2nd peak) will depend on the amount of reflection. The time delay between the direct wave (1st peak) and the reflected wave (2nd peak) will be determined by the speed of wave propagation (PWV). In the pressure pulse, effects of nitrates are attributed to a reduction in pressure wave reflection. Nitrates will therefore be expected to influence the DVP by reducing the height of the second peak. This is indeed the case with many observers reporting an

increase in "dicrotism of the DVP": a reduction in the height of the second peak and increase in the intervening "notch" between the 1st and 2nd peak.

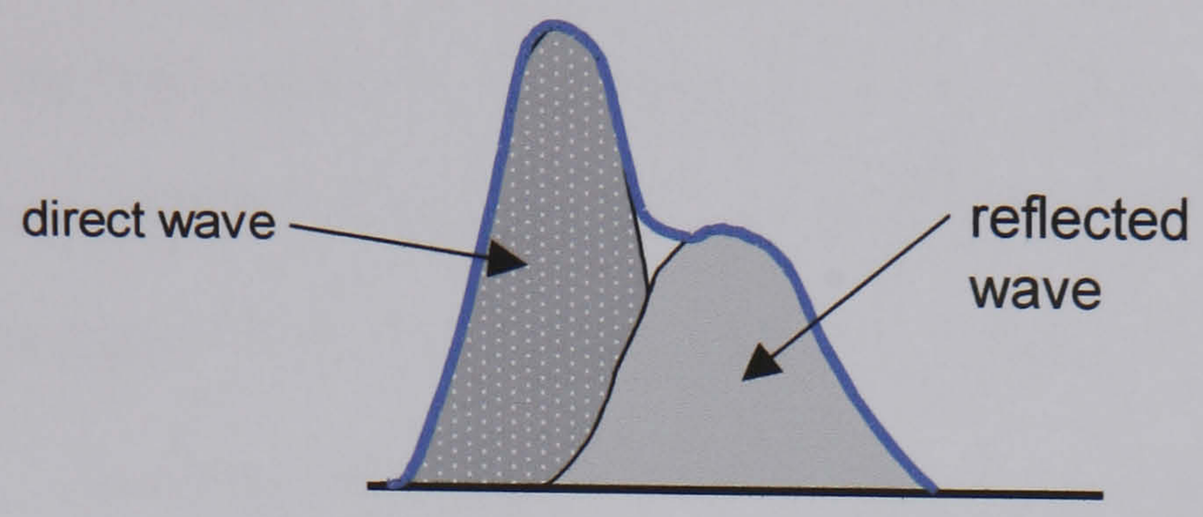

figure 30: Summation of the direct and reflected wave.

5.2 Definition of RI, a reflection index

The "dicrotic index" described by Morikawa might better be termed a reflection index. In this chapter, the use of a reflection index (RI) defined as $RI = \frac{b}{a} ? 100$ where b is the amplitude of the second wave and a the total amplitude of the pulse, is explored. This definition is not new as it has previously been used to measure effects of nitrate poisoning and other vasoactive drugs [78;94;95;151].

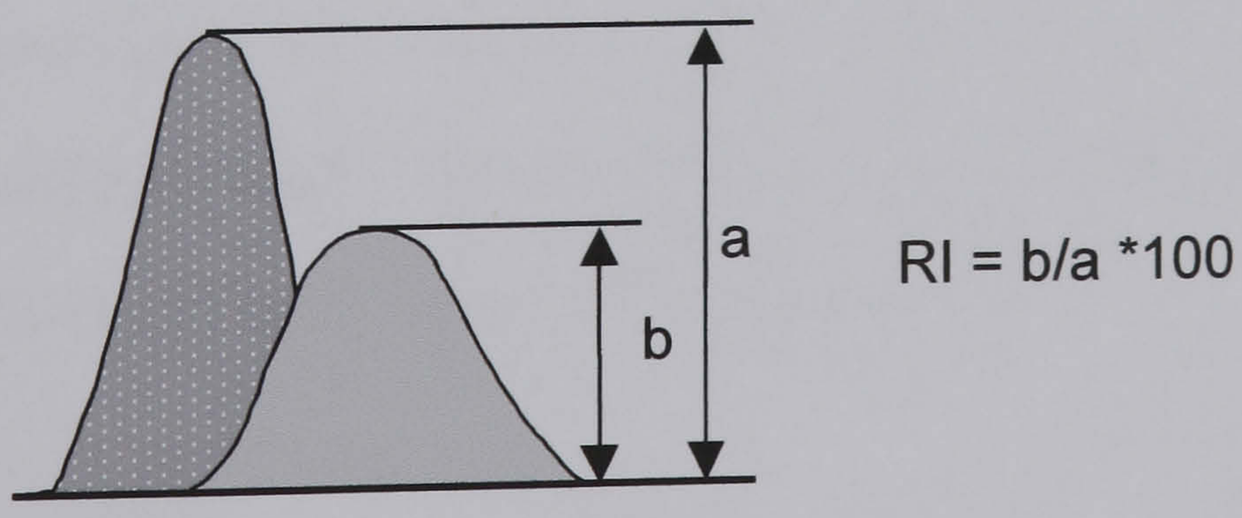

figure 31: RI definition.

5.3 Aims

The aim of this chapter was to examined the influence of vasoactive drugs on the DVP. Local intra-arterial infusions were studied to verify that the characteristics of DVP contour are not influenced by local effects. The influence of the vasodilator GTN and the vasoconstrictor angiotensin II on RI was then studied. To determine whether effects of these drugs are mediated predominantly by changes in large or small arteries, aortic pulse wave velocity and BP will be measured as well.

5.4 Study 1: Local effects

5.4.1 Methods

To check if RI could be affected by local changes in arterial characteristics, GTN was infused in the right brachial artery using a 27-gauge steel needle (Coopers Needleworks, Birmingham, UK). After baseline measurements, during infusion of saline alone, 4 cumulative doses of GTN (0.1, 0.3, 1.0 and 3.0 μg/min, David Bull Laboratories, Australia) were infused each for 5min. Forearm blood flow was measured in both arms by venous occlusion strain gauge plethysmography[142]. The mean of 5 venous occlusions during the last 2 min of each infusion period were used for analysis. The DVP was

measured simultaneously from the index finger of the left and from the right hand and was recorded immediately after forearm blood flow measurements.

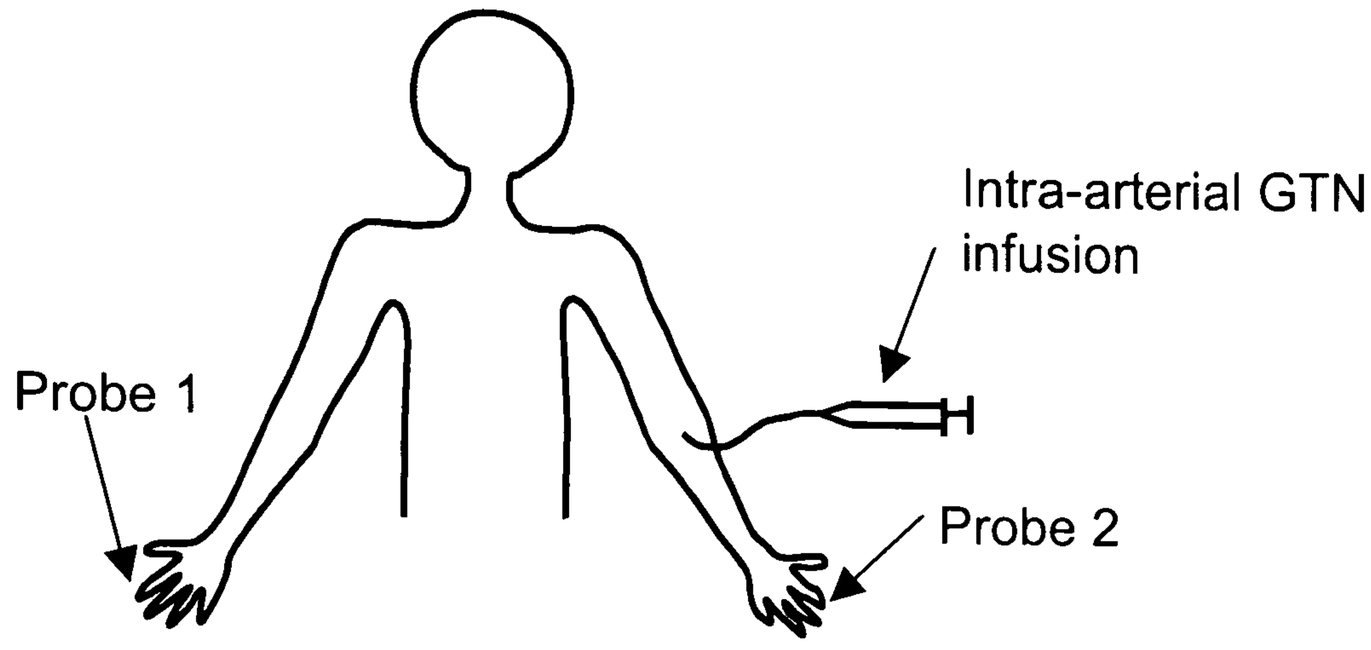

figure 32: Protocol to examine effects of local vasodilation on RI.

RI was calculated from the DVP with the algorithm explained in section 10.2.2. Briefly, when the DVP exhibits a defined peak, RI was defined as the height of the local maximum of the DVP downslope (figure 33, left panel) divided by the amplitude of the DVP. With ageing and vascular diseases, as observed by several authors[34;36;71], the second peak may disappear and only an inflection point on the downslope of the DVP is observable. In that case, RI is defined as the height of the inflection point (local maximum of the first derivative, figure 33, right panel) divided by the amplitude of the pulse.

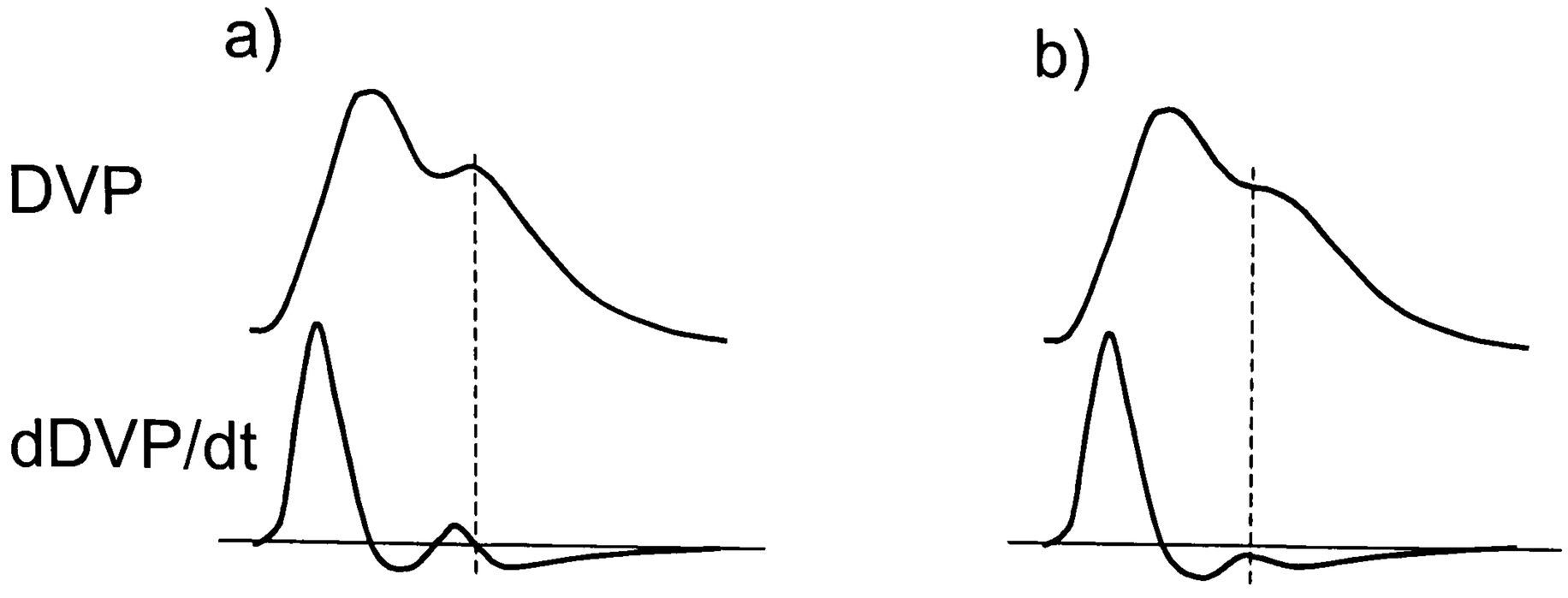

figure 33: Definition of the 2nd peak/inflection point

5.4.2 Results

Brachial infusion of GTN produced a small but significant fall in RI in both fingers. RI decreased from 60 ± 5.5 % to 53 ± 5.8 % ($P<0.05$) in the infused arm and from 63 ± 5.1% to 49 ± 6.3% ($P<0.05$) in the non-infused arm. The ratio of RI in the infused to that in the non-infused arm remained constant (figure 34). Forearm blood flow increased significantly in the infused arm from 9.8 ± 2.0 to 22.4 ± 2.4 ml/min per 100ml. There was no significant change in blood flow in the non-infused forearm. Thus the ratio of blood flow in the infused/non-infused forearm increased significantly (see figure 34, $P<0.001$ for comparison of blood flow ratio and RI ratio).

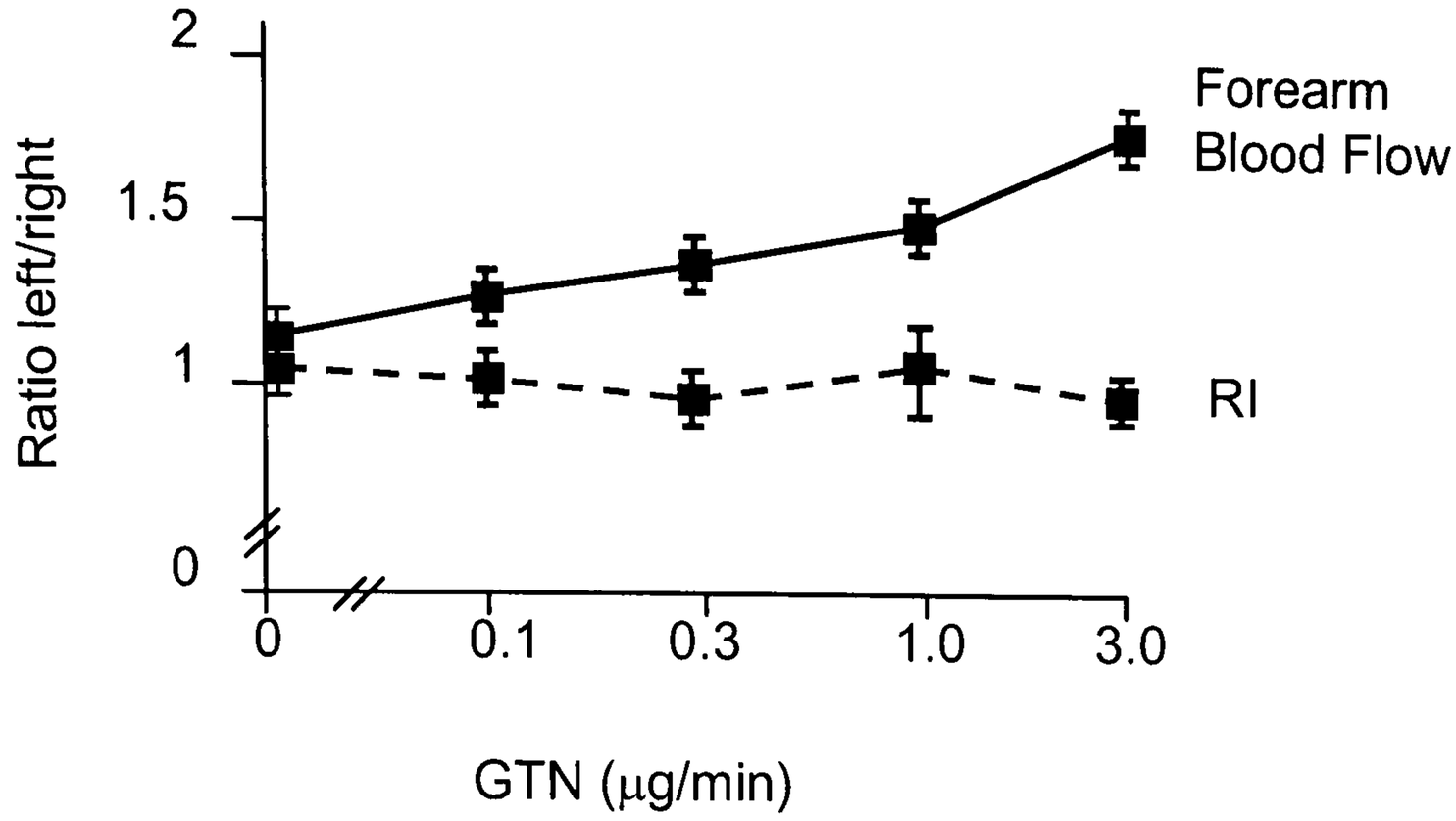

figure 34: Influence of GTN on RI and forearm blood flow
Ratio of left forearm blood flow and right forearm blood flow and ratio of RI from the DVP on the left hand and the right hand.

5.4.3 Discussion

Direct infusion of GTN into the brachial artery significantly increased total forearm blood flow in the infused arm compared to the non-infused arm but had no effect on the ratio of RI in the infused/non-infused arm. The highest dose of GTN was associated with a change in RI, but this change was of the same amplitude in both arms, suggesting that this was due to a systemic rather than a local effect. This suggests that the contour of the DVP is not determined by local effects in the arm.

5.5 Study 2: Influence of vasoactive drugs on RI and PWV

5.5.1 Methods

The influence of GTN, a vasodilator and angiotensin II, a vasoconstrictor, on the DVP was measured in 10 normotensive subjects (age: 31 ± 6.4 yrs, blood pressure: 120±13 / 62±4 mmHg, heart rate: 62±9 bpm, mean±SD). Subjects received saline vehicle, GTN and angiotensin II on 3 separate occasions according to a single-blind, randomised, 3 phase, placebo controlled, cross-over study. All subjects gave written consent for the study, which was approved by St Thomas' Hospital Research Ethics Committee. Subjects were cannulated on the right arm and were then allowed to rest for 30min. On the 3 separate days, subjects received intravenous infusions of saline for 15min and then 3 cumulative doses of GTN (3, 30 and 300 μg/min, David Bull Laboratories, Australia), angiotensin II (75,150 and 300 ng/min, Clinalfa, Germany), or 0.9% saline vehicle. The DVP and aortic PWV were measured as described in chapter 2. The mean of 3 measurements taken 5min apart during each 15min infusion period was used for analysis. BP was measured before each PWV measurements by the use of an automated oscillometric device (Dinamap 1846 SX, Critikon, US)

5.5.2 Results

During the infusion of saline vehicle, there was no significant change in HR, BP, PWV or RI. GTN decreased BP from 121±4 / 61±1 mmHg to 105±4 / 49±1 mmHg during the infusion of the highest dose ($P < 0.001$) (figure 36). HR increased from 64±4 to 80±4 bpm ($P<0.0001$). GTN produced a small but significant decrease in PWV (-0.74 m/s for the highest dose, $P < 0.05$) and a dose dependent decrease in RI of 32 ± 4.7% (% units) at the highest dose (figure 35 and figure 36).

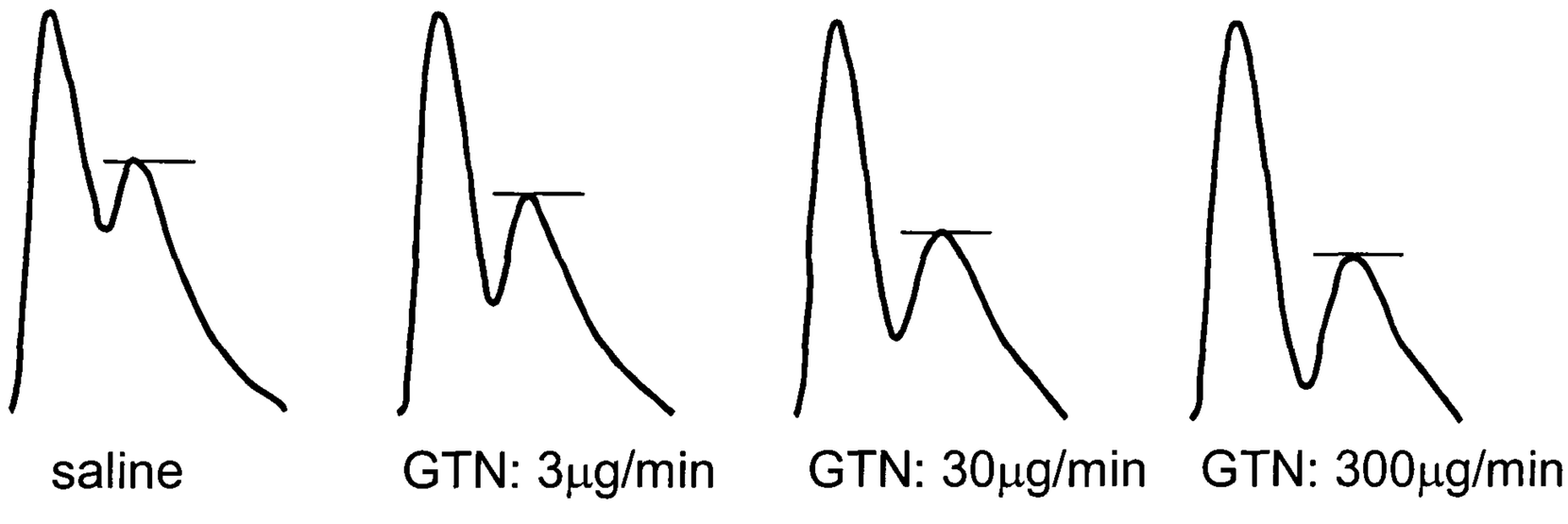

figure 35: Typical DVP after GTN in a healthy volunteer

Angiotensin II increased systolic and diastolic BP from 114±4 / 59±2 to 132±5 / 75±2 mmHg (each $P<0.0001$) without affecting HR. The change in PWV after angiotensin II infusion was small but significant (increase of 0.7 m/s for the highest dose. $P < 0.05$). Angiotensin II produced a dose dependent increase in RI (12.6 ± 2.1% for the highest dose) as shown in figure 37.

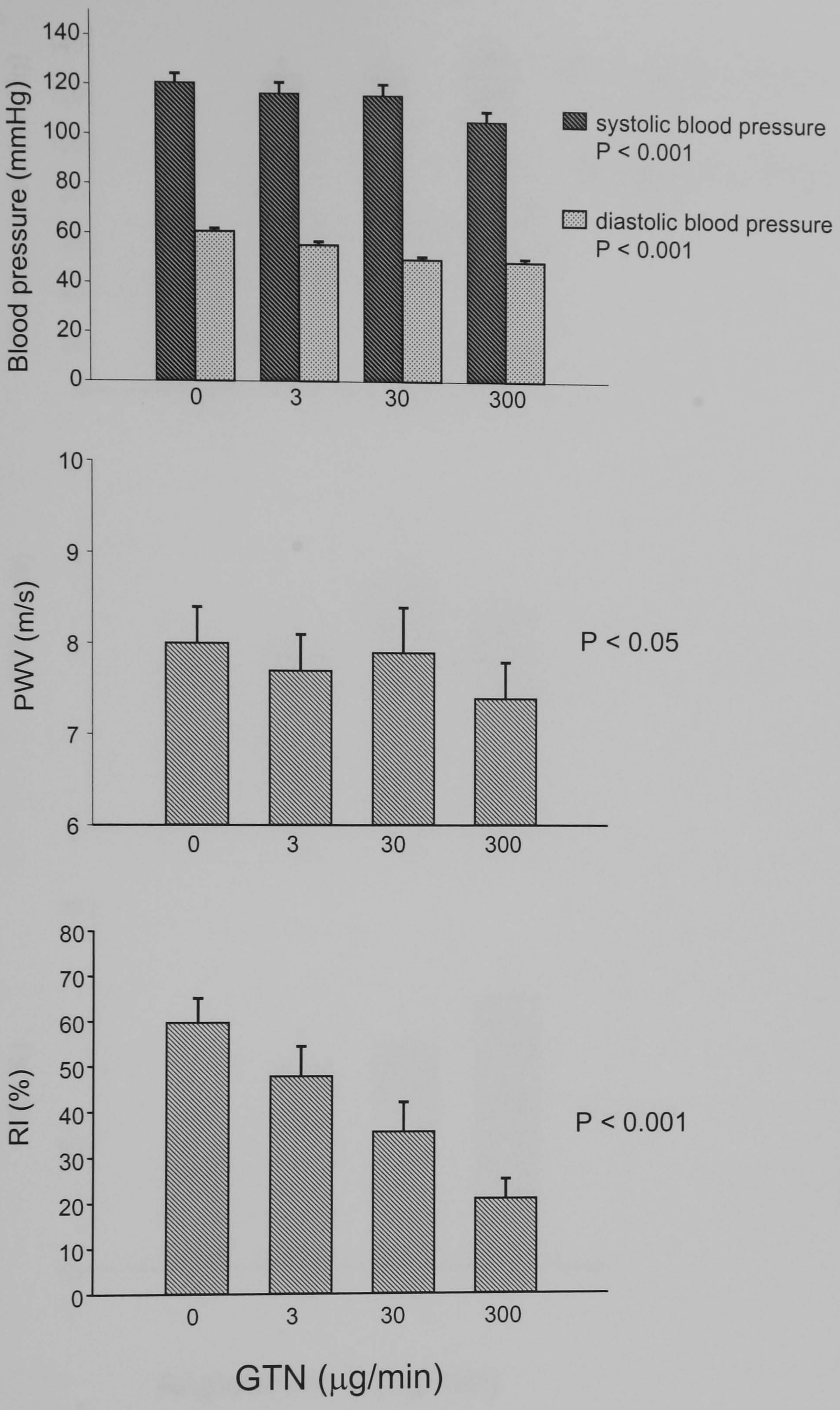

figure 36: Effect of GTN on blood pressure, PWV and RI.

P values refer to ANOVA for repeated measurements over the full dose range

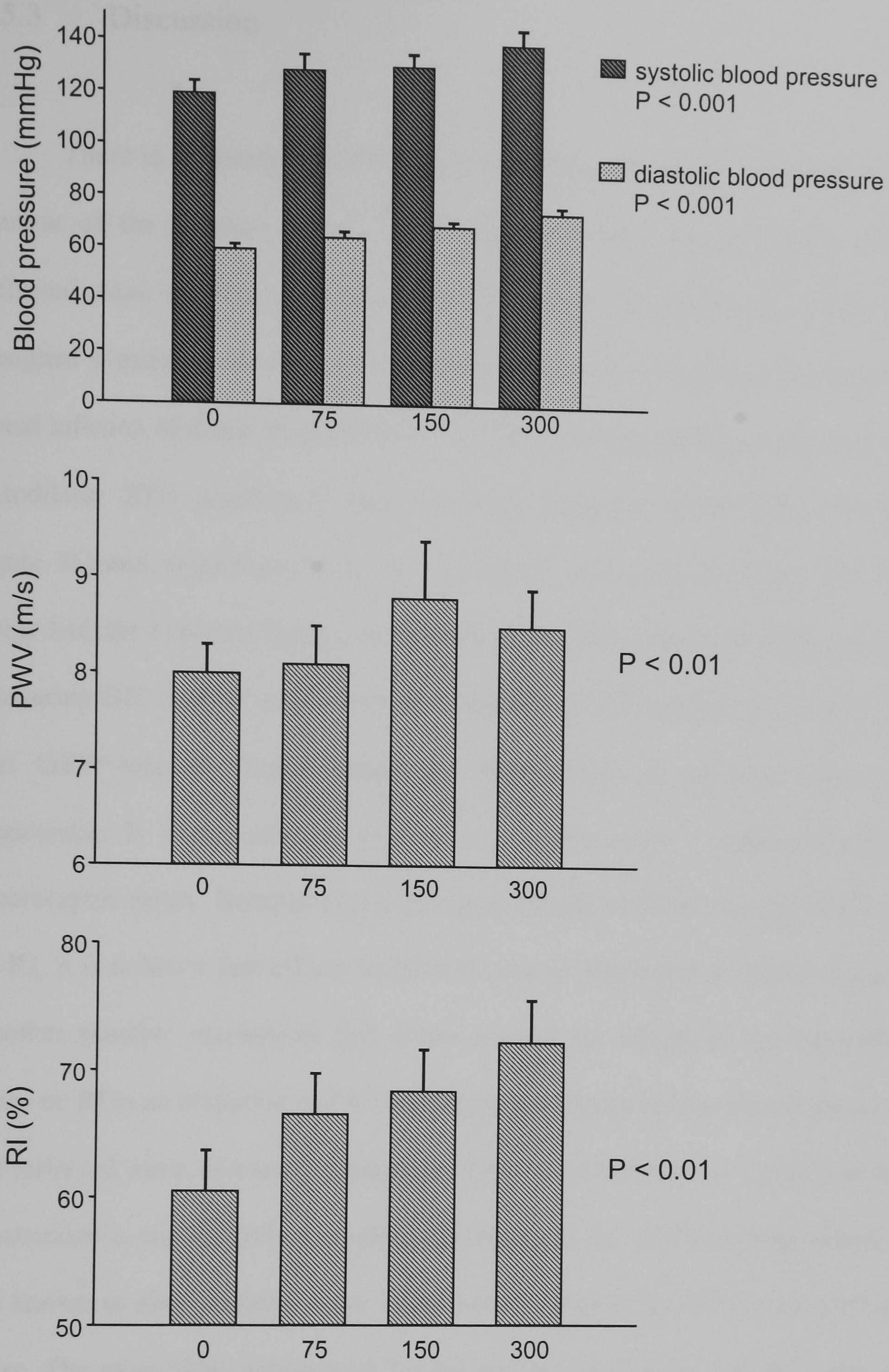

figure 37: Effect of angiotensin II on blood pressure, PWV and RI.
P values refer to ANOVA for repeated measurements over the full dose range

5.5.3 Discussion

There is an extensive literature on the effects of vasoactive drugs on the contour of the pressure wave[59;100]. Vasodilators reduce the amplitude of the reflected wave whereas vasoconstrictors increase its amplitude. This study was designed to examine the effect of a vasoconstrictor and a vasodilator on the DVP. Local infusion of drugs produced no effect. By contrast, systemic infusion of the vasodilator GTN produced a dose dependent reduction of RI (figure 35 and figure 36) and angiotensin II, a vasoconstrictor, increased RI (figure 37). The drugs had the expected effects on BP with GTN decreasing and angiotensin II increasing BP. Cardiac output was not measured in this study and it is possible that GTN reduced cardiac output by a reduction in pre-load. However, angiotensin II would also be expected to reduce cardiac output through a baroreceptor reflex. Because of the divergent effects of GTN and angiotensin II on RI, it is unlikely that effects on RI were due to alterations in cardiac output. Another possible mechanism that could account for effects of the vasoactive drugs on RI is an alteration in PWV resulting in a change in the time of arrival of the reflected wave. However, changes in PWV were minimal (< 1 m/s) and this mechanism is also unlikely to explain the change in RI. GTN and angiotensin II are known to alter pressure wave reflection as assessed by AIx in the pressure pulse. The most likely explanation for the present findings is, therefore, that an alteration in the amplitude of pressure wave reflection is responsible for the change in RI of the DVP. The major difference between AIx and RI is that AIx is caused by the addition of the reflected pressure wave with the direct pressure

wave in early systole whereas RI is influenced by the reflected wave in diastole/late systole. There may, therefore, be important differences in the estimation of pressure wave reflection by RI and AIx, AIx being more sensitive to the direct wave. RI is thus related to the amplitude of wave reflection. In the following chapter, the influence of the timing of the reflected wave will be studied.

CHAPTER 6: Estimation of large artery stiffness from the DVP: analysis of age and blood pressure related increases in large artery stiffness

6.1 Background

Ageing is accompanied by increased stiffness of large elastic arteries leading to an increase in pulse wave velocity (PWV)[8;9;21]. Premature arterial ageing as determined by an elevated aortic PWV is now recognised to be associated with risk factors for cardiovascular disease[5;16;17;69;72]. Furthermore, aortic PWV is an independent predictor of cardiovascular mortality in patients with end stage renal failure[17], in hypertensive subjects[20;69], patients aged more than 70 years of age[90], and in patients with glucose intolerance and diabetes[32].

An influence of vascular ageing on the contour of the peripheral pressure and DVP in the upper limb is also well recognised[7;60]. This change in pulse contour is likely to be due to an increase in large artery stiffness. An increase in arterial stiffness leads to an increase in PWV, decreasing the time taken for pressure waves reflected from the lower body to return to the aorta. Consequently, reflected waves arrive earlier within the cardiac cycle altering the contour of the pulse[104]. This raises the possibility that large artery stiffness may be assessed from the peripheral pulse, particularly from the DVP.

6.2 Definition of SI: an index of vascular stiffness derived from the DVP

The DVP is formed by the summation of a direct wave and reflected wave. The arm represents a common path, so the time delay between the direct

wave and the reflected wave is determined by the forward and backward propagation time along the aorta and large arteries (i.e. from the aorta to the major site of reflection and back). It is, however, not possible to measure the exact time of arrival of the reflected wave but the peak to peak time (PPT, figure 38), the time from the peak of the direct wave to the peak of the reflected wave should be a good approximation. In a previous small study (n=20), PPT was shown to be closely correlated with the pressure wave transit time from the root of the subclavian artery to the aortic bifurcation[29] ($R=0.75$, $P<0.0001$, figure 39). PPT was approximately 4 times the subclavian-iliac bifurcation transit time. Reflections arise from multiple sites but, to a first approximation, can be seen as a single reflected wave coming from an apparent site of reflection. O'Rourke et al. estimated this apparent site of wave of reflection to be mid-thigh[97;104]. The difference in path length of the reflected wave is hence approximately twice the distance from the aortic root to mid-thigh, approximately 4 times aortic length. This is close to the ratio observed between PPT and aortic transit time. The relation between PPT and aortic transit time thus supports the idea that PPT is a measure of the time taken for the direct wave to propagate to the site of reflection and back to the aortic root.

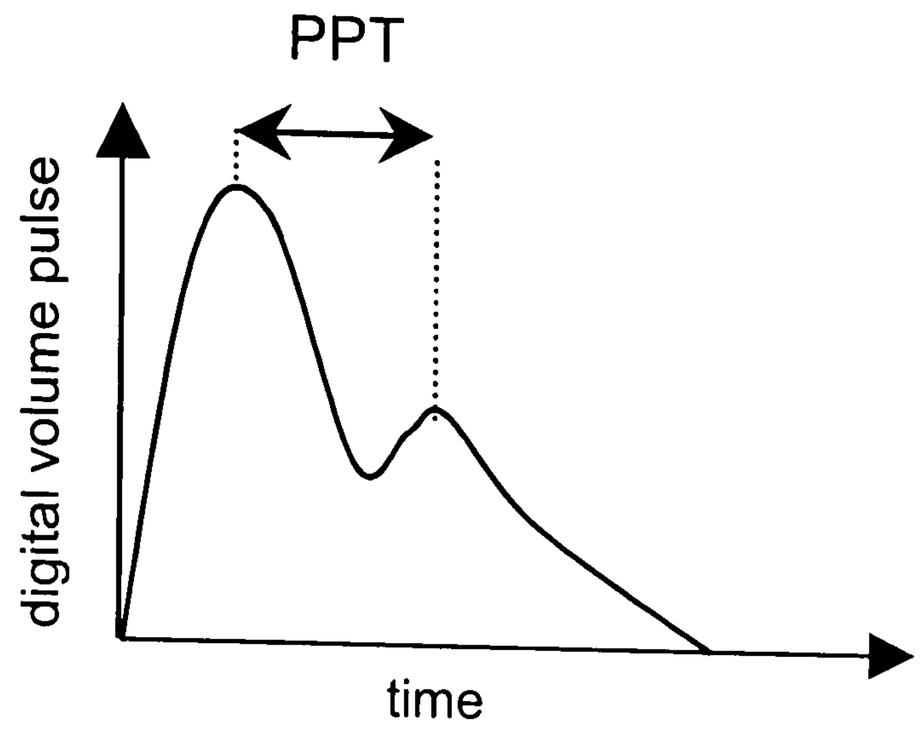

figure 38: PPT definition

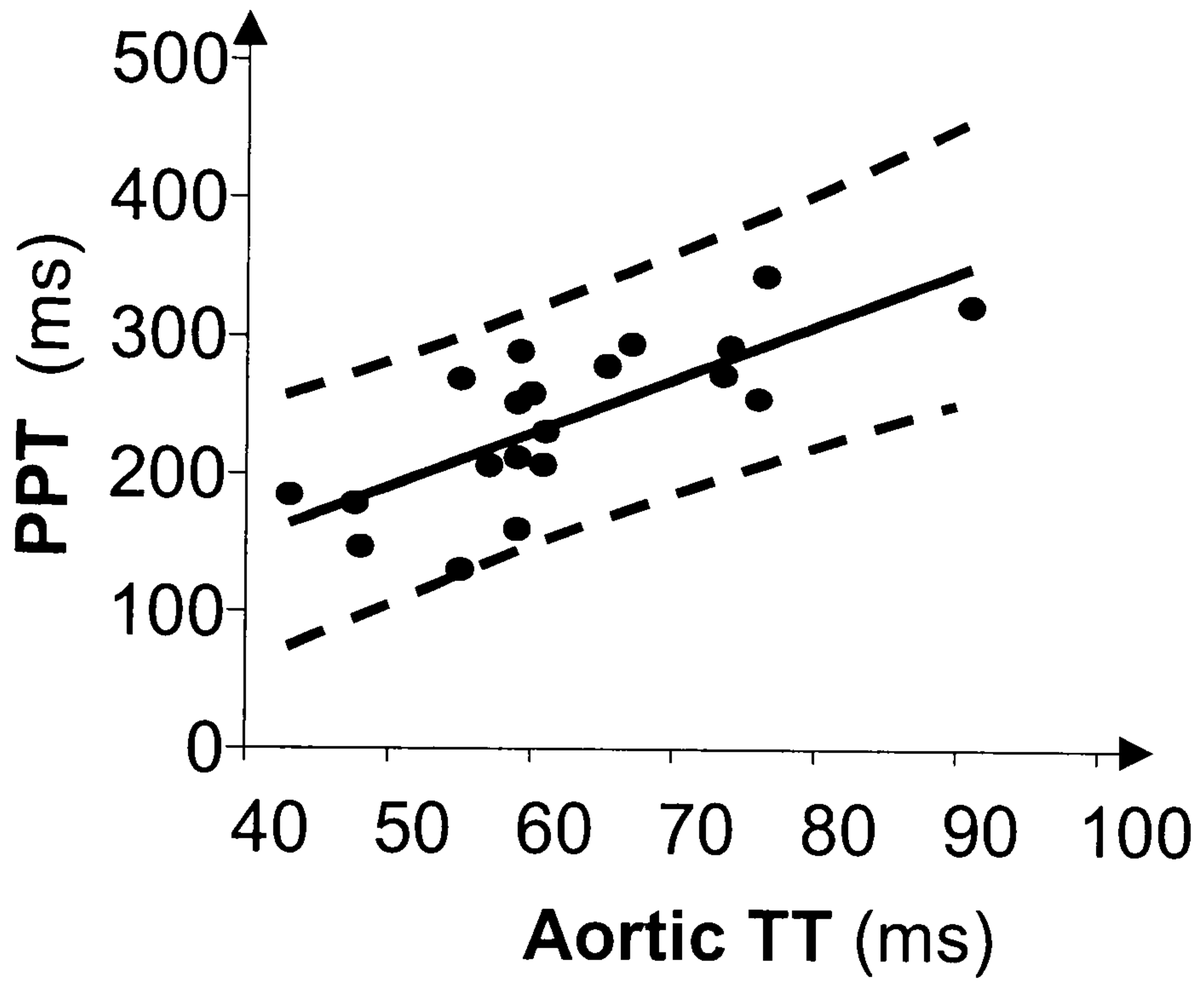

figure 39: Correlation between PPT and aortic transit time
R = 0.75, P<0.0001(from Chowienczyk et al. [29])

Peak to peak time (PPT) is thus an estimate of transit time from the aortic root to the point of reflection. PWV over this path could be estimated from path length/PPT. It is difficult to assess the exact length of the arterial path but, to a first approximation, it will be proportional to the height of the subject. For this

reason, a stiffness index (SI), was defined from the DVP as: $SI = \frac{height}{PPT}$. SI is hence expressed in m/s, in the same units as PWV, another measure of arterial stiffness.

6.3 Aims

The aim of this chapter was to examine the relationship of SI to age and BP in asymptomatic subjects and compare it with measurements of aortic PWV. To examine the sensitivity or lack thereof of SI to changes in tone of small arteries, glyceryl trinitrate (GTN) was used. GTN is known to markedly influences vascular tone[94] but has little effect on large artery PWV [64].

6.4 Methods

Aortic PWV was determined by measuring carotid to femoral transit time using the Sphygmocor (AtCor, Australia) as described in section 2.3. The distance between the sternal notch and femoral artery was used to estimate the path length between the carotid and femoral arteries.

Reproducibility of SI and PWV was assessed in 8 healthy men (aged 22 to 51 years) by obtaining 3 measurements separated by one week but otherwise under identical conditions. SI and PWV were determined in 87 asymptomatic subjects (29 women, mean age 47 years, range 21 to 68 years). No subject had a previous history of cardiovascular disease and none were receiving vasoactive

drugs. All were screened by physical examination and routine biochemistry. Subject characteristics are tabulated in table 3.

	Mean	SD	Range
Age (years)	47	13.8	21 – 68
Female/Male	29/58		
Smokers/Non-smokers	15/72		
BMI (Kg/m^2)	25	3.6	18 – 36
Diastolic BP (mmHg)	74	9	51 – 92
Systolic BP (mmHg)	125	15	91 – 178
T-cholesterol (mmol/L)	5.1	1.1	3.1 – 7.6
Triglycerides (mmol/L)	1.6	1.0	0.5 – 4.7
HDL-cholesterol (mmol/L)	1.5	0.4	0.8 – 2.5

table 3: Subject characteristics

Following at least 15 minutes resting semi-supine, 3 consecutive measurements of SI and aortic PWV were made. BP was taken as the mean of 3 measurements obtained using a mercury sphygmomanometer. Mean arterial pressure (MAP) was calculated from diastolic pressure plus one third of the pulse pressure.

Effects of vasoactive drugs on SI_{DVP} and PWV

The contour of the DVP is markedly influenced by tone in muscular arteries[29]. If SI is to provide a useful measure of stiffness in large elastic arteries it is important to establish to what extent it is sensitive to changes in smooth muscle tone. Effects of the vasodilator GTN were therefore examined in 9 healthy normotensive men aged 23 to 45 years. Subjects attended on two days according to a single blind, randomised, 2-phase, placebo controlled crossover

study design. Following 30 min resting supine, subjects received an intravenous infusion of saline for 15 min and then, on separate days, intravenous infusions of GTN (3, 30 and 300 μg/min, each dose for 15 min) and 0.9 % saline vehicle. PWV and SI were determined at 5 min intervals during the baseline period and at the end of each 15 min infusion of drug/vehicle.

The above protocols were approved by St Thomas' Hospital Research Ethics Committee and all subjects gave informed consent.

Statistics

Subject characteristics are presented as means±SD, other results as means±SE. Reproducibility was expressed as the mean WSD and WCV (see section 2.5). Associations between SI and age, BP and total serum cholesterol and between PWV and these variables were examined using univariate and multiple regression analysis. Because of co-linearity and because SBP and pulse pressure are influenced by arterial stiffness the only BP measurement used in multiple regression analysis was MAP. Effects of drugs on haemodynamic measurements were examined using analysis of variance for repeated measures.

6.5 Results

6.5.1 Reproducibility

The mean value of SI in all subjects (8.4 m/s, n=87) was of similar magnitude to that of aortic PWV (9.3 m/s). The mean within-subject standard deviations of SI and PWV in the subset of subjects who participated in the reproducibility study (n=8) were 0.062 m/s and 0.068 m/s respectively. Within-subject coefficients of variation were 9.6% and 8.8% for SI and PWV respectively (P = NS).

6.5.2 Relationship between SI, aortic PWV, age and blood pressure

Typical DVP traces in subjects of differing age are shown in figure 40. SI was correlated with PWV (R=0.65, P<0.0001). A slightly higher correlation was obtained between PPT and aorto-femoral transit time (R=0.70, P<0.0001). By univariate analysis SI was significantly correlated with age (R=0.67, P<0.0001), SBP (R=0.32, P<0.01), DBP (R=0.48, P<0.0001), MAP (R=0.45, P<0.0001) and total cholesterol (R=0.41, P<0.01) but not with pulse pressure. PWV was significantly correlated with age (R=0.67, P<0.001), SBP (R=0.47, P<0.0001), DBP (R=0.44, P<0.0001), MAP (R=0.50, P<0.0001) and correlated weakly with pulse pressure (R=0.25, P<0.05) but not with total cholesterol.

Multiple regression analysis demonstrated SI and PWV to be independently correlated with age and MAP (figure 41, R=0.69 and R=0.71 for SI and PWV respectively, each $P<0.001$ for age and $P<0.05$ for MAP). Regression coefficients relating SI and PWV to age (0.86 and 0.80 $m.s^{-1}.years^{-1}$ for SI and aortic PWV respectively) and to MAP (0.042 and 0.042 $m.s^{-1}.mmHg^{-1}$ for SI and aortic PWV respectively) were similar.

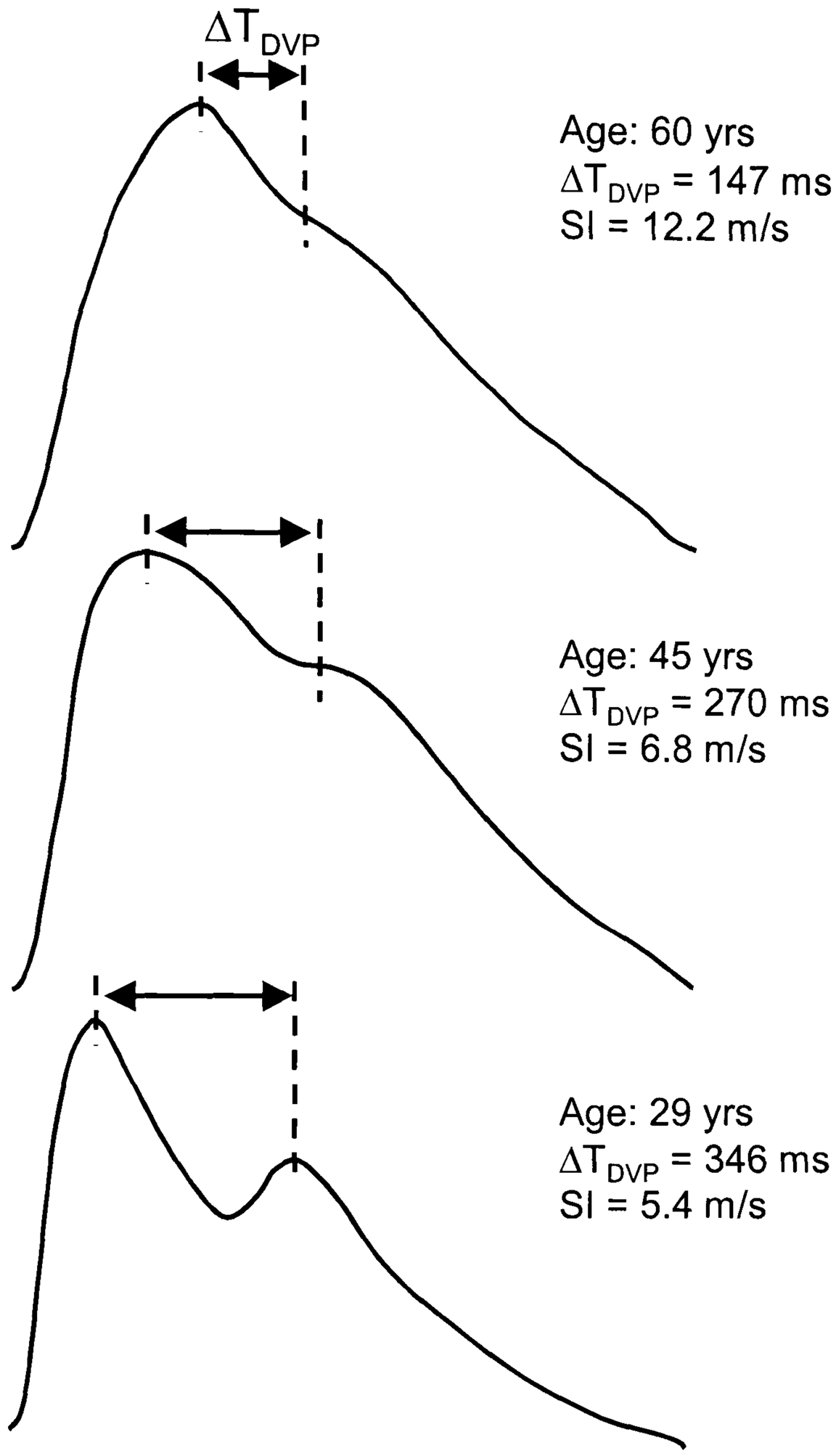

figure 40: Typical digital volume pulse (DVP) waveforms recorded in normotensive men showing the contour change with age

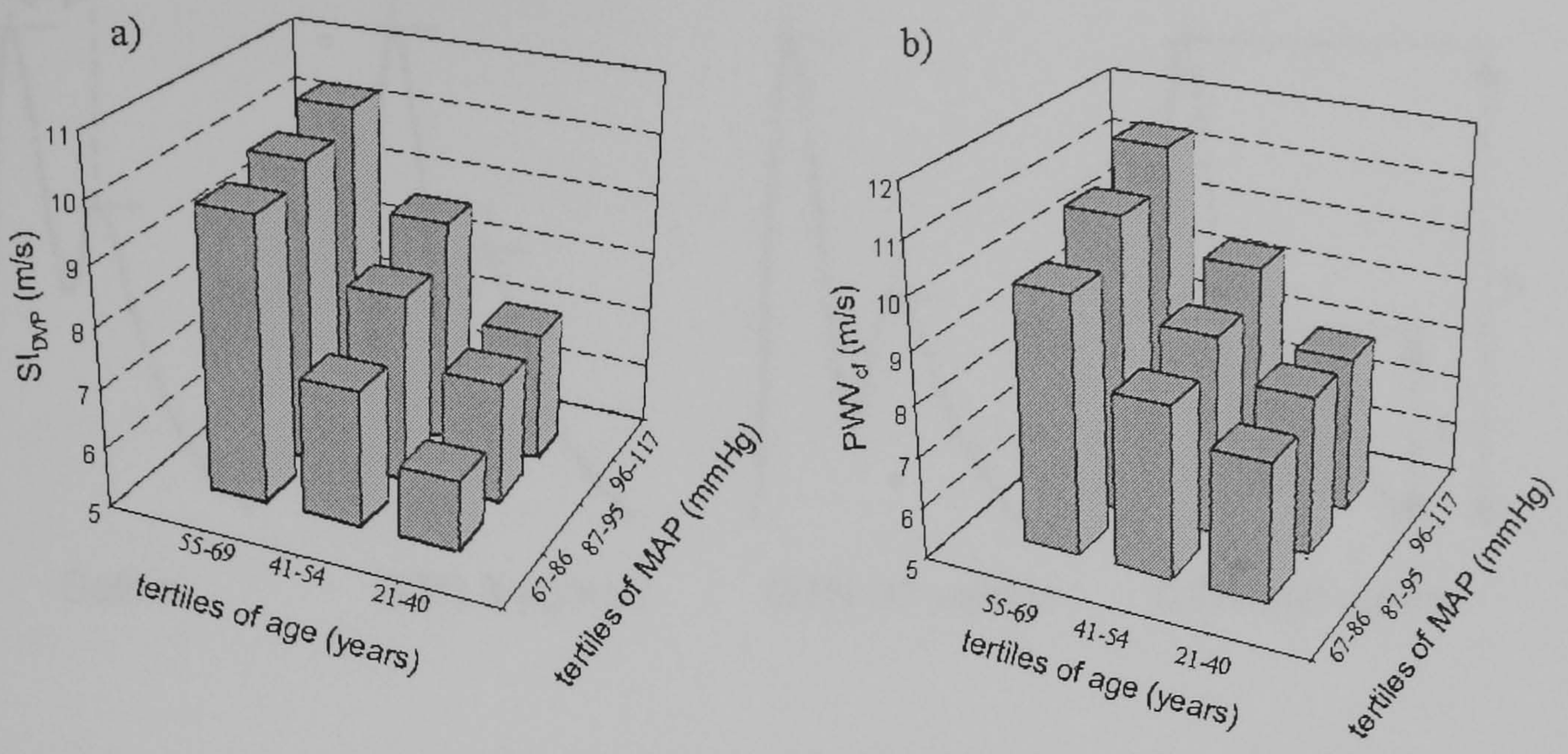

figure 41: Association of SI and PWV with age and MAP

6.5.3 Effects of GTN on SI and aortic PWV

During intravenous infusion of saline vehicle there was no significant change in HR, BP, SI, or PWV. GTN decreased BP from 125±5/62±2 to 109±4/48±1 ($P<0.001$). GTN produced profound changes in the height of the diastolic peak of the DVP relative to the systolic peak (figure 42) reducing the second peak to systolic peak reflection index (RI) from 64±3 to 29±6% ($P<0.0001$). Effects on SI were relatively modest and of comparable magnitude to those on PWV (figure 43). GTN decreased SI by 0.9 m/s (from 6.5±0.19 at baseline to 5.3±0.27 m/s, $P<0.001$) at the highest dose and PWV by 0.9 m/s (from 8.1± to 7.2 m/s, $P<0.05$) at the highest dose.

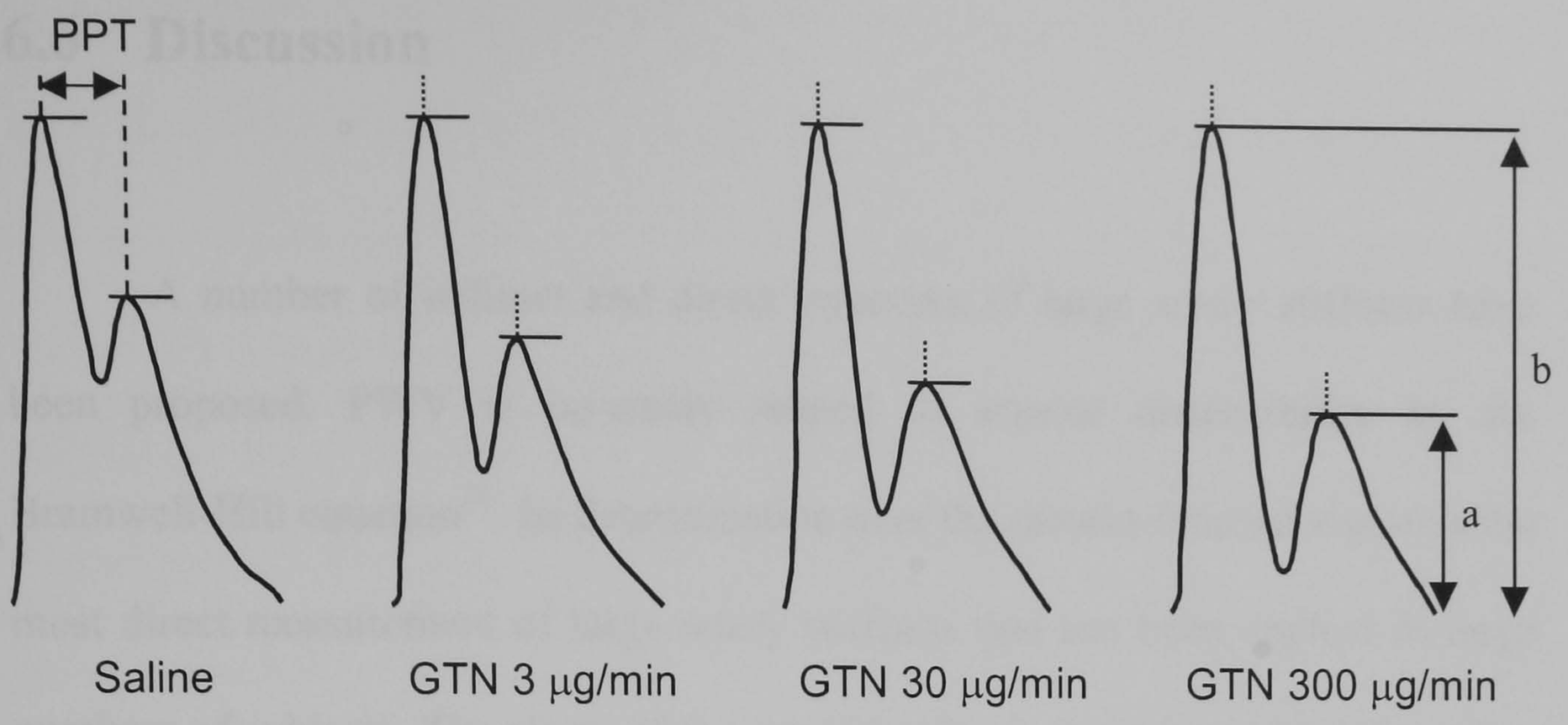

figure 42: Influence of GTN on SI

Effects of intravenous infusions of glyceryl trinitrate (GTN) on the digital volume pulse (DVP) in a healthy subject. The major change is the height of the diastolic component of the waveform (assessed by the reflection index RI=a/b) rather than time between the systolic and diastolic peaks (PPT) and hence in the stiffness index (SI).

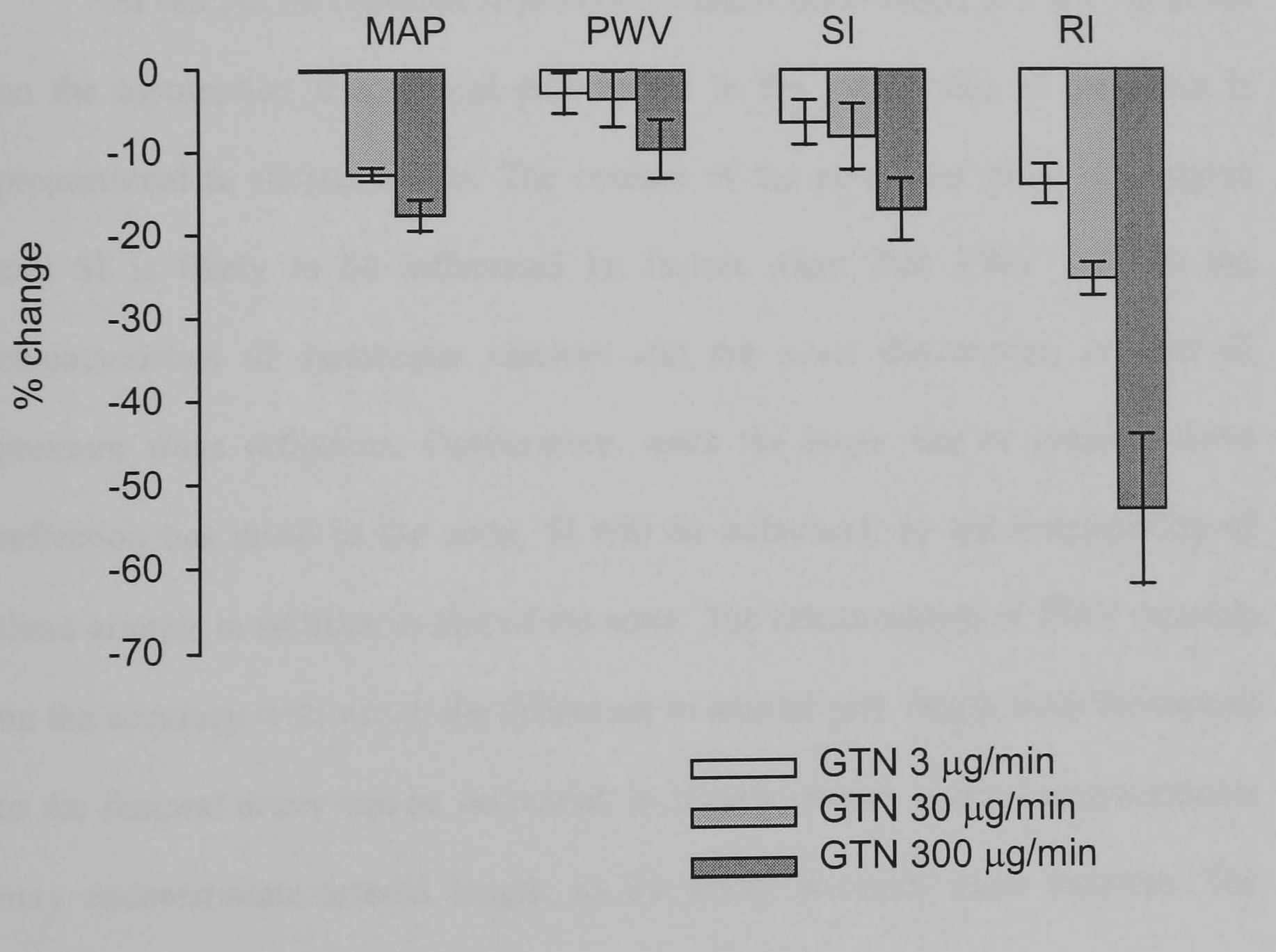

figure 43: Haemodynamic changes after GTN

Mean change from baseline(n=9) in mean arterial pressure (MAP), stiffness index (SI), aortic pulse wave velocity (PWV) and reflection index (RI) following glyceryl trinitrate (GTN).

6.6 Discussion

A number of indirect and direct measures of large artery stiffness have been proposed. PWV is inversely related to arterial distensibility by the Bramwell-Hill equation[21]. Its determination over the carotid-femoral region is the most direct measurement of large artery stiffness that has been applied in large numbers of subjects. The shape of the arterial pulse is determined by pulse wave velocity. On the aortic pressure pulse, the augmentation index (AIx) has been proposed as a measure of arterial stiffness[112;146]. However, although AIx exhibits a reasonable correlation with PWV under basal conditions, vasoactive drugs cause it to change markedly and independently of PWV[64].

SI can not be expected to provide identical information to PWV. SI relies on the assumption that arterial path length to the major sites of reflection is proportional to subject height. The contour of the peripheral pulse is complex and SI is likely to be influenced by factors other than PWV such as the characteristics of ventricular ejection and the exact distribution of sites of pressure wave reflection. Furthermore, since the major site of pressure wave reflection lies distal to the aorta, SI will be influenced by the distensibility of these arteries in addition to that of the aorta. The determination of PWV depends on the accuracy with which the difference in arterial path length from the carotid to the femoral artery can be estimated. In elderly people, surface measurements may underestimate arterial length, as the artery becomes more tortuous. The distance is also difficult to estimate accurately in obese subjects.

Despite these reservations the correlation between SI and PWV is striking, being higher than that reported for other widely used indices of arterial stiffness such as systemic arterial compliance (SAC) for which the correlation with PWV has been reported as 0.47 in healthy subjects[73]. A slightly higher correlation was observed between transit time measured directly and PPT consistent with some inaccuracy in the determination of length contributing to the difference between SI and PWV. The similarity of the relationship between SI, age and BP with that between PWV, age and BP supports the concept that SI and PWV are influenced by similar factors. The similarity of these relationships suggests that variation between SI and PWV relates at least in part to experimental errors inherent in determining one or both of these measurements rather than to a systematic difference.

In addition to the timing of reflected pressure waves, the contour of the arterial pulse is influenced by the amplitude of wave reflection. Pressure wave reflection is dependent on vascular tone of small muscular arteries and vasoactive drugs may influence reflection independently of effects on large artery stiffness and hence PWV. To investigate whether such changes in reflection influence SI, effects of GTN on SI and PWV were examined. As expected, GTN caused large changes in the contour of the DVP but these were limited mainly to an alteration in the height of the diastolic component so that changes in PPT and hence SI were modest and of comparable magnitude to those of PWV. This supports the concept that SI is influenced predominantly by large elastic artery stiffness unlike AIx derived from the pressure pulse[64].

In conclusion, SI is correlated with PWV and varies with age and BP in similar manner to PWV. It is influenced by vasoactive drugs to a similar extent as is PWV. It may be a valuable index to assess large artery stiffness at least in asymptomatic subjects.

CHAPTER 7: Comparison of direct and second derivative analysis of the DVP

7.1 Background

Studies presented in chapter 5 and 6 suggest that the DVP can be used to assess effects of vasoactive drugs and of ageing. Interest in this application has also received much attention by investigators in Japan. Here, however, a completely different approach to the analysis of the DVP has been taken. Features of the second derivative of the DVP (the "acceleration photoplethysmogram", d^2DVP/dt^2) have been used to study the influence of vasoactive drugs[131;132] and the association with age[19;45;52;131;133], blood pressure (BP)[19;45] and pulse wave velocity (PWV)[45] and on the DVP (see section 1.4). Typically, the d^2DVP/dt^2 comprises 5 waves called the a, b, c, d and e waves as shown in figure 44. The relative heights of these waves (b/a, c/a, d/a and e/a ratios), particularly the d/a ratio, have been related to age, BP and actions of vasoactive drugs[19;133].

The main problem with this approach is that interpretation of these indices is not straightforward and it is difficult to relate them to biomechanical properties of the cardiovascular system.

7.2 Aims

The aim of this study was to compare the indices RI and SI derived from the DVP with indices derived from the d^2DVP/dt^2. The repeatability and reproducibility of these indices, their association with age and change in response to vasoactive drugs were studied.

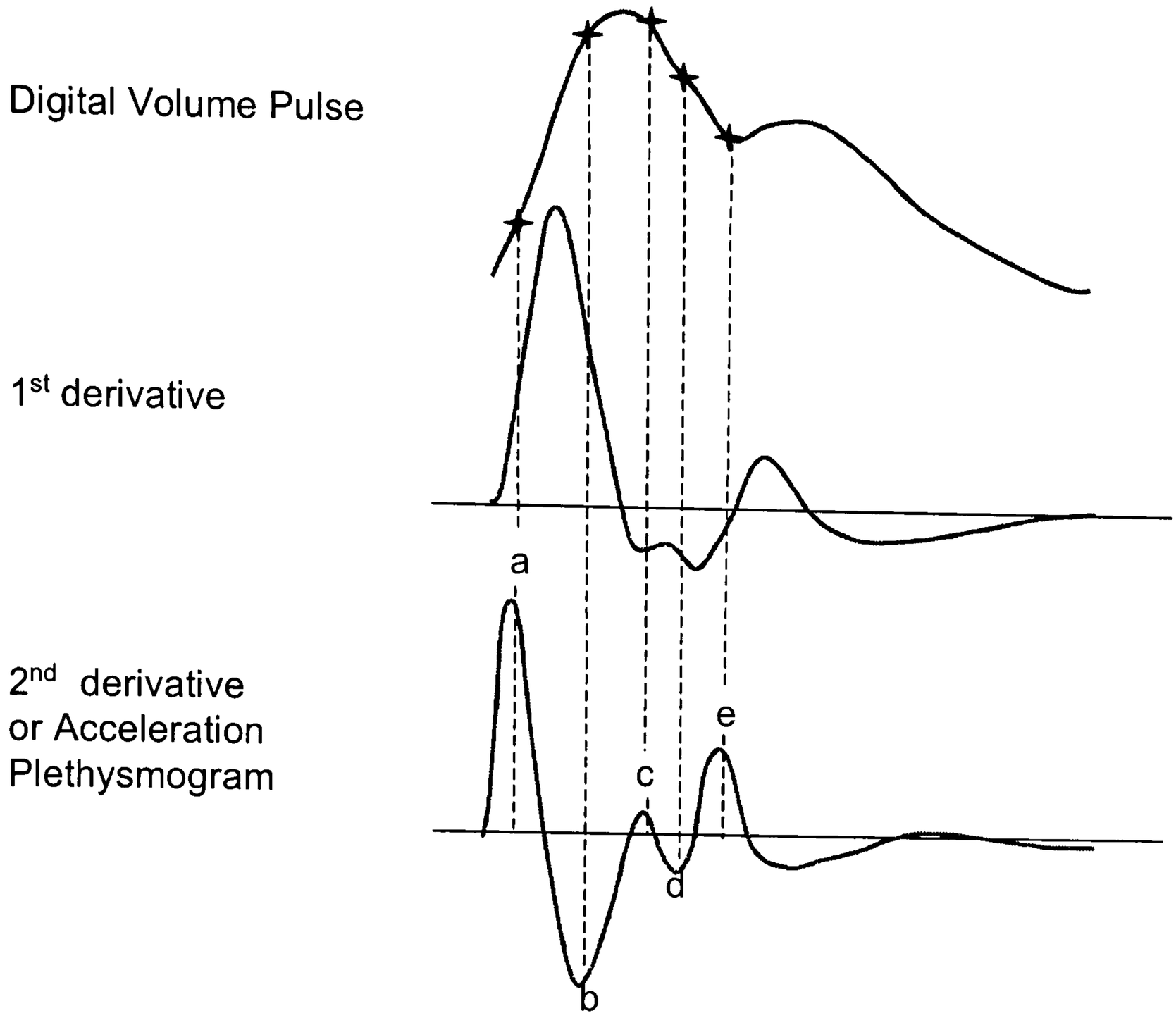

figure 44: 2nd derivative of the DVP

Definition of the a, b, c, d and e waves

7.3 Methods

The DVP was measured from the index finger of the right hand as described in section 2.2. Measurements were obtained with subjects supine after at least 20 min resting in a quiet temperature controlled clinical laboratory. DVP waveforms were recorded over at least 10 cardiac cycles and averaged to obtain a

single waveform from which RI and SI were calculated as previously described in sections 5.2 and 6.2.

To calculate the b/a, c/a, d/a and e/a ratios, the DVP signal was digitally filtered (low pass filter to remove the high frequency noise amplified by differentiation) and then differentiated twice to obtain the second derivative (d^2DVP/dt^2). The a-wave was defined as the maximum of the d^2DVP/dt^2. The b, c, d and e waves were determined as the 1st, 2nd, 3rd and 4th consecutive zero-crossings of the 3rd derivative after the a-wave (see figure 44). Cardiac cycles for which the a, b, c, d or e waves could not be identified were not analysed. The indices a, b, c, d and e were determined for each cardiac cycle and mean values from a minimum of 10 cycles used for analysis. Takazawa et al. described an ageing index defined as the (b-c-d-e)/a ratio[133]. This index was also calculated.

As differentiating is a high-pass filter process, the cut-off frequency of the low pass-filter could influence the shape of d^2DVP/dt^2 and in particular the relative height of the a, b, c, d, and e-waves. To test this, 3 different cut-off frequencies for the low pass filter were used: 10, 12 and 16 Hz. Previous investigators have used cut-off frequencies of 10 Hz [19] and 16 Hz [132].

The digital filter used was a Remez filter with passband frequency (Fp) and stopband frequency (Fs, as defined in figure 45) set to 10Hz, 12Hz or 16Hz and 12.5, 14.5 or 18.5Hz respectively.

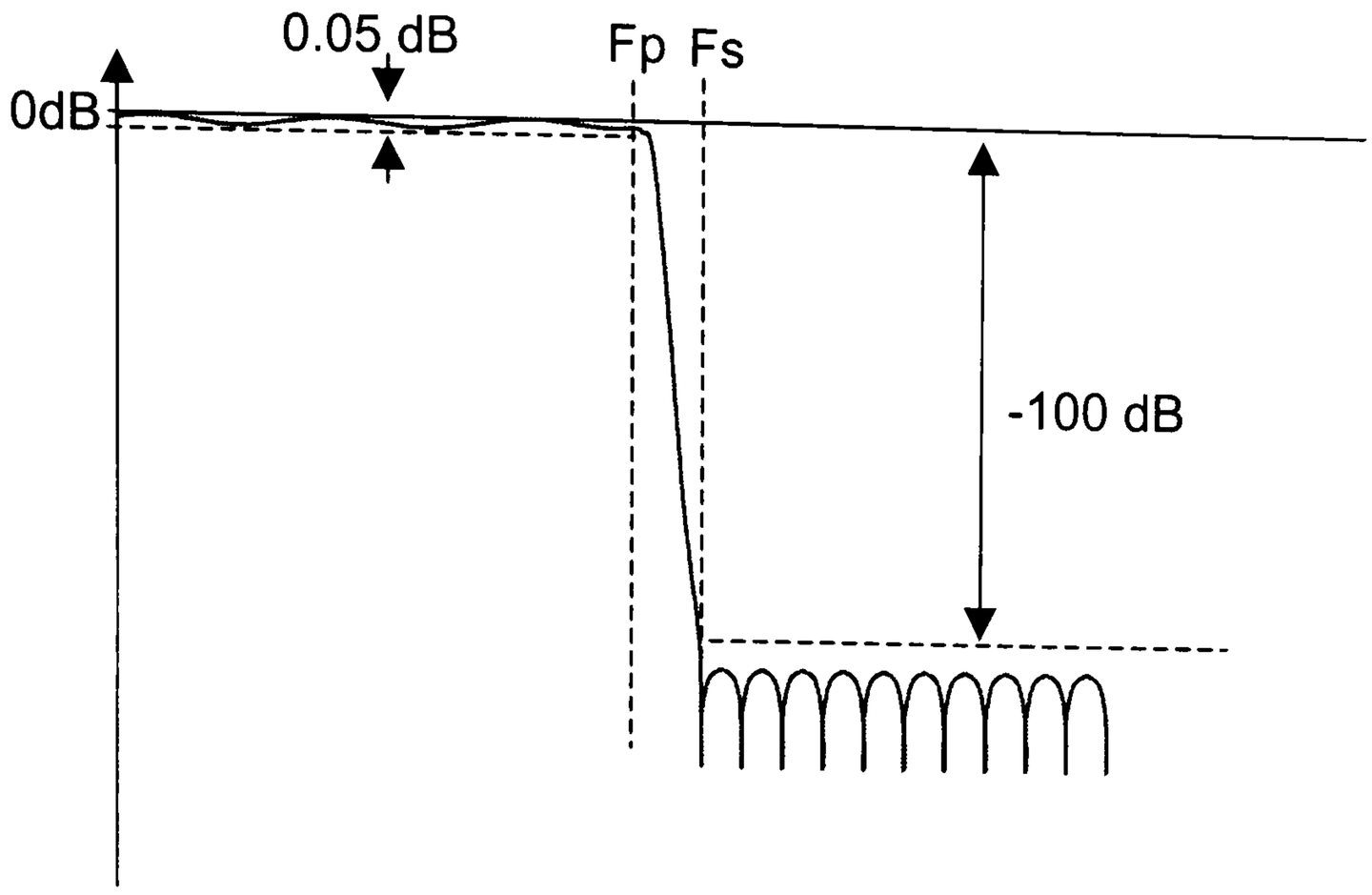

figure 45: Remez digital filter

Fp : Passband frequency, Fs : Stopband frequency

7.4 Study 1: repeatability and reproducibility

7.4.1 Methods

Eight healthy men (age: 31.5 ± 7 yrs, BP: 121±14 / 62±5 mmHg, means ± SD) attended on 4 different occasions separated by at least 3 days. The DVP and d^2DVP/dt^2 were obtained during 3 consecutive recordings after at least 20 min rest in a temperature control room.

Repeatability was assessed as the mean within-subjects standard deviation (WSD) of measurements obtained on the same day and reproducibility as the WSD of measurements made on different days. Repeatability and

reproducibility were also expressed as the within subject coefficient of variation (WCV) as described in section 2.5.

For measurements highly correlated with age (SI and d/a), the WSD was expressed in equivalent years of vascular ageing as determined from the slope of the regression lines relating SI to age and d/a to age.

WSD and WCV were calculated for indices obtained after the 3 different filters (10Hz, 12Hz and 16Hz) in order to investigate the influence of the cut-off frequency and to choose the optimum cut-off frequency for further analysis.

7.4.2 Results

As shown in figure 46, the cut-off frequency used in the filtering process significantly affects the values of the indices b/a and e/a derived form the d^2DVP/dt^2. Values of c/a and d/a are not so affected by the cut-off frequency used. RI and SI were independent of the cut-off frequency (values differed by less than 0.1%). Table 4 shows the reproducibility and the repeatability values of RI, SI and the indices derived from the d^2DVP/dt^2 after 10Hz filtering. The repeatability and reproducibility of RI and SI were not affected by the cut-off frequency of the digital filter. However, indices derived from the d^2DVP/dt^2 were less repeatable and less reproducible after filtering at 12Hz and 16 Hz than after filtering at 10Hz (data not shown) filtering.

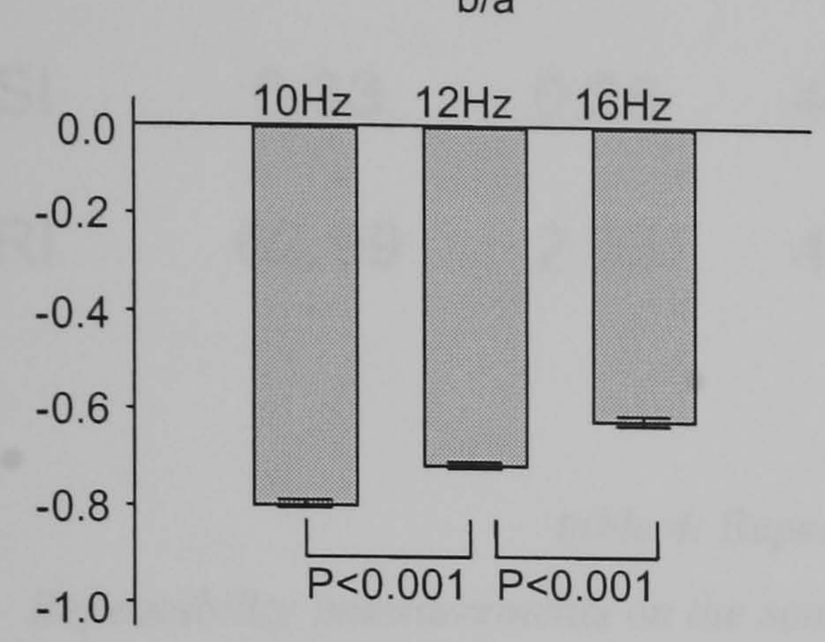

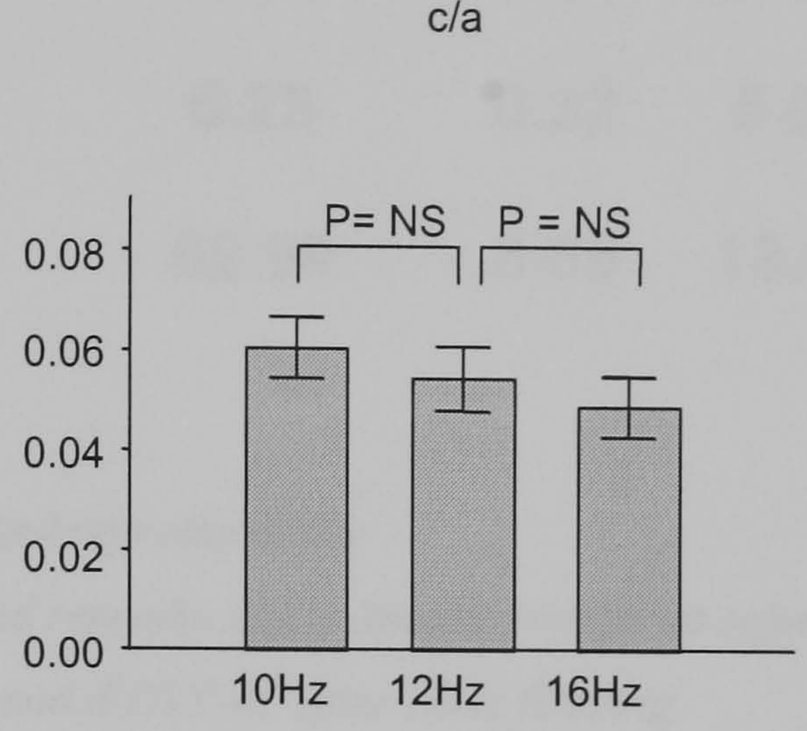

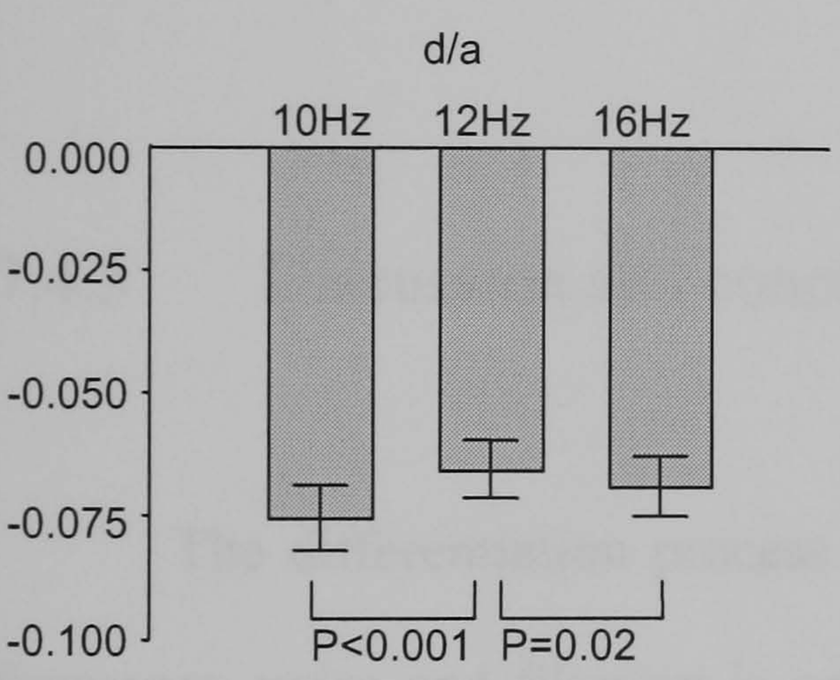

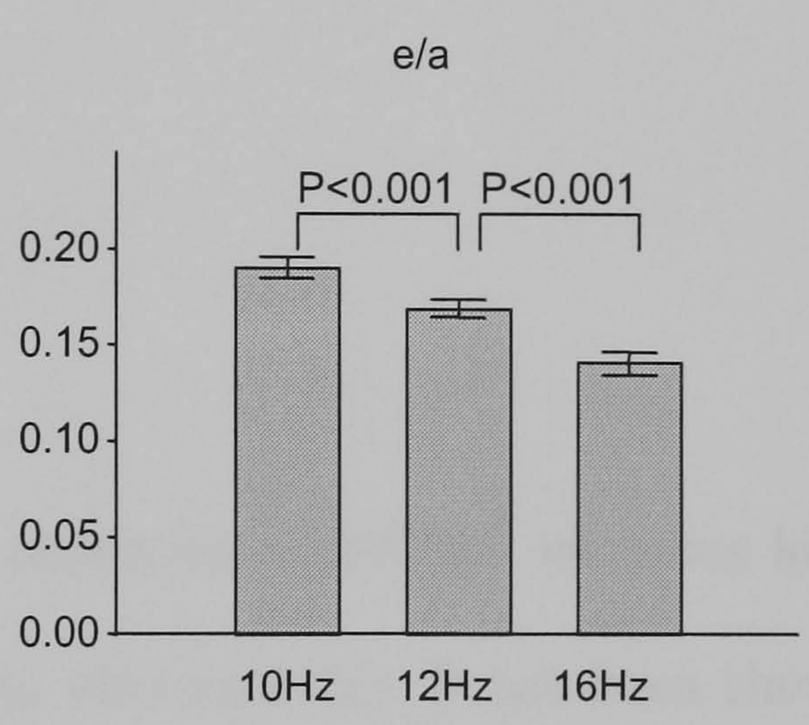

figure 46: d^2DVP/dt^2 indices obtained after different low-pass filters

Mean b/a, c/a, d/a and e/a indices using 10, 12 and 16Hz low-pass filtering.

	Repeatability			Reproducibility		
	mean	WSD	WCV	mean	WSD	WCV
b/a	-0.79	0.04	4.88%	-0.79	0.05	5.96%
c/a	0.06	0.02	33.64%	0.06	0.05	80.27%
d/a	-0.08	0.02	20.76%	-0.08	0.03	43.91%
e/a	0.19	0.02	12.23%	0.19	0.04	21.86%
SI	6.33	0.28	4.39%	6.23	0.32	5.08%
RI	62.99	2.93	4.65%	62.99	8.69	13.80%

table 4: Repeatability and reproducibility

Repeatability (measurements on the same day) and reproducibility (measurements on separate days) of indices derived from the DVP and d^2DVP/dt^2 after 10Hz filtering

7.4.3 Discussion and conclusion

The differentiation process used to obtain the d^2DVP/dt^2 increases high frequency noise and filtering is necessary to eliminate this. It has been shown that most of the information in the arterial pulse is contained in the first 10 harmonics[121]. For a HR of 60 beats per minutes, this means that most the information of the DVP is below 10Hz. However, the 2nd derivative is affected more by higher frequencies. Bortolotto et al. used a 10Hz low pass-filter[19] when assessing the d^2DVP/dt^2 whereas Takazawa et al. used a 16 Hz filter[132]. The results of this study show that the cut-off frequency does affect the indices derived from the d^2DVP/dt^2 (the b/a, c/a, d/a and e/a ratios) whereas RI and SI

from the DVP are not influenced by this. The detection of a, b, c, d and e wave is frequency dependent. However for d/a (the most used index) similar values are obtained using filter cut-offs of 10 and 16Hz. With higher frequency cut-offs, signal noise increases (figure 47).

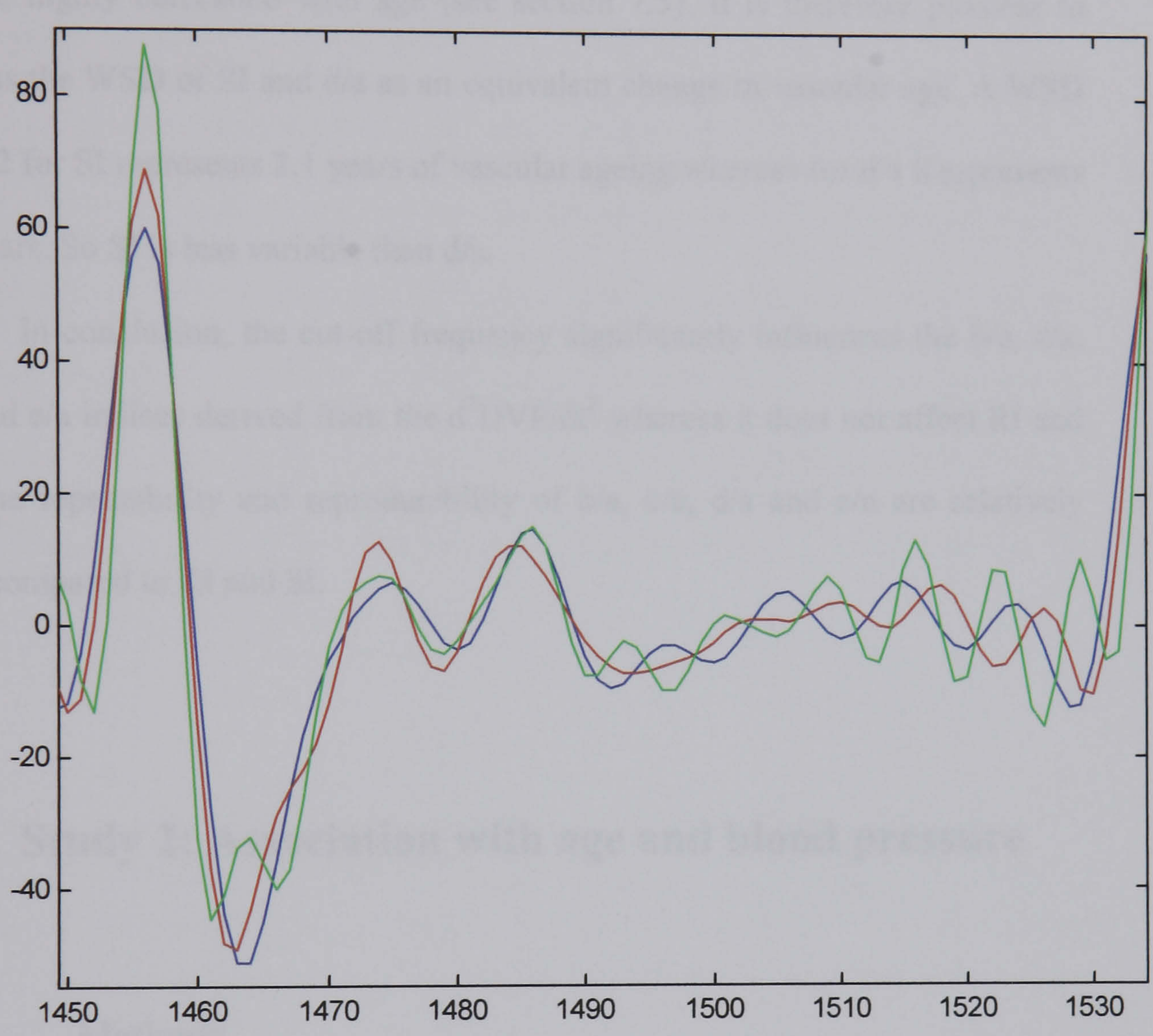

figure 47: Example of the d^2DVP/dt^2 after different low-pass filters: 16Hz low pass (green), 12Hz (red) and 10Hz (blue).

The best reproducibility and repeatability for the indices derived from the d^2DVP/dt^2 were achieved with the 10Hz filter. Subsequent studies were, therefore, done using this filter.

The WCV for the d^2DVP/dt^2 indices was high but with the mean value of these indices being close to zero, the WCV is difficult to interpret and the WSD provides more information. Of the various d^2DVP/dt^2 indices, d/a was the most reproducible (lowest WSD). It was, however, more variable than RI or SI probably because the d^2DVP/dt^2 is more affected by high frequency noise. SI and d/a are highly correlated with age (see section 7.5). It is therefore possible to express the WSD of SI and d/a as an equivalent change in vascular age. A WSD of 0.32 for SI represents 2.1 years of vascular ageing whereas for d/a it represents 5.4 years. So SI is less variable than d/a.

In conclusion, the cut-off frequency significantly influences the b/a, c/a, d/a and e/a indices derived from the d^2DVP/dt^2 whereas it does not affect RI and SI. The repeatability and reproducibility of b/a, c/a, d/a and e/a are relatively poor compared to RI and SI.

7.5 Study 2: Association with age and blood pressure

7.5.1 Methods

The DVP and d^2DVP/dt^2 were obtained in 124 men aged from 20 to 74 years, with no history of diabetes or cardiovascular disease other than hypertension (9 out of 24 had a previous diagnosis of hypertension). No subjects were taking vasoactive drugs. Subjects rested supine in a warm room for at least

20 min, and then 3 recordings, each of 20s, of the DVP were made at 5 minute intervals. d^2DVP/dt^2 was obtained as described in section 7.1.

7.5.2 Results

Correlation coefficients for b/a, c/a, d/a, e/a, RI and SI with age, systolic blood pressure (SBP), diastolic blood pressure (DBP) and mean blood pressure (MAP) are summarised in table 5. SI was strongly associated with age and BP. Of the d^2DVP/dt^2 indices, d/a showed the strongest association with age (figure 48) and BP with correlation coefficients of similar magnitude to those for SI. Multiple regression analysis showed both d/a and SI to be independently correlated with age and MAP (each $P<0.05$). The coefficient of correlation for the ageing index, (b-c-d-e)/a, described by Takazawa et al.[133] with age for the data in this study was 0.654 ($p<0.001$).

	b/a	c/a	d/a	e/a	SI_{DVP}	RI_{DVP}
age	0.51 *	-0.53 *	-0.66 *	0.08	0.63 *	0.24
SBP	0.19	-0.17	0.39 *	0.17	0.48 *	0.08
DBP	0.18	-0.24	0.57 *	0.28	0.68 *	0.28
MAP	0.16	-0.13	0.41 *	0.23	0.51 *	0.18

table 5: Correlation between age, BP and indices derived from the DVP and the d^2DVP/dt^2.
($P<0.01$)*

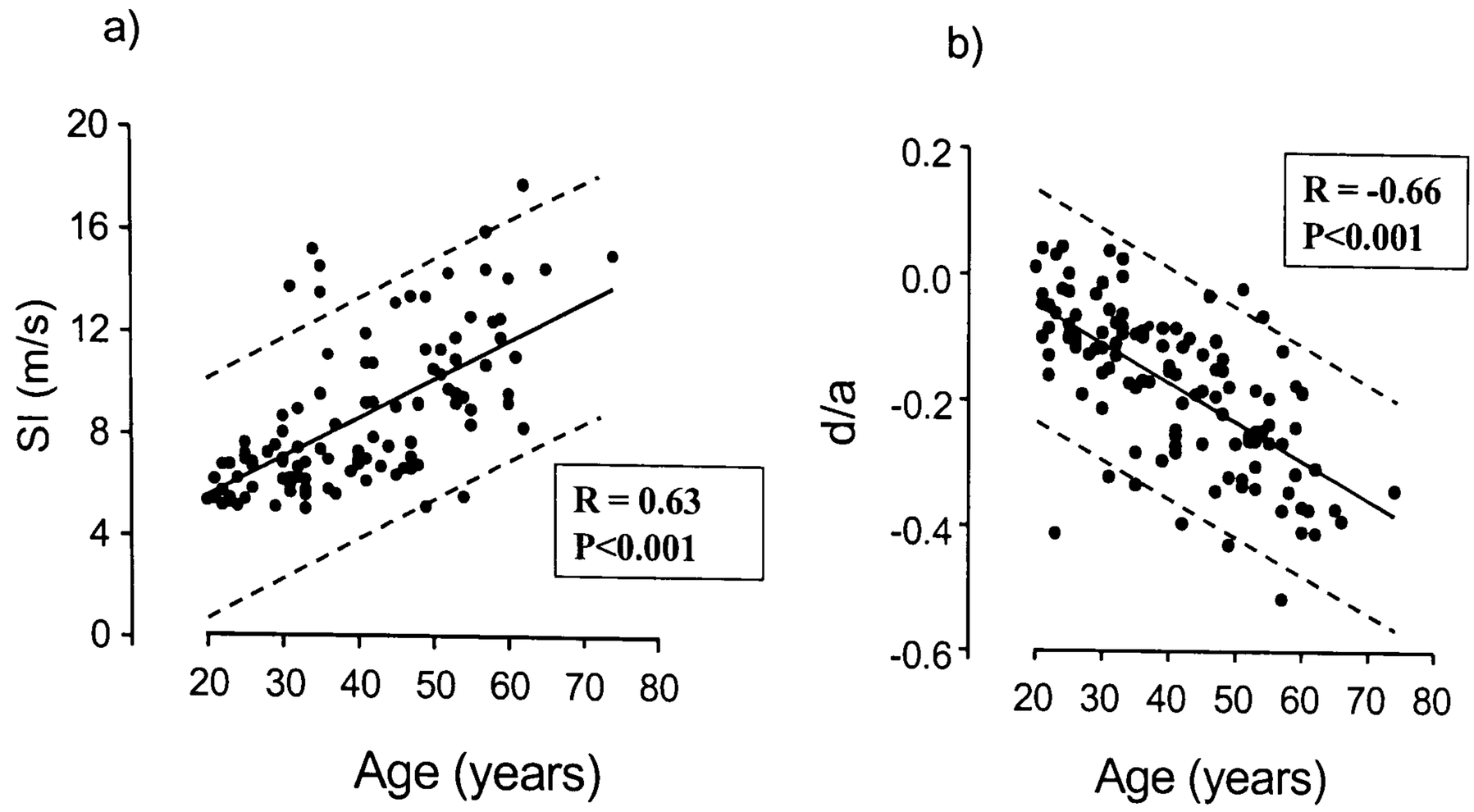

figure 48: a) SI versus age b) d/a versus age in 124 men.

7.5.3 Discussion and conclusion

Results of this study confirm those in chapter 6, that SI is strongly correlated with age and BP. Despite the influence of vasoactive drugs on RI as described in chapter 5, RI was only poorly correlated with BP. Findings from this study with regard to the second derivative indices are broadly in agreement with those of Takazawa et al.[133] and Imanaga et al.[52]: b/a ratio increases with age, whereas c/a and d/a decrease with age. However no relationship between e/a and age was observed. The correlation reported by Takazawa et al. was, however, relatively small (R = -0.25) with 600 subjects. The present study in 124 subjects may be too small to find a weak relationship between e/a and age.

Takazawa et al. found a strong correlation with the ageing index and age (R=0.80). In the present study, the ageing index was slightly less correlated with

age (R=0.65) than the d/a ratio (R=0.66). As the ageing index incorporates e/a and no relation between age and e/a ratio was found, the ageing index seems to offer no advantage over the d/a ratio in assessing ageing, at least in asymptomatic subjects. This may not be the case in subjects with cardiovascular diseases. Takazawa et al.[133] found an increased ageing index ($p<0.01$) in patients with hypertension, diabetes, ischemic heart disease and hypercholesterolemia compared with age matched controls. Bortolotto et al.[19] found patients with atherosclerotic alterations also had a higher ageing index ($p<0.001$). In the present data, the small number of hypertensive subjects did not allowed a comparison of differences in the ageing index between hypertensive and normotensive men.

The indices b/a, c/a and d/a from the d^2DVP/dt^2 are correlated with age and only d/a is correlated with BP as well. These results are in agreement with those of Takazawa et al.[132;133]. The correlation of SI with age and BP is similar to that between d/a, age and BP.

7.6 Study 3: effects of vasoactive drugs

7.6.1 Methods

10 healthy volunteers (31 ±6 years) attended on 3 days according to a single blind randomised, 3-phase, placebo controlled crossover study design. After 20min rest supine, saline was infused and the DVP was recorded 3 times at

5 minutes intervals. The DVP was then recorded during infusion of angiotensin II (75, 150 and 300 ng/min, Clinalfa, Läufelfingen, Germany) or of GTN (3, 30, 300 μg/min, David Bull Laboratories, Australia) and saline vehicle. The GTN data of one of the volunteers was discarded due to poor quality. The d^2DVP/dt^2 was calculated as described in section 7.3.

7.6.2 Results

During intravenous infusion of saline vehicle, there was no significant change in HR, BP, RI, SI or d^2DVP/dt^2 indices. Angiotensin II produced a dose dependent increase in MAP from 78±8 to 93±8 mmHg at the highest dose ($P<0.001$), an increase in RI ($P<0.01$, figure 49) and a decrease in d/a ($P<0.001$, figure 49). GTN produced a dose dependent decrease in MAP from 82±8 to 67±4 mmHg ($P<0.001$), and a decrease in RI ($P<0.001$, figure 50) but d/a did not change in a dose dependent manner (figure 50). The other d^2DVP/dt^2 indices b/a, c/a and e/a did not show a consistent response to angiotensin II and GTN. The vasoactive agents produce a change in SI of 2.6m/s for angiotensin II and –1.3m/s for GTN.

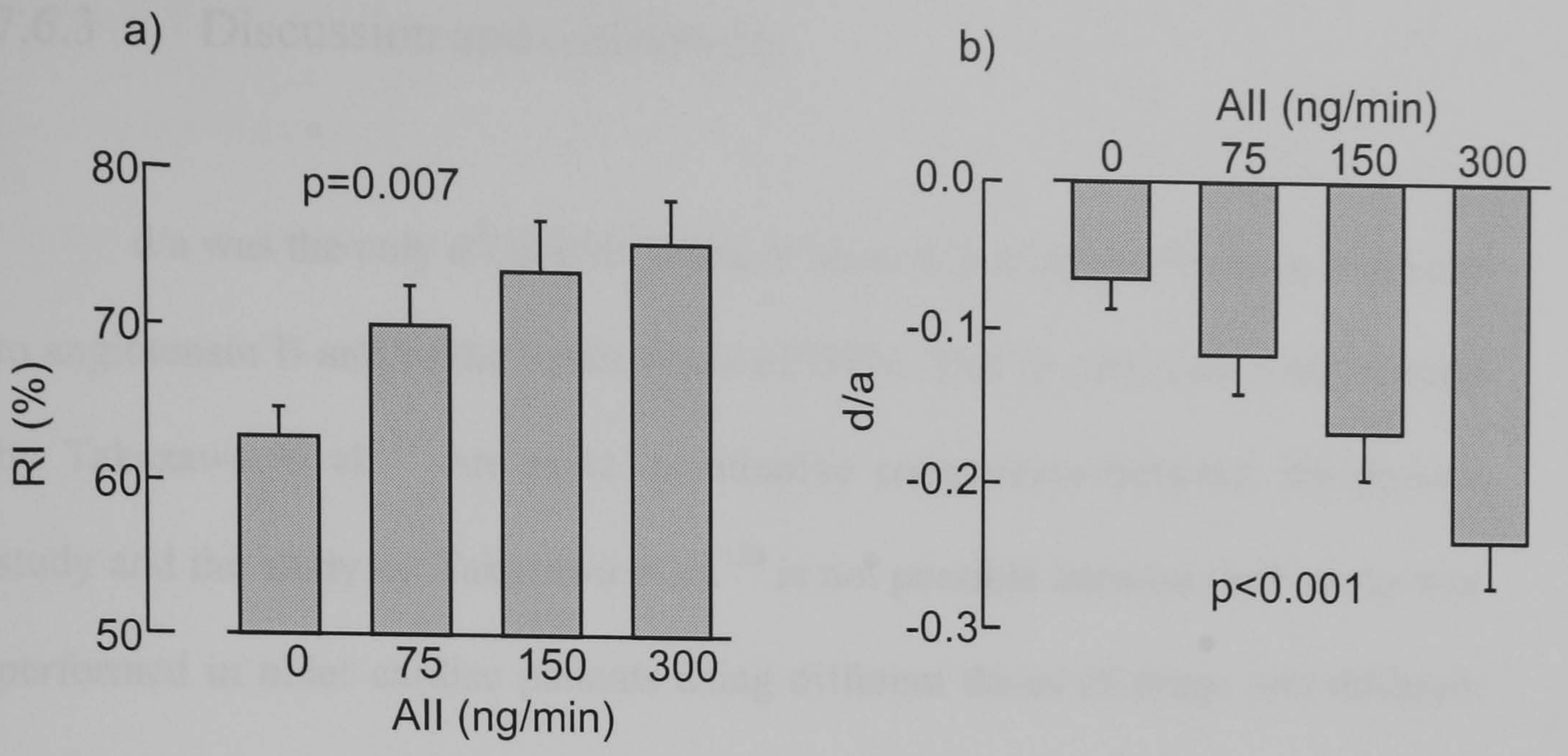

figure 49: Effects of angiotensin II (AII) on a) RI and b) d/a

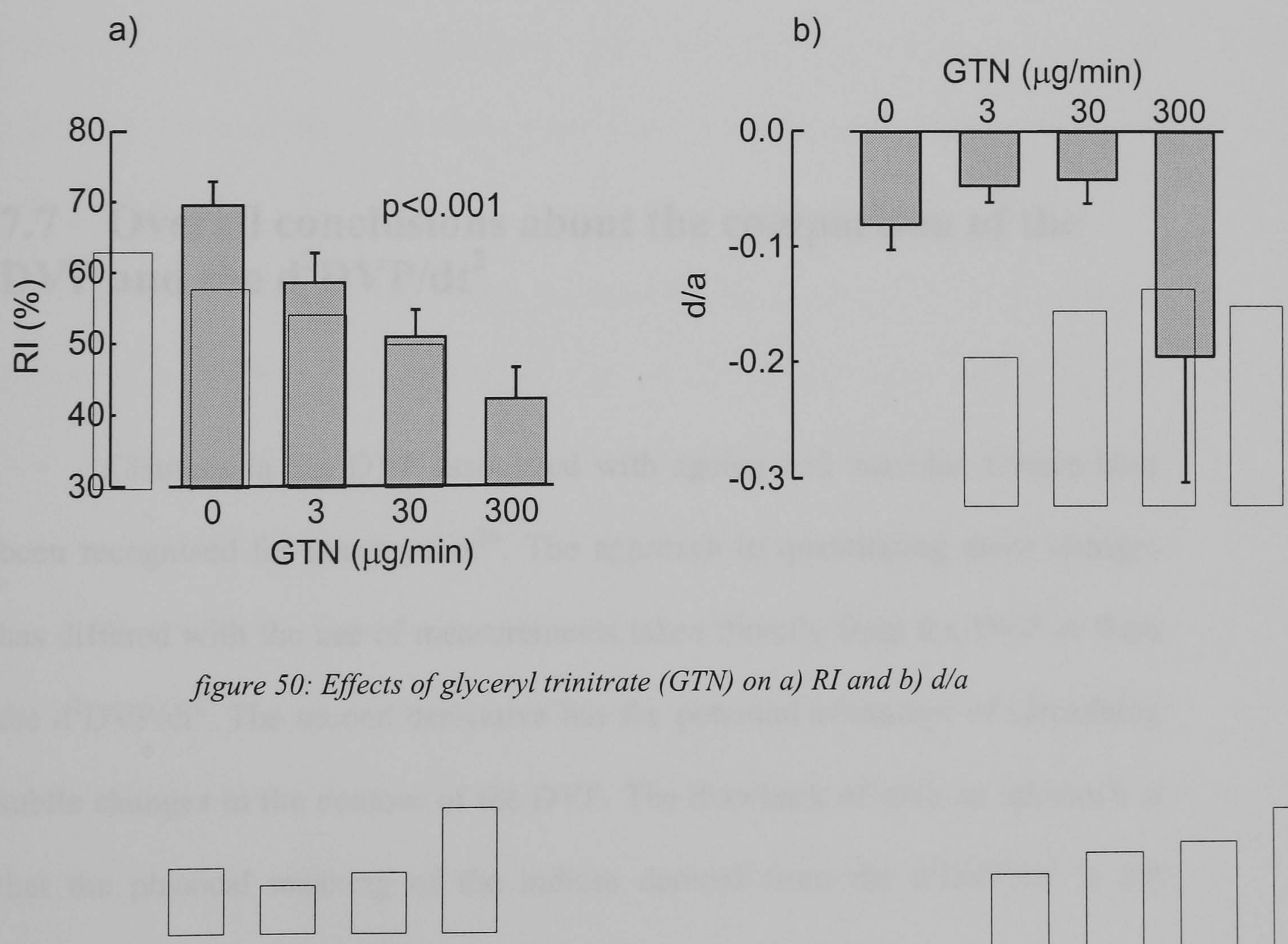

figure 50: Effects of glyceryl trinitrate (GTN) on a) RI and b) d/a

7.6.3 Discussion and conclusion

d/a was the only d^2DVP/dt^2 index to show a consistent change in response to angiotensin II and to the lower doses of GTN. This is consistent with a study by Takazawa et al.[133] An exact quantitative comparison between the present study and the study by Takazawa et al.[133] is not possible because their study was performed in older cardiac patients using different doses of drugs and different routes of administration.

Of the various d^2DVP/dt^2 indices, d/a was also the most reproducible (see section 7.4) with the lowest WSD. RI was, however, more repeatable and reproducible and showed a consistent response to both vasoactive agents. The use of the 2nd derivative does not seems to improve the detection of vasoactive change in the vasculature.

7.7 Overall conclusions about the comparison of the DVP and the d^2DVP/dt^2

Changes in the DVP associated with ageing and vascular disease have been recognised for many years[36]. The approach to quantitating these changes has differed with the use of measurements taken directly from the DVP or from the d^2DVP/dt^2. The second derivative has the potential advantage of identifying subtle changes in the contour of the DVP. The drawback of such an approach is that the physical meaning of the indices derived from the d^2DVP/dt^2 is not

obvious. Furthermore, values of indices derived from the d^2DVP/dt^2 depend on the cut-off frequency of the filter used to eliminate noise. Using the second derivative might help to detect particular characteristics of the waveform, but it is sensitive to filtering characteristics and/or noise.

In section 5.1, an interpretation of RI and SI in terms of pressure wave reflection and large artery stiffness was presented. In the present study, RI showed no significant correlation with age but was markedly influenced by angiotensin II and GTN in a dose dependent manner, consistent with an effect of these drugs on the tone of small arteries. Of the d^2DVP/dt^2 indices, d/a was the most reproducible, was the most highly correlated with age and showed a consistent response to angiotensin II. This might explain why it is the ratio the most used by other investigators. However, d/a did not change in a dose response manner in response to GTN. The influence of angiotensin II on d/a and the correlation of d/a with age suggests that d/a is influenced both by large and small arteries. As a measure of vascular tone, therefore, d/a may be more difficult to interpret than RI.

As expected for an index of large artery stiffness, SI was strongly positively correlated with age and BP. d/a was also highly negatively correlated with age. The relative merits of these indices in detecting vascular ageing will be mainly determined by their degree of change relatively to their reproducibility and their sensitivity (or lack of sensitivity) to confounding factors. Comparison of repeatability and reproducibility of d/a and SI is difficult because mean values of d/a are close to zero. For this reason the WSD was expressed as an equivalent change in vascular age. Variability of SI as assessed by WSD on different days was equivalent to 2.1 years of vascular ageing whereas that of d/a was equivalent

to 5.4 years. Ideally, SI and d/a should be compared to PWV. This was not possible due to time constraints. However the correlation of SI with PWV in another group of subjects is presented in section 6.5.2 and the coefficient of correlation was 0.67 ($P<0.0001$). Hashimoto et al. have compared d/a with aortic PWV, a measure of aortic stiffness[45]. Although PWV and d/a are both correlated with age and BP, they were only weakly correlated to each other ($R=0.24$) whereas a strong correlation between SI and PWV was observed ($R=0.65$, see section 6.5.2). Changes in SI in response to vasoactive drugs were small and could be explained by changes in BP. By contrast, d/a changed to a greater degree. The better reproducibility of SI compared to d/a, less marked change after vasoactive agents but similar correlation with age and BP suggest that SI may be as useful if not a better measure of vascular ageing in healthy men.

In conclusion, in asymptomatic volunteers, RI may be a better index to track the effects of vasoactive drugs than indices such as d/a from the second derivative. SI is equally strongly associated with age as d/a, but shows less variability and thus may be a more reliable index of vascular ageing. The use of the second derivative may not be necessary to interpret useful characteristics of the DVP.

CHAPTER 8: Clinical Applications

Potential uses of the DVP as a simple tool to investigate vascular function are explored in this chapter. Applications examined are: endothelial function, vascular function in pregnancy and epidemiological screening using the example of the association of vascular function with birth weight.

8.1 Endothelial function

8.1.1 Background

With the recognition that atherosclerosis is initiated by injury to the endothelium, there has been much interest in endothelial-derived substances as markers or mediators of atherogenesis. Endothelium derived nitric oxide (NO) has received most attention. In addition to being an important vasodilator, NO has anti-atherogenic properties, including inhibition of the expression of adhesion molecules, inhibition of platelet adhesion and aggregation and inhibition of vascular smooth muscle proliferation[93]. Decreased availability of endothelium-derived nitric oxide (NO) is thought to be of major importance in the initiation and progression of atherosclerotic vascular disease[102]. Impaired endothelium-dependent vasodilation mediated by NO is observed at the earliest stages of vascular disease and, in the presence of most recognised risk factors for vascular disease, is evident before development of clinical sequel[1]. In such subjects endothelium-dependent vasomotor function is predictive of future ischaemic events[117;122;130]. Interventions that reduce the progression of vascular

disease such as lipid lowering drugs are associated with improved endothelial function[1]. The potential for NO to play a causal role in the beneficial effects of such interventions is demonstrated by animal models where pharmacological[24;103] or genetic[26;67] modulation of NO synthase is seen to influence atherogenesis. Existing techniques for assessing endothelial function involve intra-arterial injection of an endothelium-dependent vasodilator (usually acetylcholine) into a local vascular bed such as the forearm or involve measuring the vasomotor response to a physical stimulus such as an increase in shear stress. The only accepted non-invasive technique involves measuring dilation of the brachial artery in response to an increase in blood flow generated by reactive hyperaemia[25]. The change in brachial artery diameter is at the limit of resolution of high quality ultrasound imaging systems. The technique requires expensive equipment and extreme attention to detail: reliable results can only be obtained by an ultrasonographer with extensive experience in the method. There is thus a real need for a simple and robust test of endothelial function. The sensitivity of the DVP to exogenously administered NO donors (as described in sections 1.4 and 5.1) raises the possibility that it should also be sensitive to stimulated NO release from the endothelium and hence, given an appropriate stimulus, could be used as a simple test of endothelial function[140]. Work in the department of clinical pharmacology at St Thomas' Hospital has previously shown that the β_2-agonist salbutamol acts to stimulate NO release[35]. The aim of the present study was to determine whether salbutamol could be used to assess endothelial function.

8.1.2 Aim

To determine whether salbutamol produces a similar change in the DVP to GTN and to investigate whether the response to salbutamol is impaired in subjects with type 2 diabetes, a group known to have endothelial dysfunction

8.1.3 Methods

20 healthy controls (n=20) and 20 type II diabetes (n=20) were recruited with the approval of St Thomas' Hospital Research Ethics Committee. Patients with type-II diabetes were recruited from the diabetic clinic of St-Thomas' hospital. They were managed by diet alone or by diet plus oral hypoglycaemic therapy. No patients had complications other than background retinopathy. Control non-diabetic subjects were recruited concurrently and were similar in terms of age and gender distribution. Subject characteristics are shown in table 6. After 30min rest supine, DVP, HR and BP were measured at 5 minutes interval. The DVP was measured as described in section 2.2. GTN (500 μg sublingually) was then administered and BP and DVP measurements were made 3 min after GTN. Twenty minutes later, when DVP and BP returned to baseline, salbutamol (400 μg) was given by inhalation through a spacer. DVP and BP were measured 10 and 15 min after inhalation. The mean measurements at these times was used for analysis.

	Control subjects (n=20)	Diabetics (n=20)
Gender (M/F)	15/5	13/7
Smokers / Non-smokers	4/16	5/15
Age (years)	44 ± 6.9	48 ± 10
SBP (mmHg)	123 ± 17	131 ± 21
DBP (mmHg)	71 ± 13	78 ± 12
BMI (kg/m^2)	24 ± 2.5	28 ± 4.7 *
Glucose (mmol/L)	4.8 ± 0.6	10.3 ± 5.3 *
HbA1c (%)	4.9 ± 0.6	7.7 ± 2.0 *
T-Chol (mg/dl)	189 ± 31	201 ± 46
Triglycerides (mg/dl)	115 ± 71	230 ± 186
HDL (mg/dl)	54 ± 12	46 ± 12

table 6: Subjects Characteristics

** $P < 0.05$, data are presented as mean ± SD*

8.1.4 Results

The effect of salbutamol and GTN on HR and BP were similar in the 2 groups (see table 7). At baseline, values of RI were similar in controls and patients with diabetes. Salbutamol and GTN both produced a fall in RI. The response to GTN was similar in controls and patients with diabetes but that to salbutamol was significantly less in patients with type II diabetes (see figure 51).

		control subjects	diabetics
ΔHR (bpm)	GTN	9.8 ± 1.6*	7.1 ± 1.2*
	Salbutamol	6.5 ± 1.2*	5.6 ± 1.2*
ΔSBP (mmHg)	GTN	0.3 ± 3.0	1.6 ± 3.1
	Salbutamol	-2.7 ± 1.9	-5.4 ± 2.1
ΔDBP (mmHg)	GTN	-2.0 ± 2.3	-6.4 ± 2.6
	Salbutamol	-6.1 ± 1.4*	-6.7 ± 1.4*

table 7: Changes in heart rate and blood pressure after GTN and salbutamol

*ΔHR: change in heart rate; ΔSBP: change in systolic blood pressure; ΔDBP change in diastolic blood pressure (*P<0.05)*

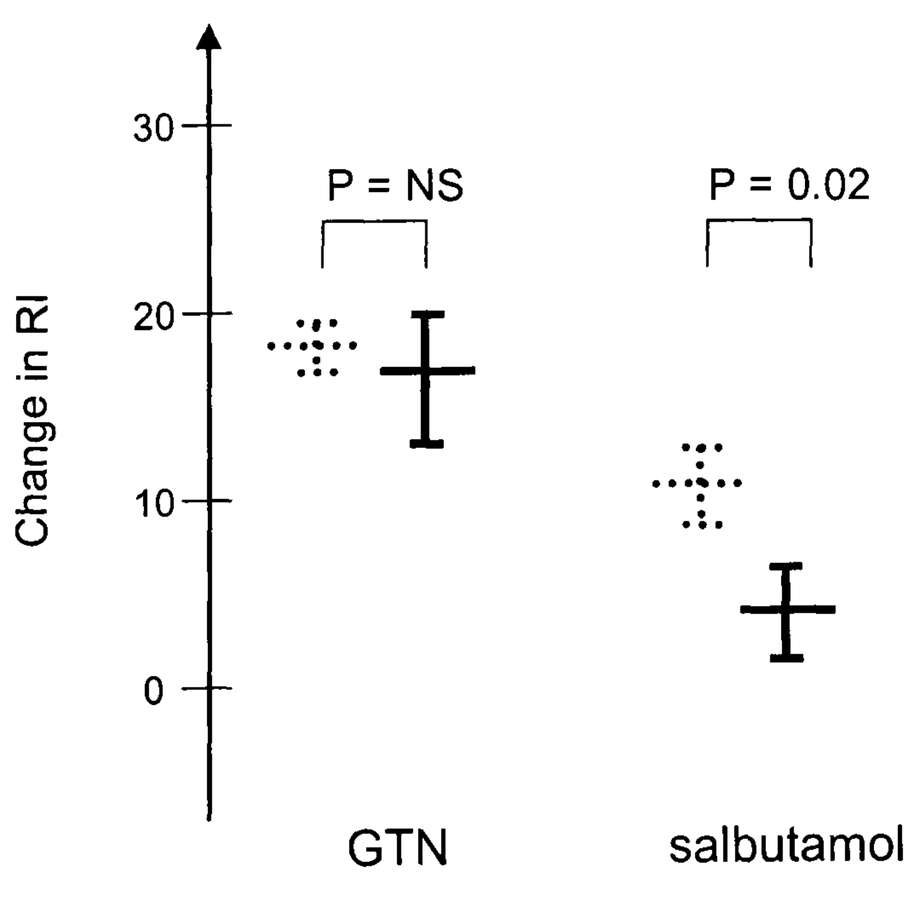

figure 51: Change in RI in control and diabetic subjects

Change of RI (%) from baseline after sublingual GTN and inhaled salbutamol in controls (dashed lines) and in type II diabetes (solid lines)

8.1.5 Discussion

GTN produces vasodilation through its metabolism in vascular smooth muscle to nitric oxide or a nitrosothiol[37]. Salbutamol stimulates nitric oxide release from the endothelium through the L-arginine-NO pathway. Salbutamol should therefore have similar effects on the DVP as GTN[140]. This study confirms that both salbutamol and GTN reduce RI and confirms observations from animals work. In patients with endothelial dysfunction, characterised by an abnormal L-arginine-NO pathway, such as those in type II diabetes, a blunted response to salbutamol would be expected. Results of the present study support this and suggest that the DVP response to salbutamol might be used as a simple test of endothelial function. Other investigators have explored this concept using the pressure pulse rather than the DVP[47;74;75;144]. Wilkinson et al.[144] have examined the response of aortic AIx (obtained by transformation of the radial pulse) to salbutamol. They found this to be impaired in hypercholesterolaemic patients compared with normo-cholesterolaemic controls. They also demonstrated a correlation between the AIx response to salbutamol and forearm blood flow response to brachial artery infusion of acetylcholine (a standard test of endothelial function). As described in chapter 4, the pressure pulse is closely related to the DVP but the aortic AIx relies on a transfer function (see chapter 3) and is influenced by factors (HR, PWV, ejection pattern) other than vasodilation. RI is measured on the diastolic part of the DVP and may be more closely related to vasodilation (see section 5.5). A similar approach, based on examining response of the radial AIx to salbutamol or terbutaline, has been shown to be NO

dependent[47;74;75]. Hayward et al.[47] have also shown that the radial AIx response to salbutamol can distinguish between subjects with coronary diseases and normal controls subjects. This reinforces the observation made in chapter 3, that similar information can be obtained from the radial and aortic AIx.

In conclusion, the DVP response to salbutamol has potential as a simple test of endothelial function. To fully assess this, its reproducibility and sensitivity in detecting a change in endothelial function needs to be compared with conventional techniques.

8.2 Pre-eclampsia

8.2.1 Background

Normal human pregnancy is characterised by an increase in cardiac output and a reduction in peripheral arterial resistance, which occurs from the 12th week of gestation. The mechanism involved in the reduction of peripheral resistance is unknown although increased endothelial synthesis of nitric oxide has been proposed[118]. Pre-eclampsia is a disease process arising usually in the 2nd half of pregnancy and is characterised by hypertension, proteinuria and sometimes oedema. Pre-eclampsia complicates 5 to 10% of pregnancies and is a major cause of maternal and foetal morbidity and mortality[137]. The only cure is delivery. The management of pre-eclampsia starts with screening for the development of hypertension and proteinuria as these are usually not associated with symptoms. Once hypertension is discovered, the patient is admitted to hospital for close monitoring. However, there is a high rate of false-positive cases (and false-negative as well) at a great cost to the Health Service. There is a need for an early reliable test for pre-eclampsia. Pre-eclampsia is characterised by an increase in peripheral resistance and pressor activity, reduced cardiac output and reduced perfusion of vascular beds. Present methods for measuring peripheral resistance and cardiac output are either labour intensive or invasive.

8.2.2 Aim

The aim of this study was to investigate if DVP contour analysis, a simple, non-invasive and rapid method, could be used to monitor changes in arterial function due to pre-eclampsia.

8.2.3 Methods

10 women with pre-eclampsia, diagnosed according to the ISSHP definition[33] were studied shortly after admission, before initiation of anti-hypertensive treatment. Women who had diabetes and hypertension before pregnancy were excluded. 20 normotensive pregnant women of similar age and gestation were studied in the ante-natal clinic as controls. The DVP was measured as described in section 2.2.

8.2.4 Results

Subjects characteristics are tabulated in table 8.

	n	gestation	age (yrs)	HR (bpm)	SBP (mmHg)	DBP (mmHg)
normal pregnant	20	34 ± 3.7	29 ± 6.5	90 ± 2.1	121 ± 4.5	69 ± 2.2
pre-eclampsia	10	36 ± 4.2	28 ± 6.0	84 ± 5.0	151 ± 3.1**	99 ± 4.6**

table 8: Subjects characteristics

Values are means ± SD except for heart rate and blood pressure (means ± SE)

**P < 0.01, ** P<0.001 compared to healthy pregnant women*

RI and SI were significantly increased in women with pre-eclampsia, as shown in figure 52.

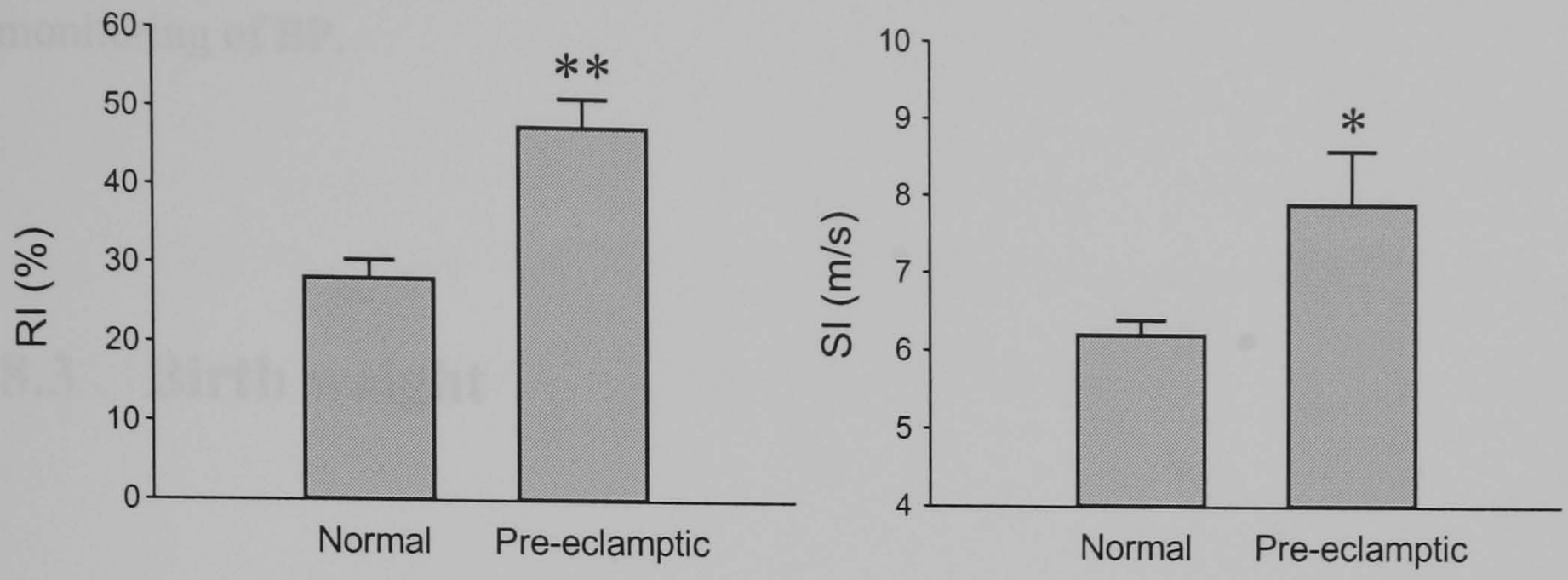

figure 52: RI and SI in pregnancy

RI and SI measured on the DVP in healthy pregnant women and women with pre-eclampsia

**P<0.01, **P<0.001 compared to healthy pregnant women*

8.2.5 Discussion

These results show that both RI and SI are increased in pre-eclampsia compared to values in normal pregnant women. The increase in RI is consistent with an increase in vascular tone affecting both resistance arteries (and hence causing an increase in BP) and in more proximal arteries causing an increase in pulse wave reflection. The increase in SI may results from increased stiffness of the aorta and large arteries. From these data, however, it is not possible to determine if the increase in SI is a primary phenomenon or is secondary to the increase in BP. These results demonstrating a difference in DVP indices between women with pre-eclampsia and healthy pregnant women suggest that the DVP

may be useful in the prediction of pre-eclampsia. Prospective evaluation of such an approach will be required however to determine whether the DVP is more sensitive/specific in screening for pre-eclampsia compared with conventional monitoring of BP.

8.3 Birth weight

8.3.1 Background

Barker et al.[10-13;86;113] have studied the association of birth weight with hypertension and cardiovascular events occurring in later life. There have been over 80 studies demonstrating a relationship between birth weight and hypertension. Law et al.[70] and Huxley et al.[50] in a meta-analyse suggest that overall, a 1kg difference in birth weight corresponds to a 3.5 mmHg change in adult SBP[70]. However, a recent meta-analysis in which studies have been weighted to account for size, suggests that the strength of the BP-birth weight association may have been over estimated[49]. An increasing risk of adult hypertension has also been linked to "catch-up growth"[50]. The association between birth weight and BP is seen from early childhood through to late adulthood. There are relatively few studies examining the relationship between birth weight and arterial properties. An association between arterial compliance and birth weight has been reported[86] in children as young as 9 years of age[85]. The DVP waveform is determined by characteristics of the arterial tree including

arterial stiffness (compliance). It is possible, therefore, that the DVP exhibits a different contour in subjects with low birth weight.

8.3.2 Aim

The aim of this study was to test if birth weight is associated with a change in contour of the DVP in healthy adolescent subjects.

8.3.3 Methods

Students (n=96, 48 women) aged 16 to 25 years living with their parents were studied with the approval of St Thomas' Hospital Research Ethics Committee. The majority were attending the 6th form of a Secondary School in North London. BP (mean of 3 readings seated) was measured using an automated oscillometric method (Omron 705CP, Omron, Japan) with appropriate sized cuff. Birth weight was obtained by maternal recall. The PulseTrace device, described in section 2.2.3, was used to obtain RI and SI. The mean of 3 recordings was used. The relationship between BP, RI, SI and birth weight was examined in each sex by regression analyses. No adjustments were made for current weight (or other anthropometric characteristics) because in previous series in young adults there was no association between these characteristics and RI or SI and because adjustment of birth weight associations for current weight and other confounding factors has been criticised[49].

8.3.4 Results

Mean (±SD) BP was 117±10/75±8 mmHg and birth weight 3.3±0.4 Kg. There was no significant correlation (in either sex) between BP and birth weight or between SI and birth weight. In men, RI was not significantly correlated with birth weight (R=0.19, P=NS) but, in women, RI was strongly negatively correlated with birth weight (R=-0.52, P<0.001, see figure 53)

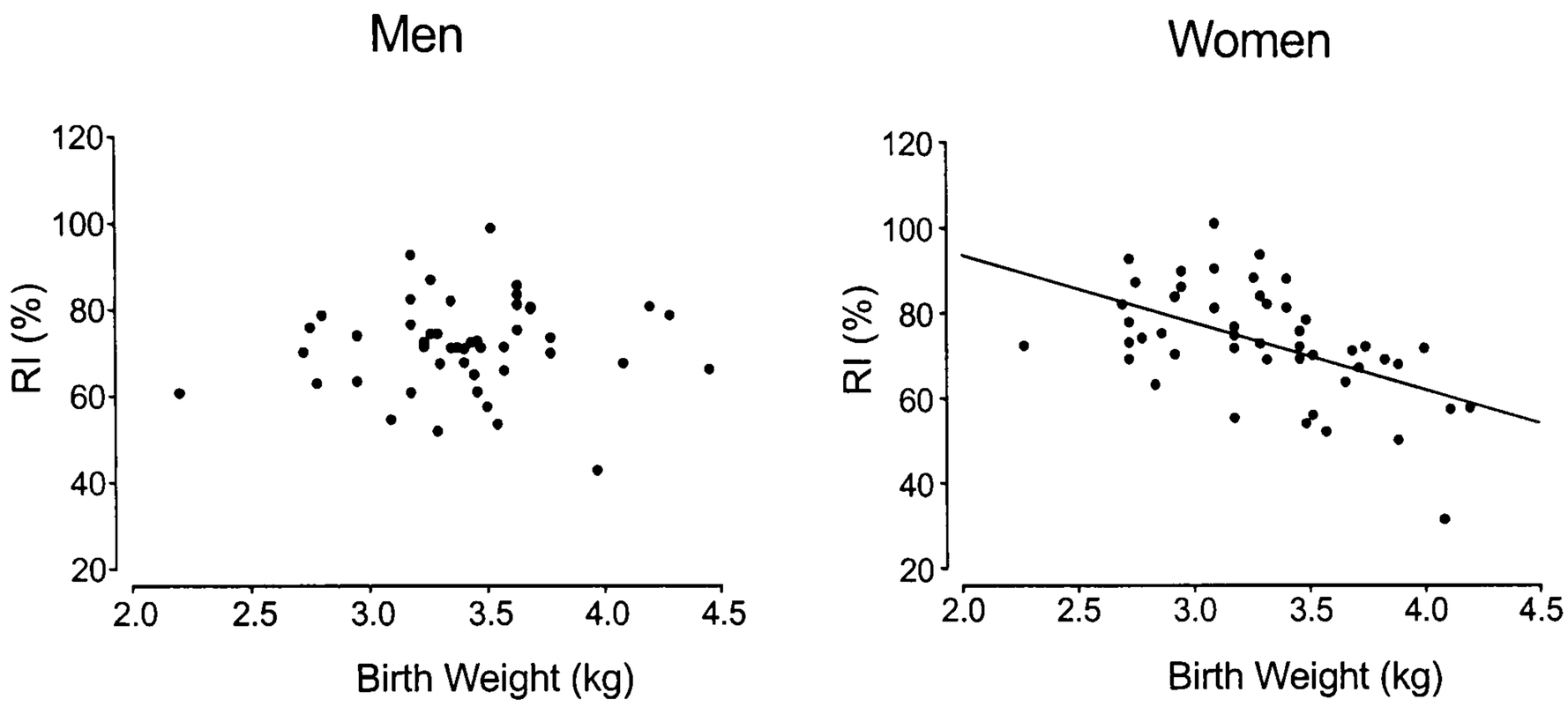

figure 53: Correlation of RI with birth weight
in men (left panel, R = 0.19 , P = NS) and women (right panel, R = -0.52, P < 0.001)

8.3.5 Discussion

The lack of association between BP and birth weight is consistent with the recent analysis by Huxley et al.[49] (our study had insufficient power to detect a weak association). The negative correlation between RI and birth weight in female students suggests that low birth weight may be associated with altered structure of small arteries (the major site of reflection). The lack of association

between RI and birth weight in men is at first sight surprising but studies in young adults shows that the association between birth weight and BP is stronger in women than in men[50]. It is possible that the growth spurt obscures birth weight related programming of arterial properties and such effects may be more apparent in young men rather than women due to the later growth spurt in men.

In adults, low birth weight has been associated with a increase in arterial stiffness[86] but these results were not corrected for BP which was higher in subjects with low birth weight. SI is a measure of large artery stiffness and is determined mainly by aortic stiffness and, in this study, SI was not related to birth weight. In 9 year old children, carotid stiffness has been found to be related to birth weight[85]. This apparent conflict with the present study could relate to the limited power of our study to detect a weak association between SI and birth weight or to differences between arterial beds.

In conclusion, the present study suggests that marked variations in the properties of the arterial tree as measured with the DVP, may be associated with birth weight in young women, independently of BP. Gender specific associations of birth weight with arterial properties deserve further study.

CHAPTER 9: Overall discussion

Characteristics of the pressure pulse contour are understood in terms of direct and reflected waves. Indices derived from pressure pulse contour analysis such as the aortic AIx have been used to examine effects of ageing, hypertension, and vasoactive drugs. Most investigators have used the central pressure pulse derived by applying a transfer function (TF) to the peripheral pressure pulse. The analysis presented in chapter 3 suggests that a TF may not be necessary to study wave reflection. The peripheral pulse contains the same information as the central pulse regarding wave transit time and reflection. The shape of the peripheral pulse can be used directly to study wave reflection without mathematical transformation to the central pulse. A transfer function is, however, required to estimate central SBP.

The DVP can be obtained more simply than the pressure pulse and with less training. In chapter 4, the relation between DVP and pressure pulse was examined and the DVP found to contain the same information than the pressure pulse. Like the pressure pulse, the DVP can be interpreted as the summation of a direct wave and a reflected wave. A reflection index, RI, has been defined to quantify the amplitude of wave reflection whereas timing of the reflected wave and hence large artery PWV is estimated with a stiffness index, SI. Data presented in chapters 5 and 6 suggest that these indices behave as expected. SI is strongly associated with age and BP, major determinants of arterial stiffness but is little influenced by vasoactive drugs. By contrast, RI changes in response to vasoactive drugs but show little association with age and BP. Other investigators have analysed the second derivative of the DVP. However, as shown in chapter 7, the benefit of using indices from the second derivative is not obvious and the interpretation of such indices is problematic. RI seems to be a better index to

track vasoactive changes, and SI correlates better with age and BP, major contributors to large artery stiffness.

Although, at present, the pressure pulse is more widely used that the DVP, work presented in chapter 8 suggests the DVP has important potential clinical applications. Obtaining the DVP is very simple and rapid with no discomfort to the patient and requires no particular training for the operator. For these reasons, it could be a particularly useful tool to study arterial structure/function especially in situations where large numbers of subjects need to be studied or in subjects in whom more complicated methods are difficult to apply such as in children and pregnant women. Although further studies are required, the DVP may prove to be a useful tool to examine endothelial function, the arterial mechanism involve in pre-eclampsia and in the arterial modelling associated with low birth weight.

Perhaps the largest and potentially the most useful application of DVP is the assessment of large artery stiffness. Aortic PWV has recently been shown to be a powerful predictor of cardiovascular mortality. If similar information could be obtained from the DVP, this simple measurement could be useful in identify patients at risk and targeting preventative treatment. Work presented in chapter 6 shows that SI correlates well with PWV in healthy men over the age range 21 – 69 years. In older subjects, the inflection point on the down-slope of the DVP waveform may be difficult to identify. In these cases a more sophisticated analysis of the shape of the waveform may be required. Nevertheless, the correlation of SI with PWV in healthy subjects shows that important information relating to vascular stiffness and hence cardiovascular risk can be obtained from the DVP. This will need to be verified in a prospective outcome study.

In conclusion, the DVP contains similar information to the pressure pulse. It is influenced by characteristics of the systemic circulation. The DVP is a potentially useful tool for the rapid analysis of arterial structure and function.

CHAPTER 10: Appendices

10.1 Algorithm to calculate the average pulse

10.1.1 Overview

This algorithm is used on the DVP or pressure signal to calculate the average pulse. First, the foot of the pulses are detected. Individual pulses are normalised to calculate the average pulse.

10.1.2 Detection of the foot of the pulses

- 4 points averaging process of the signal to reduce electrical noise (optional)
- Calculation of the 1st derivative of the signal (derv)
- Detection of the maximum value of the signal (MaxDerv)
- Calculation of a threshold: Thres = MaxDerv*0.6
- Test on every samples if derv(i) > Thres. If true, then a new pulse is identified and the zero crossing of the 1st derivative before that is the foot of the pulse (see figure 54).
- By processing the entire signal, an array containing the time of the foot of each pulse is obtained.

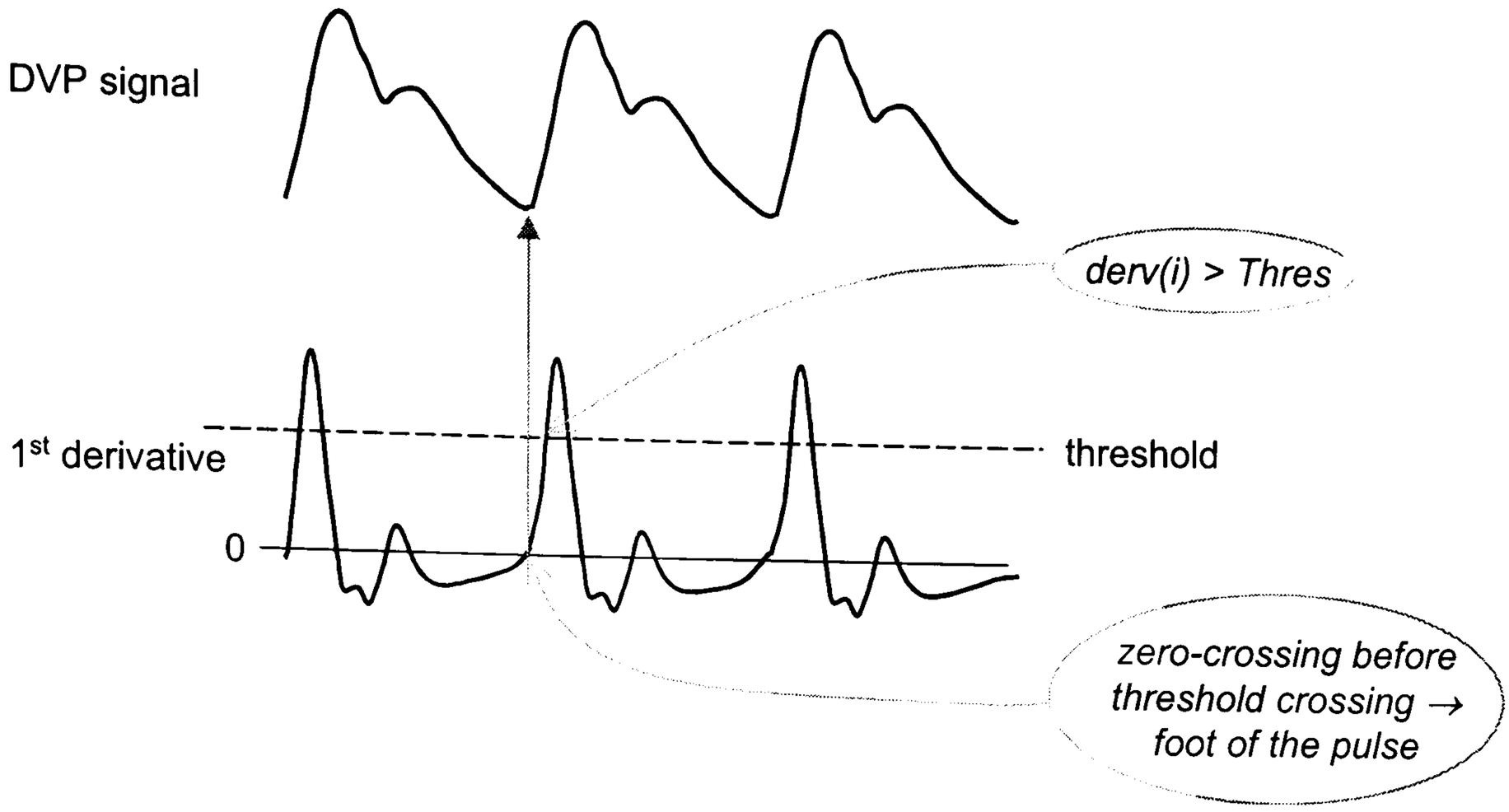

figure 54: Detection of the foot of the pulse

10.1.3 Obtaining the averaged pulse

- A pulse is defined as the signal between 2 consecutive feet
- The DC "drift" component is removed (figure 55)

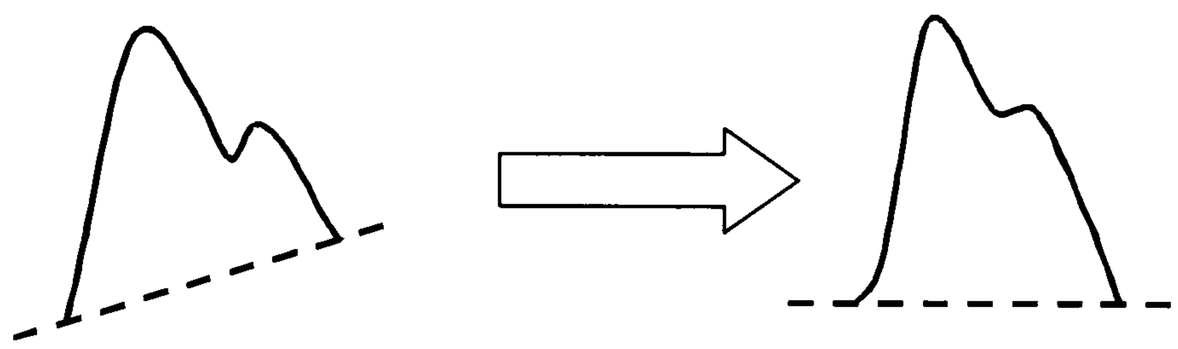

figure 55: Removal of the DC "drift" component

- Period normalisation by interpolation (linear interpolation is sufficient because there is little difference between the original duration of the pulse and the normalised period) (figure 56).

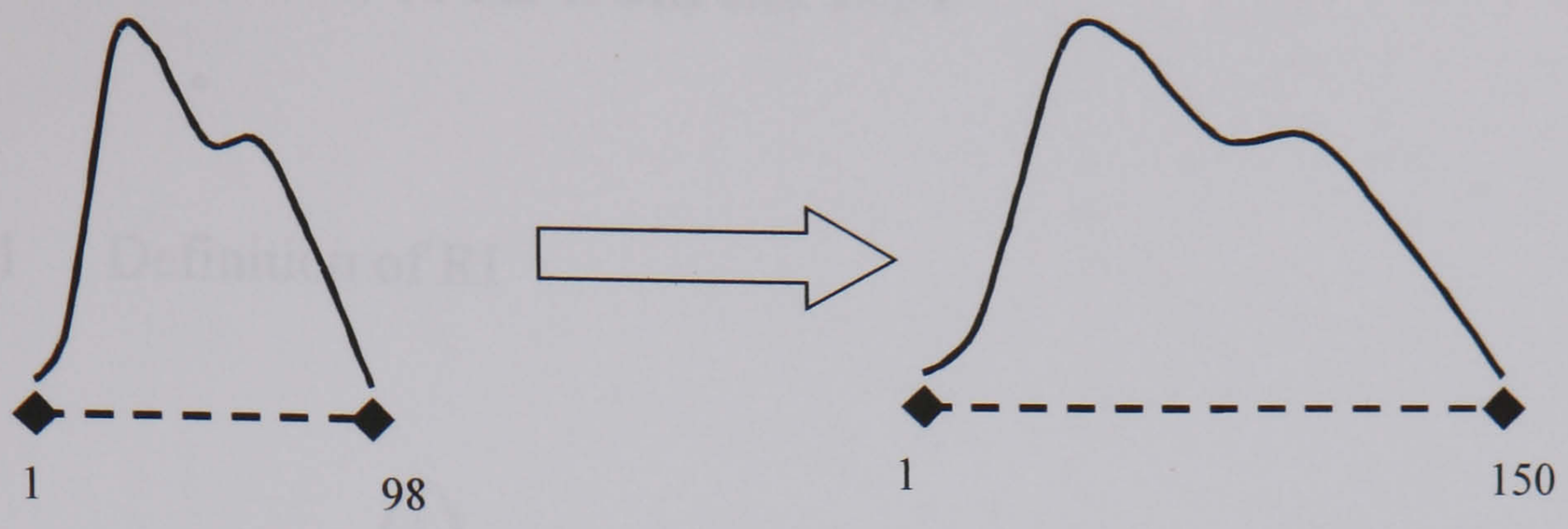

figure 56: Period normalisation

? Amplitude normalisation

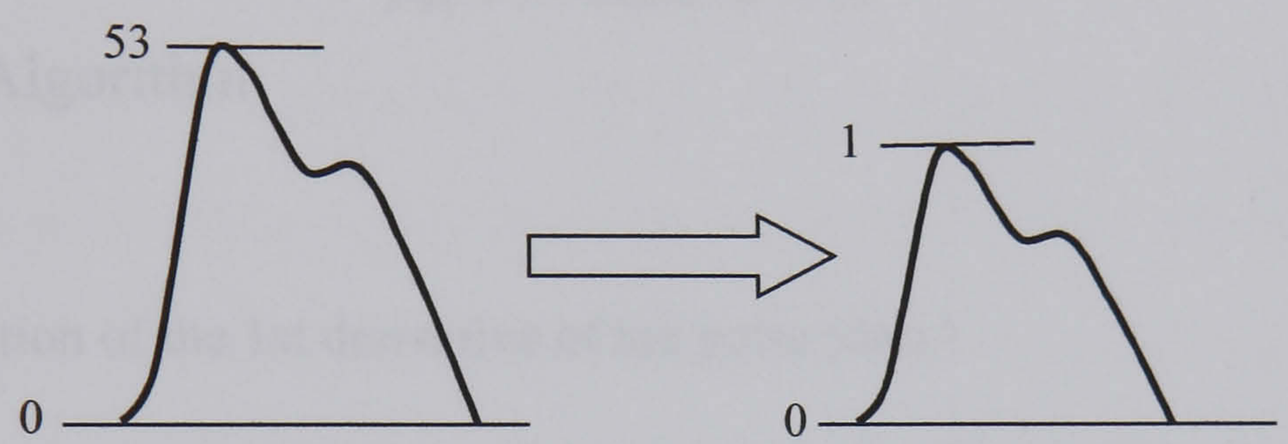

figure 57: Amplitude normalisation

? Normalised pulses are ensemble averaged.

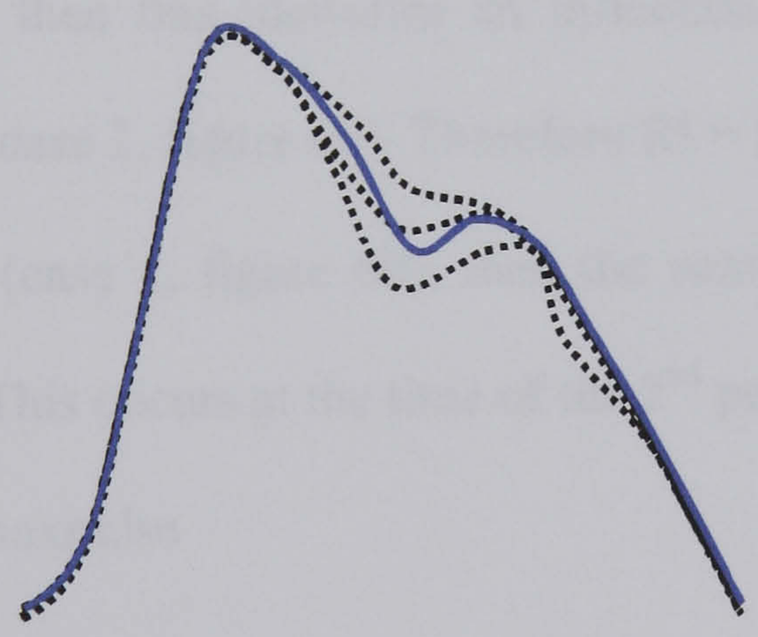

figure 58: Ensemble averaging of pulses (average pulse in blue)

10.2 Calculation of RI from the DVP

10.2.1 Definition of RI

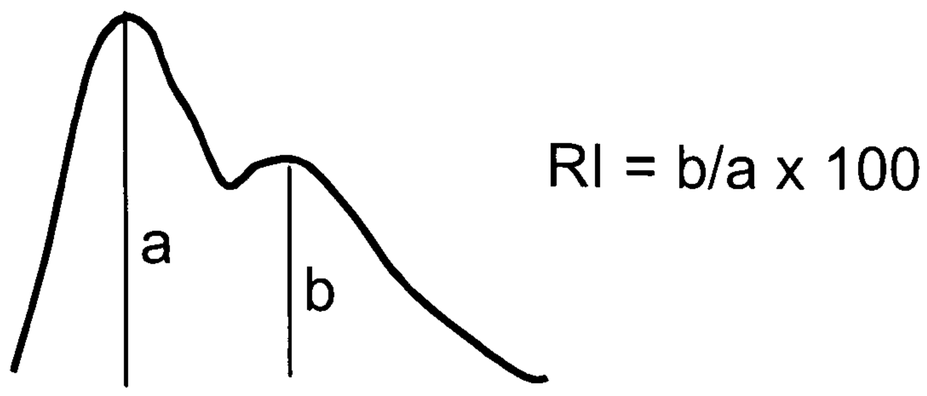

figure 59: Definition of RI

10.2.2 Algorithm

- Calculation of the 1st derivative of the pulse (derv)
- Find of the maximum value and time of the pulse (maxpulse, maxpos)
- Identification of the time (t_{inf}) of the maximum of the 1st derivative in the "search window" (inflection point). The "search window" is set to be after the max of the pulse and shorter than the full length of the pulse.
- If derv[t_{inf}] is <0, then this identifies an inflection point and there is no second peak (as in case 2, figure 60). Therefore RI = DVP[t_{inf}] / maxpulse
- If DVP[t_{inf}] is >0 (case 1, figure 60), then the next zero-crossing point of derv is identified. This occurs at the time of the 2nd peak. Therefore RI = DVP[t_{peak}] / maxpulse

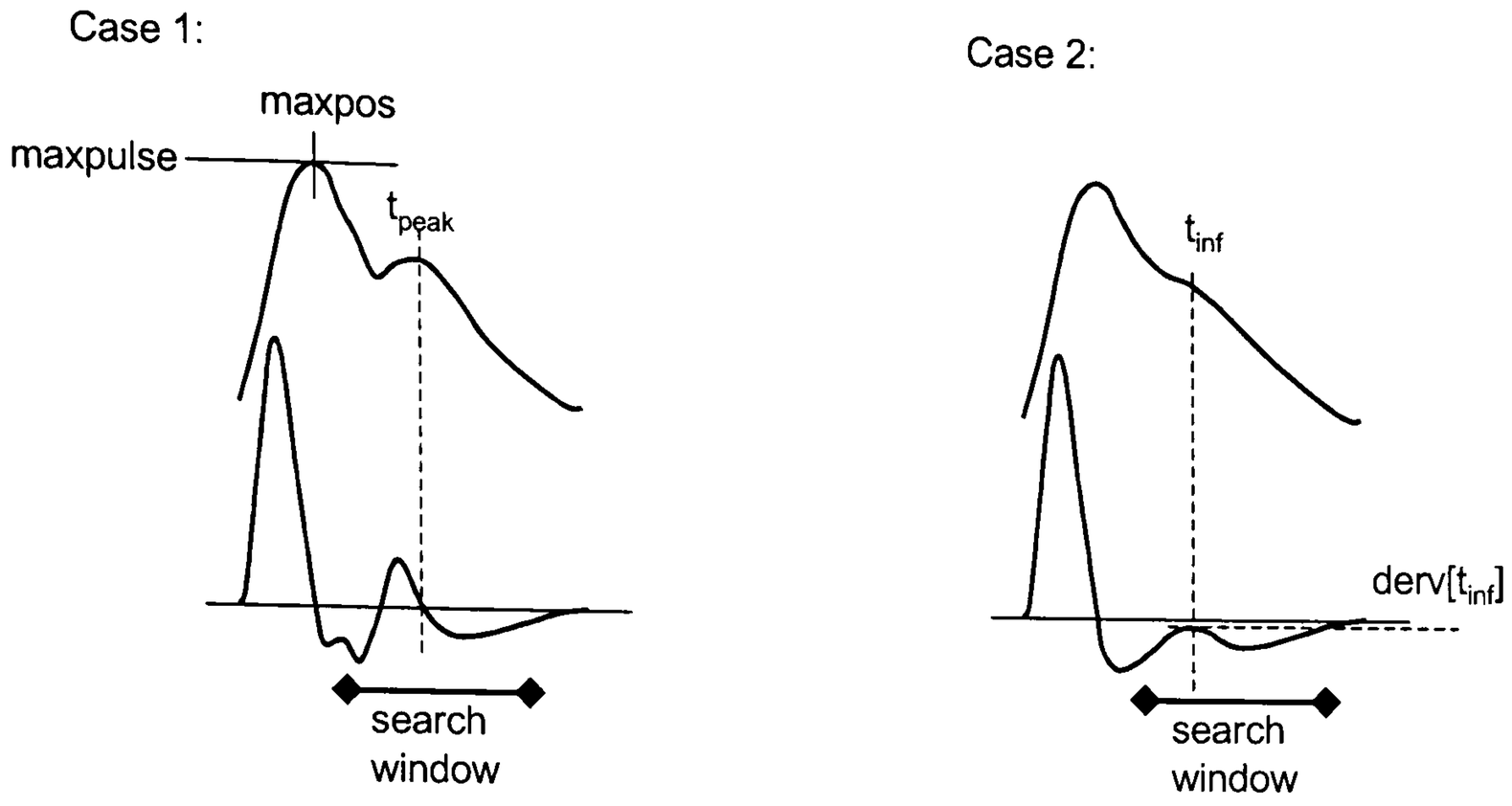

figure 60: Determination of the notch to calculate RI

As described in section 6.5.2 and figure 40, DVP waveforms such as in the above case 1 would usually be found in young healthy volunteers. With aging, the DVP waveform changes to a contour like the one shown in case 2. In subjects with especially stiff arteries, it is possible that no peak or inflection point is present. On the waveforms obtained for this thesis, less than 1% of the traces had no peak/inflection point and hence were not analysable. It is, however, important to note that very few subjects aged more than 75years old were studied and that on an older cohort, more DVP traces might not be analysable.

10.3 Calculation of SI from the DVP

10.3.1 Definition of SI

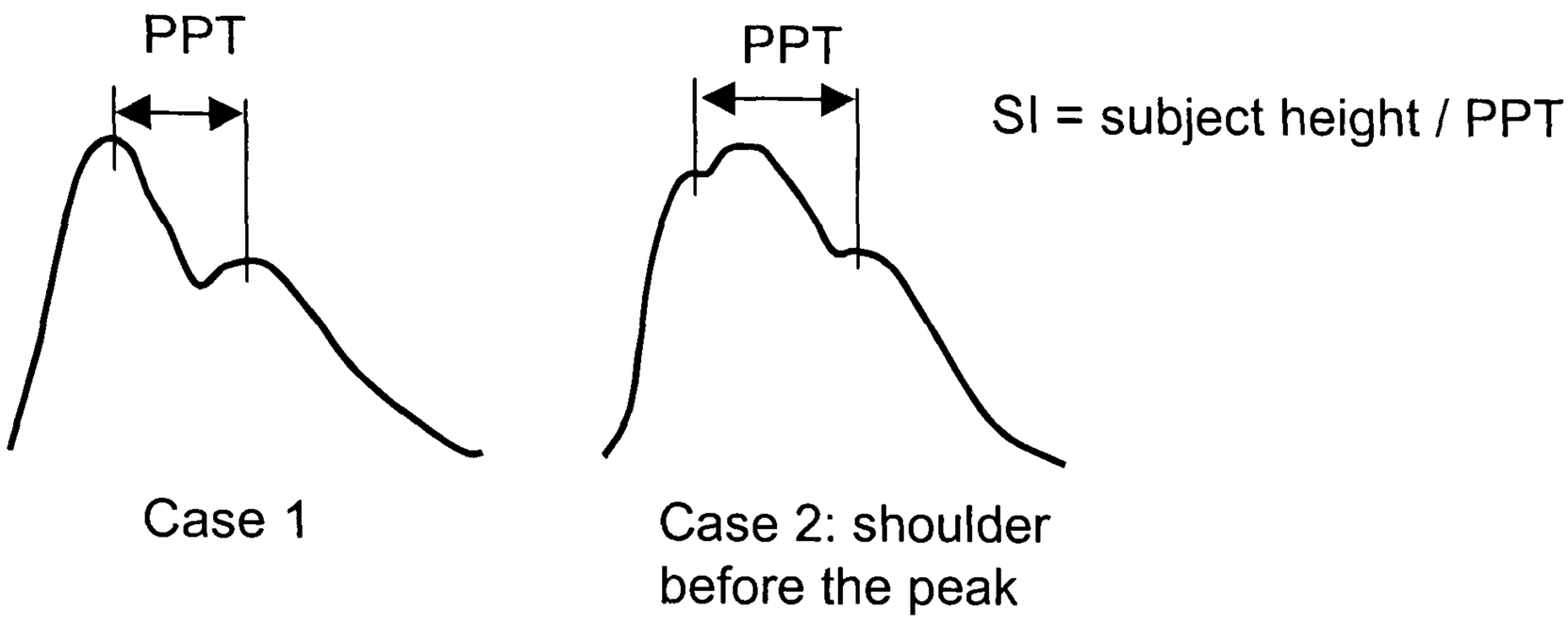

figure 61: Definition of SI

SI is defined as the height of the subject divided by the time between the 2 peaks, the peak to peak time (PPT).

$$PPT = T_2 - T_1$$

where T_1 = maxpos or $t_{shoulder}$ (see following case 1 and 2)

and $T_2 = t_{peak}$ or t_{inf} (as described in section 10.2.2)

10.3.2 Algorithm

Case 1:

- Find of the maximum of the DVP (maxpulse, maxpos)
- Find the time of inflection point t_{inf} as described in paragraph 10.2

- Calculate the peak to peak time, PPT = (t_{inf} – maxpos)/Fs with Fs being the sampling frequency
- Calculate SI from the subject height. SI = height / PPT

Case 2: Shoulder before the peak

Here there are 2 cases, the shoulder could be a inflection point (case 2a) or a peak (case 2b). In both case the notch is determined as described in the section 10.2 (timing of the notch: t_{inf}).

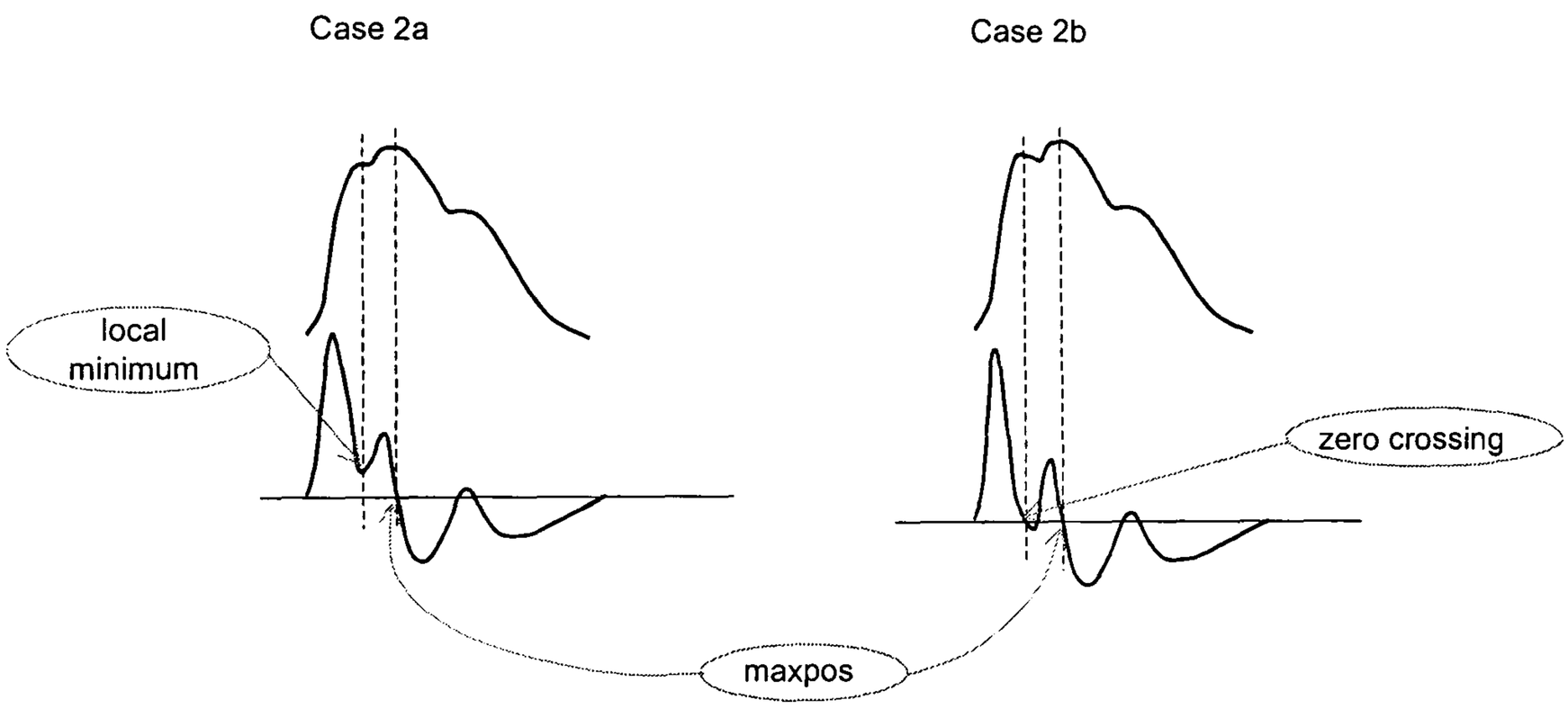

figure 62: Determination of PPT

So the algorithm is as follows:

- Find of the max of the pulse (maxpulse, maxpos)
- Find the time of the inflection point as described in the section 10.2 (t_{inf})
- Find the maximum of the derivative (abscissa: dervmaxpos)
- Determine if there is a zero crossing on the 1st derivative between dervmaxpos and t_{inf}.

- If there is a (or 2) zero-crossing(s), we are in the case 2b and the abscissa of the shoulder is the zero-crossing point the nearest to t_{inf} (abscissa: $t_{shoulder}$).
- If there is no zero-crossing, we are in case 2a. The local minimum need to be find. It can be find by using the 2 second zero-crossing of the 2nd derivative before t_{inf} (abscissa: $t_{shoulder}$).
- Calculate the peak to peak time, PPT = $(t_{inf} - t_{shoulder})/Fs$ (or PPT = $(t_{peak} - t_{shoulder})/Fs$) with Fs being the sampling frequency
- Calculate SI from the subject height. SI = height / PPT

10.3.3 Accuracy of the SI measurement

SI is calculated from subject height and PPT and there error in SI will come mainly form the estimation of PPT. The process of linear interpolation to obtain an average pulse (section 10.1.3) gives a "sampling frequency" of 150*HR/60 (where HR is heart rate in beats per minute). So for the averaged pulse, the error in estimating PPT is 1/(2.5*HR)/2 seconds (sampling period divided by 2). For HR = 40 bpm, the error in estimating PPT would be ±5ms, for HR = 60 bpm, ±3ms and for HR = 100 bpm, ±2ms.

In section 6.5.2, SI was measured in 87 asymptomatic subjects. In this cohort the slowest HR was 36 bpm and the lowest PPT value was 118ms (not on the same subject). So in the worst scenario, the error in PPT is ±5.5ms representing an error of ±4.7% in PPT and an error of ±4.6% in SI (see calculation details below). This is however the worst case scenario, in the same

cohort, the mean HR was 67bpm and PPT 218ms which gives an error of ±1.4% in estimating SI.

Calculation to evaluate the error in estimating SI:

The error in estimating PPT is: $\mathrm{err} = \frac{1}{2} \times \frac{1}{2.5 \times \mathrm{HR}}$

The error on SI in % is: (H being the subject height):

$$\mathrm{SI\_error} = \frac{100}{2} \times \frac{\frac{H}{PPT - err} - \frac{H}{PPT + err}}{\frac{H}{PPT}} = 100 \times \frac{PPT \times err}{PPT^2 - err^2}$$

10.4 Volume / Pressure Transfer Function

This appendix relates to the method to derive the DVP to pressure transfer function defined as:

$$TF = \frac{FFT(Pressure)}{FFT(Volume)}$$

There are several methods to evaluate TF. The one used in chapter 2 is based on frequency domain analysis of the average pulses. Determinations of the TF were performed using with Matlab 5.2.

10.4.1 Determining the TF for each individual

The DVP and the pressure pulse (radial and/or digital) were measured simultaneously for at least 6 consecutive heart beats. First, the average DVP (Vpulse) and the average pressure pulse (Ppulse) were calculated as described in appendix 10.1. After this algorithm, Vpulse and Ppulse were both time normalised to have a fixed duration of 150 samples independent of the HR.

A discrete Fourier transform was performed using the in-built fast Fourier transform(FFT) function of Maltab. This function can perform a discrete FFT on a signal, irrespective of the number of samples. If the number of samples is a power of two, a fast radix-2 fast-Fourier transform algorithm is used. If the length of the signal is not a power of two, a slower algorithm is employed. The only difference is the computing time. With the performance of the computer used for this analysis and the size of input signals (Vpulse and Ppulse), computing time was not an issue and so the FFT was performed on 150 points. Therefore the output of the FFT was on 150 points. The 1^{st} sample representing the mean of the signal, the 2^{nd} sample the fundamental and the 3^{rd} sample the 1^{st} harmonic and so on. In the rest of the text, the mean, the fundamental and the harmonics will be refer as "harmonics". For a signal from a subject whose HR is 60bpm, the 10 first harmonics of the FFT represents the FFT from 0 to 10Hz. For a subject whose HR is 120bpm, it represents the FFT from 0 to 20 Hz. A TF for each subject can be computed by dividing the 10 first harmonics of FFT(Ppulse) by the 10 first harmonics of FFT(Vpulse).

10.4.2 Averaging individual TF

With the above method, applying an FFT to a single pulse, an individual TF (ITF) is obtained for each subject. It is represented by an array of complex numbers corresponding to the harmonics of the waveform. Because the period of the pulse has been normalised, the frequency of each harmonic depends on the HR. To calculate the general transfer function (GTF), an averaging process needs to be applied to the ITFs. Two options were tried:

1. averaging the ITF values after interpolation of these to the same frequency.
2. averaging the ITF values for each harmonics.

The method used did not significantly change the reconstruction of the pressure pulse and therefore option 2 was used as it involves less data manipulation.

The generalised TF (GTF) was calculating by averaging the amplitude and phase of the ITFs.

$$ITF_k = \begin{bmatrix} A_{1k} \cdot \exp(-i \cdot \varphi_{1k}) \\ A_{2k} \cdot \exp(-i \cdot \varphi_{2k}) \\ \vdots \\ A_{10k} \cdot \exp(-i \cdot \varphi_{10k}) \end{bmatrix}$$

$$GTF = \begin{bmatrix} \sum_k A_1 \cdot \exp\left(-i \cdot \sum_k \varphi_1\right) \\ \sum_k A_2 \cdot \exp\left(-i \cdot \sum_k \varphi_2\right) \\ \vdots \\ \sum_k A_{10} \cdot \exp\left(-i \cdot \sum_k \varphi_{10}\right) \end{bmatrix} \cdot \frac{1}{n}$$

This method gave the smallest SD and the best reconstructed pulse compared to an averaging process based on the real and imaginary part.

10.4.3 Pulse reconstruction

The pressure pulse was reconstructed from the DVP and then compared to the measured pressure pulse. The reconstructed pressure pulse was calculated as follows where IFFT stands for Inverse Fast Fourier transform.

$$P_{recons} = IFFT(GTF \cdot FFT(Vpulse))$$

Vpulse is the average DVP and was computed as described in section 10.1. So, as described earlier, the Fourier transform of Vpulse is obtained for samples corresponding to each harmonics. The GTF was therefore resampled to the same number of samples as the pulse using the 10 first harmonics and setting values for higher harmonics to 10^{-6} (equivalent to a low pass filter).

Bibliography

1. Anderson TJ. Assessment and treatment of endothelial dysfunction in humans. *J Am Coll Cardiol*. 1999;34:631-638.

2. Asmar R. Arterial Stiffness and Pulse Wave Velocity: clinical applications. Elsevier, 1999.

3. Asmar RG, London GM, O'Rourke ME et al. Improvement in blood pressure, arterial stiffness and wave reflections with a very-low-dose perindopril/indapamide combination in hypertensive patient: a comparison with atenolol. *Hypertension*. 2001;38:922-926.

4. Asmar R. Effect of hypertensive agents on arterial stiffness as evaluated by pulse wave velocity. *Am J Cardiovasc Drugs*. 2001;1:387-397.

5. Asmar R, Rudchini A, Blacher J et al. Pulse Pressure and aortic pulse wave are markers of cardiovascular risk in hypertensive. *Am J of Hypertension*. 2001;14:91-97.

6. Avolio AP. Multi-branched model of the human arterial system. *Med &Biol &Eng &Comput*. 1980;18:709-718.

7. Avolio AP. Ageing and wave reflection. *Journal of Hypertension*. 1992;10:S83-S86.

8. Avolio AP, Chen S-G, Wang R-P et al. Effects of aging on changing arterial compliance and left ventricular load in a northern Chinese urban community. *Circulation*. 1983;68:50-58.

9. Avolio AP, Fa-Quan D, Wei-Qiang L et al. Effects of aging on arterial distensibility in populations with high and low prevelance of hypertension: comparison between urban and rural communities in China. *Circulation*. 1985;71:202-210.

10. Barker DJ, Bull AR, Osmond C et al. Fetal and placental size and risk of hypertension in adult life. *BMJ*. 1990;301:259-262.

11. Barker DJ, Osmond C. Low birth weight and hypertension. *BMJ*. 1988;297:134-135.

12. Barker DJ, Osmond C, Golding J et al. Growth in utero, blood pressure in childhood and adult life, and mortality from cardiovascular disease. *BMJ*. 1989;298:564-567.

13. Barker DJ, Winter PD, Osmond C et al. Weight in infancy and death from ischaemic heart disease. *Lancet*. 1989;2:577-580.

14. Bass A, Walden R, Hirshberg A et al. Pharmacokinetic activity of nitrites evaluated by digital pulse volume recording. *J Cardiovasc Surg*. 1989;30:395-397.

15. Benetos A, Asmar R, Asmar R et al. Arterial stiffness, hydrochlorothiazide and converting enzyme inhibition in essential hypertension. *Journal of Human Hypertension*. 1996;10:77-82.

16. Blacher J, Asmar R, Djane S et al. Aortic pulse wave velocity as a marker of cardiovascular risk in hypertensive patients. *Hypertension*. 1999;33:1111-1117.

17. Blacher J, Guerin AP, Pannier B et al. Impact of aortic stiffness an survival in end-stage renal disease. *Circulation*. 1999;99:2434-2439.

18. Bland JM, Altman D. Statistical methods for assessing agreement between two methods of clinical measurement. *The Lancet*. 1986;8:307-310.

19. Bortolotto LA, Blacher J, Kondo T et al. Assessment of vascular aging and atherosclerosis in hypertensive subjects: Second derivative of photoplethysmogram versus pulse wave velocity. *Am J of Hypertension*. 2000;13:165-171.

20. Boutouyrie P, Tropeano AI, Asmar R et al. Aortic stiffness is an independent predictor of primary coronary events in hypertensive patients: a longitudinal study. *Hypertension*. 2002;39:10-15.

21. Bramwell JC, Hill AV. The velocity of the pulse wave in man. *Proceedings of the Royal Society, London, Ser B*. 1922;93:298-306.

22. Broadbent WH. The pulse. London:Cassell ed. 1890.

23. Buschmann M, et al. Comparison of the effects of two different galenical preparations of glyceryl trinitrate on pulmonary artery pressure and on the finger pulse curve. *Eur J Clin Pharmacol*. 1993;44:451-456.

24. Cayatte AJ, Palacino JJ, Horten K et al. Chronic inhibition of nitric oxide production accelerates neointima formation and impairs endothelial function in hypercholesterolemic rabbits. *Arterioscler Thromb*. 1994;14:753-759.

25. Celermajer DS, Sorensen KE, Gooch VM et al. Non-invasive detection of endothelial dysfunction in children and adults at risk of atherosclerosis. *The Lancet*. 1992;340:1111-1115.

26. Channon KM, Qian H, George SE. Nitric oxide synthase in atherosclerosis and vascular injury: insights from experimental gene therapy. *Arterioscler Thromb Vasc Biol*. 2000;20:1873-1881.

27. Chen C-H, Nevo E, Fetics BJ et al. Estimation of central aortic pressure waveform by mathematical transformation of radial tonometry pressure. *Circulation*. 1997;95:1827-1836.

28. Chen C-H, Ting C-T, Nussbacher A et al. Validation of carotid artery tonometry as a mean of estimating augmentation index of ascending aortic pressure. *Hypertension*. 1996;27:168-175.

29. Chowienczyk PJ, Kelly RP, MacCallum H et al. Photoplethysmographic assessment of pulse wave reflection: blunted response to endothelium-dependent beta2-adrenergic vasodilation in type II diabetes mellitus. *J Am Coll Cardiol*. 1999;34:2007-2014.

30. Cockcroft JR, McEniery CM, Wilkinson IB. Pseudo hypertension of youth: too much of a good thing? *Am J Hypertens*. 2003;16:262-264.

31. Cohn JN, Finkelstein SM, McVeigh GE et al. Noninvasive pulse wave analysis for the early detection of vascular disease. *Hypertension*. 1995;26:503-508.

32. Cruickshank K, Riste L, Anderson SG et al. Aortic pulse-wave velocity and its relationship to mortality in diabetes and glucose intolerance: an integrated index of vascular function? *Circulation*. 2002;106:2085-2090.

33. Davey DA, MacGillivray I. The classification and definition of the hypertensive disorders of pregnancy. *Am J Obstet Gynecol*. 1988;158:892-898.

34. Dawber TR, Thomas HE, Jr., McNamara PM. Characteristics of the dicrotic notch of the arterial pulse wave in coronary heart disease. *Angiology*. 1973;24:244-255.

35. Dawes M, Chowienczyk PJ, Ritter JM. Effects of inhibition of the L-arginine/nitric oxide pathway on vasodilation caused by beta-adrenergic agonists in human forearm. *Circulation*. 1997;95:2293-2297.

36. Dillon JB, Hertzman AB. The form of the volume pulse in the finger pad in health, arteriosclerosis, and hypertension. *Am Heart J*. 1941;21:172-190.

37. Feelisch M. Biotransformation to nitric oxide of organic nitrates in comparison to other nitrovasodilators. *Eur Heart J*. 1993;14 Suppl I:123-132.

38. Fetics BJ, Nevo E, Chen C-H et al. Parametric model derivation of transfer function for noninvasive estimation of aortic pressure by radial tonometry. *IEEE Trans Biomed Eng*. 1999;46:698-706.

39. Finkelstein SM, Collins VR, Cohn JN. Arterial vascular compliance response to vasodilators by Fourier and pulse contour analysis. *Hypertension*. 1988;12:380-387.

40. Franck O. Die Grundform des arteriellen Pulses. Erste Abhandlung. Mathematische Analyse. *Zeitschriff für Biologie*. 1899;37:483-526.

41. Goetz RH. Plethysmography of the skin in the investigation of peripheral vascular diseases. *Brit J Surg*. 1940;27:506-520.

42. Guerin AP, Pannier B, Marchais SJ et al. Effects of antihypertensive agents on carotid pulse contour in humans. *Journal of Human Hypertension*. 1992;6:S37-S40.

43. Hallock P. Arterial elasticity in man in relation to age as evaluated by the pulse wave velocity method. *Arch Inter Med*. 1934;54:770-798.

44. Hannemann RE, Stoltman WP, Bronson EC et al. Digital plethysmography for assessing erythrityl tetranitrate bioavailability. *Clinical Pharma Ther*. 1981;35-39.

45. Hashimoto J, Chonan K, Aoki Y et al. Pulse wave velocity and the second derivative of the finger photoplethysmogram in treated hypertensive patients: their relationship and associating factors. *J Hypertens*. 2002;20:2415-2422.

46. Haynes F, Ellis LB, Weiss S. Pulse wave velocity and arterial elasticity in arterial hypertension, arteriosclerosis and related conditions. *Am Heart J*. 1936;11:385-401.

47. Hayward CS, Kraidly M, Webb CM et al. Assessment of endothelial function using peripheral waveform analysis: a clinical application. *J Am Coll Cardiol*. 2002;40:521-528.

48. Hertzman AB. The blood supply of various skin areas as estimated by the photoelectric plethysmograph. *Am J Physiol*. 1939;124:328-340.

49. Huxley R, Neil A, Collins R. Unravelling the fetal origins hypothesis: is there really an inverse association between birthweight and subsequent blood pressure? *Lancet*. 2002;360:659-665.

50. Huxley RR, Shiell AW, Law CM. The role of size at birth and postnatal catch-up growth in determining systolic blood pressure: a systematic review of the literature. *J Hypertens*. 2000;18:815-831.

51. Ignarro LJ, Buga GM, Wood KS et al. Endothelium-derived relaxing factor produced and released from artery and vein is nitric oxide. *Proc Natl Acad Sci U S A*. 1987;84:9265-9269.

52. Imanaga I, Hara H, Koyanagi S et al. Correlation between wave components of the second derivative of plethysmogram and arterial distensibility. *Jpn Heart J*. 1998;39:775-784.

53. Imholz BPM, Wieling W, Van Montfrans Ga et al. Fifteen years experience with finger arterial pressure monitoring; assessment of the technology. *Cardiovasc Res*. 1998;38:605-616.

54. Kannel WB, Dawber TR, McGee DL. Perspectives on systolic hypertension. The Framingham study. *Circulation*. 1980;61:1179-1182.

55. Karamanoglu M, Feneley MP. On-line synthesis of the human ascending aortic pressure pulse from the finger pulse. *Hypertension*. 1997;1416-1424.

56. Karamanoglu M, Gallagher DE, Avolio AP et al. Functional origin of reflected pressure waves in a multibranched model of the human arterial system. *Am J Physiol*. 1994;267:H1681-H1688.

57. Karamanoglu M, Gallagher DE, Avolio AP et al. Pressure wave propagation in a multibranched model of the human upper limb. *Am J Physiol*. 1995;269:H1363-H1369.

58. Karamanoglu M, O'Rourke MF, Avolio AP et al. An analysis of the relationship between central aortic and peripheral upper limb pressure waves in man. *European Heart Journal*. 1993;14:160-167.

59. Kelly RP, Gibbs H, O'Rourke MF et al. Nitroglycerin has more favourable effects on left ventricular afterload than apparent from

measurement of pressure in a peripheral artery. *European Heart Journal*. 1990;11:138-144.

60. Kelly RP, Hayward C, Avolio AP et al. Noninvasive determination of age-related changes in the human arterial pulse. *Circulation*. 1989;80:1652-1659.

61. Kelly RP, Hayward C, Ganis J et al. Noninvasive registration of the arterial pressure pulsewave for measuring high-fidelity applanation tonometry. *J Vasc Med Biol*. 1989;1:142-149.

62. Kelly RP, Hayward C, Winter D et al. Non-invasive determination of ageing changes in the arterial pulse. *FASEB Journal*. 1988;2.

63. Kelly RP, Karamanoglu M, Gibbs H et al. Noninvasive carotid pressure wave registration as an indicator of ascending aortic pressure. *J Vasc Med Biol*. 1989;1:241-247.

64. Kelly RP, Millasseau SC, Ritter JM et al. Vasoactive drugs influence aortic augmentation index independently of pulse-wave velocity in healthy men. *Hypertension*. 2001;37:1429-1433.

65. Klemsdal TO, Andersson TLG, Matz J et al. Vitamin E restores endothelium dependent vasodilatation in cholesterol fed rabbits: in vivo measurements by photoplethysmography. *Cardiovasc Res*. 1994;28:1-6.

66. Korteweg DJ. Über die Fortpflanzungsgesschwindigkeit des Schalles in elastischen Rohren. *Annals of Physics and Chemistry (NS)*. 1878;5:520-537.

67. Kuhlencordt PJ, Gyurko R, Han F et al. Accelerated atherosclerosis, aortic aneurysm formation, and ischemic heart disease in apolipoprotein E/endothelial nitric oxide synthase double-knockout mice. *Circulation*. 2001;104:448-454.

68. Latham RD, Westerhof N, Sipkema P et al. Regional wave travel and reflections along the human aorta: a study with six simultaneous micromanometric pressures. *Circulation*. 1985;72:1257-1269.

69. Laurent S, Boutouyrie P, Asmar R et al. Aortic stiffness is an independent predictor of all-cause and cardiovascular mortality in hypertensive patients. *Hypertension*. 2001;37:1236-1241.

70. Law CM, Shiell AW. Is blood pressure inversely related to birth weight? The strength of evidence from a systematic review of the literature. *J Hypertens*. 1996;14:935-941.

71. Lax H, Feinberg A, Cohen BM. Studies of the arterial pulse wave and its modification in the presence of human arteriosclerosis. *J Chronic Dis*. 1956;3:618-631.

72. Lehmann ED, Hopkins KD, Rawesh A et al. Relation between number of cardiovascular risk factors/events and non-invasive Doppler ultrasound assessments of aortic compliance. *Hypertension*. 1998;32:565-569.

73. Liang Y-L, Teede H, Kotsopoulos D et al. Non-invasive measurements of arterial structure and function; repeatability, interrelationships and trial sample size. *Clin Sci*. 1998;95:669-679.

74. Lind L, Hall J, Johansson K. Evaluation of four different methods to measure endothelium-dependent vasodilation in the human peripheral circulation. *Clin Sci (Lond)*. 2002;102:561-567.

75. Lind L, Pettersson K, Johansson K. Analysis of endothelium-dependent vasodilation by use of the radial artery pulse wave obtained by applanation tonometry. *Clin Physiol Funct Imaging*. 2003;23:50-57.

76. London GM, Blacher J, Pannier B et al. Arterial wave reflections and survival in end-stage renal failure. *Hypertension*. 2001;38:434-438.

77. London GM, Guerin AP, Pannier B et al. Increased systolic pressure in chronic uremia, role of arterial wave reflections. *Hypertension*. 1992;20:10-19.

78. Lund F. Digital pulse plethysmography (DPG) in studies of the hemodynamic response to nitrates - A survey of recording methods and principles of analysis. *Acta Pharmacol Toxicol*. 1986;59:76-86.

79. Mackensie J. The study of the pulse. Arterial, venous and hepatic and of the movements of the heart. Edinburg: Pentland ed. 1902.

80. Mahmud A, Feely J. Spurious systolic hypertension of youth: fit young men with elastic arteries. *Am J Hypertens*. 2003;16:229-232.

81. Mahmud A, Feely J. Acute effect of Caffeine on Arterial stiffness and aortic pressure waveform. *Hypertension*. 2001;38:227-231.

82. Mahomed FA. The Physiology and clinical use of the sphygmograph. *Medical Times and Gazette, London*. 1872;1:62-65.

83. Mahomed FA. The aetiology of Bright's disease and the prealbuminuric stage. *Med Chir Trans*. 1874;57:197-228.

84. Mahomed FA. On the sphygmographic evidence of arterio-capillary fibrosis. *Trans Pathlo Soc*. 1877;28:393-397.

85. Martin H, Hu J, Gennser G et al. Impaired endothelial function and increased carotid stiffness in 9-year-old children with low birthweight. *Circulation*. 2000;102:2739-2744.

86. Martyn CN, Barker DJ, Jespersen S et al. Growth in utero, adult blood pressure, and arterial compliance. *Br Heart J*. 1995;73:116-121.

87. McDonald DA, Taylor MG. The hydrodynamics of the arterial circulation. *Progress in Biophysics and Chemistry*. 1959;9:107-173.

88. McVeigh GE, Bratteli CW, Morgan DJ et al. Age-Related Abnormalities in Arterial Compliance Identified by Pressure Pulse Contour Analysis: Aging and Arterial Compliance. *Hypertension*. 1999;33:1392-1398.

89. McVeigh GE, Morgan DJ, Finkelstein SM et al. Vascular abnormalities associated with long-term cigarette smoking identified by arterial waveform analysis. *Am J of Medecine*. 1997;102:227-231.

90. Meaume S, Benetos A, Henry OF et al. Aortic pulse wave velocity predicts cardiovascular mortality in subjects >70 years of age. *Arterioscler Thromb Vasc Biol*. 2001;21:2046-2050.

91. Miyai N, Miyashita K, Arita M et al. Noninvasive assessment of arterial distensibiliy in adolescents using the second derivative of photoplethysmogram waveform. *Eur J Appl Physiol*. 2001;86:119-124.

92. Moens AI. Die Pulskurve. Leiden ed. 1878.

93. Moncada S, Palmer RM, Higgs EA. Nitric oxide: physiology, pathophysiology, and pharmacology. *Pharmacol Rev*. 1991;43:109-142.

94. Morikawa Y. Characteristic pulse wave caused by organic nitrates. *Nature*. 1967;841-842.

95. Morikawa Y, Matsuzaka J, Kuratsune M et al. Plethysmographic study of effects of alcohol. *Nature*. 1968;220:186-187.

96. Müller O, Weis E. Über die Topographie, die Entstehung und die Bedeutung des menschlichen Sphygmogramms. *Deutsches Arch f klin Med*. 1911;105:321.

97. Murgo JP, Westerhof N, Giolma JP et al. Aortic input impedance in normal man: relationship to pressure waveforms. *Circulation*. 1980;63:105-116.

98. Murrell W. Nitro-glycerine as a remedy for angina pectoris - part 1. *The Lancet*. 1879;80:80-81.

99. Murrell W. Nitro-glycerine as a remedy for angina pectoris - part 2. *The Lancet*. 1879;80:113-115.

100. Murrell W. Nitro-glycerine as a remedy for angina pectoris - part 3. *The Lancet*. 1879;80:151-152.

101. Murrell W. Nitro-glycerine as a remedy for angina pectoris - part 4. *The Lancet*. 1879;80:225-226.

102. Napoli C, Ignarro LJ. Nitric oxide and atherosclerosis. *Nitric Oxide*. 2001;5:88-97.

103. Naruse K, Shimizu K, Muramatsu M et al. Long-term inhibition of NO synthesis promotes atherosclerosis in the hypercholesterolemic rabbit thoracic aorta. PGH2 does not contribute to impaired endothelium-dependent relaxation. *Arterioscler Thromb*. 1994;14:746-752.

104. Nichols WW, O'Rourke MF. McDonald's blood flow in arteries. Theoretical, experimental and clinical principles. Oxford University Press, Inc, New York, 1999.

105. O'Brien E, Petrie J, Littler W et al. An outline of the revised British Hypertension Society protocol for the evaluation of blood pressure measuring devices. *J Hypertens*. 1993;11:677-679.

106. O'Brien E, Petrie J, Littler W et al. The British Hypertension Society protocol for the evaluation of automated and semi-automated blood pressure measuring devices with special reference to ambulatory systems. *J Hypertens*. 1990;8:607-619.

107. O'Rourke MF, Pauca A, Jiang XJ. Pulse wave analysis. *Br J Clin Pharmacol*. 2001;51:507-522.

108. O'Rourke MF, Vlachopoulos C, Graham RM. Spurious systolic hypertension in youth. *Vasc Med*. 2000;5:141-145.

109. O'Rourke MF. Pressure and flow waves in systemic arteries and the anatomical design of the arterial system. *J Appl Physiol*. 1967;23:139-149.

110. O'Rourke MF, Avolio AP. Pulsatile flow and pressure in human systemic arteries: studies in man and in a multi-branched model of the human systemic arterial tree. *Circ Res*. 1980;46:363-372.

111. O'Rourke MF, Kelly RP, Avolio AP. The arterial pulse. Philadelphia: Lea & Febiger ed. 1992.

112. O'Rourke MF, Mancia G. Areterial stiffness. *Journal of Hypertension*. 1999;17:1-4.

113. Osmond C, Barker DJ, Slattery JM. Risk of death from cardiovascular disease and chronic bronchitis determined by place of birth in England and Wales. *J Epidemiol Community Health*. 1990;44:139-141.

114. Palmer RM, Ferrige AG, Moncada S. Nitric oxide release accounts for the biological activity of endothelium-derived relaxing factor. *Nature*. 1987;327:524-526.

115. Pauca AL, O'Rourke MF, Kon ND. Prospective evaluation of a method for estimating ascending aortic pressure from the radial artery pressure waveform. *Hypertension*. 2001;38:932-937.

116. Peñáz J. Photoeletric measurement of blood pressure, volume and flow in the finger. *Digest 10th Int Conf Med Biol Eng p104, Dresden, Germany*. 1973.

117. Perticone F, Ceravolo R, Pujia A et al. Prognostic significance of endothelial dysfunction in hypertensive patients. *Circulation*. 2001;104:191-196.

118. Poston L. Maternal vascular function in pregnancy. *J Hum Hypertens*. 1996;10:391-394.

119. Quan H, Shih WJ. Assessing reproducibility by the within-subject coefficient of variation with random effects models. *Biometrics*. 1996;52:1195-1203.

120. Rang HP, Dale MM, Ritter JM et al. Pharmacology. 2003.

121. Safar ME. Editorial review: Pulse pressure in essential hypertension: clinical and therapeutical implications. *Journal of Hypertension*. 1989;7:769-776.

122. Schachinger V, Britten MB, Zeiher AM. Prognostic impact of coronary vasodilator dysfunction on adverse long-term outcome of coronary heart disease. *Circulation*. 2000;101:1899-1906.

123. Schinz A, Gottsauner A, Schnelle K. Digital pulse plethysmography: a sensitive test of the pharmacodynamics of nitrates - reproducibility and quantitation of the technique. Nitrate III. Kardiovaskulare Wirkungen. 1999: 117-122.

124. Segers P, Carlier S, Pasquet A et al. Individualizing the aorto-radial pressure transfer function: feasibility of a model-based approach. *Am J Physiol*. 2000;279:H542-H549.

125. Segers P, Qasem A, De Backer T et al. Peripheral "oscillatory" compliance is associated with aortic augmentation index. *Hypertension*. 2001;37:1434-1439.

126. Siebenhofer A, Kemp C, Sutton A et al. The reproducibility of central aortic blood pressure measurements in healthy subjects using applanation tonometry and sphygmocardiography. *J Hum Hypertens*. 1999;13:625-629.

127. Soderstrom S, Nyberg G, O'Rourke MF et al. Can a clinically useful aortic pressure wave be derived from a radial pressure wave? *Br J Anaesth*. 2002;88:481-488.

128. Stengele E, Winkler F, Trenk D et al. Digital pulse plethysmography as a non-invasive method for predicting drug-induced changes in left ventricular preload. *Eur J Clin Pharmacol*. 1996;50:279-282.

129. Sugimachi M, Kawada T, Shishido T et al. Estimation of arterial mechanical properties from aortic and tonometric arterial pressure waveforms. *Methods of information in medecine*. 1997;36:250-253.

130. Suwaidi JA, Hamasaki S, Higano ST et al. Long-term follow-up of patients with mild coronary artery disease and endothelial dysfunction. *Circulation*. 2000;101:948-954.

131. Takada H, Washino K, Harrell JS et al. Acceleration plethysmography to evaluate aging effect in cardiovascular system. *Medical Progress through Technology*. 1997;21:205-210.

132. Takazawa K, Fujita M, Yabe K et al. Clinical usefulness of the second derivative of a plethysmogram (acceleration plethysmogram). *Journal of Cardiology*. 1993;23:207-217.

133. Takazawa K, Tanaka N, Fujita M et al. Assessment of vasoactive agents and vascular aging by second derivative of the photoplethysmograph waveform. *Hypertension*. 1998;32:365-370.

134. Taylor MG. An experimental determination of the propagation of fluid oscillations in a tube with a visco-elastic wall; together with an analysis of hte characteristics required in an electrical analogue. *Phys Med Biol*. 1959;4:63-82.

135. Taylor MG. The input impedance of an assembly of randomly branching elastic tubes. *Biophysical Journal*. 1966;6:29-51.

136. Ting C-T, Chen C-H, Chang M-S et al. Short- and long-term effects of antihypertensive drugs on arterial reflections, compliance, and impedance. *Hypertension*. 1995;26:524-530.

137. U.S.Department of health and human services. National high blood pressure education program (NHBPEP). Working group report on high blood pressure in pregnancy. National Institutes of Health Publication, editor. 91, 3029. 1991.

138. Vlachopoulos C, Hirata K, O'Rourke MF. Effect of caffeine on aortic elastic properties and wave reflection. *J Hypertens*. 2003;21:563-570.

139. Wagner F, Siefert F, Trenk D et al. Relationship between pharmacokinetics and hemodynamic tolerance to isosorbibe-5-mononitrate. *Eur J Clin Pharmacol*. 1990;38:S53-S59.

140. Weinberg PD, Habens F, Kengatharan M et al. Characteristics of the pulse waveform during altered nitric oxide synthesis in the rabbit. *Br J Pharmacol*. 2001;133:361-370.

141. Westerbacka J, Wilkinson IB, Cockcroft JR et al. Diminished Wave Reflection in the Aorta. A Novel Physiological action of insulin on large Blood Vessels. *Hypertension*. 1999;33:1118-1122.

142. Whitney RJ. The measurement of volume changes in human limbs. *J Physiol (London)*. 1953;121:1-27.

143. Wilkinson IB, Franklin SS, Hall IR et al. Pressure amplification explains why pulse pressure is unrelated to risk in young subjects. *Hypertension*. 2001;38:1461-1466.

144. Wilkinson IB, Hall IR, MacCallum H et al. Pulse-wave analysis: clinical evaluation of a noninvasive, widely applicable method for assessing endothelial function. *Arterioscler Thromb Vasc Biol*. 2002;22:147-152.

145. Wilkinson IB, Prasad K, Hall IR et al. Increased central pulse pressure and augmentation index in subjects with hypercholesterolemia. *J Am Coll Cardiol*. 2002;39:1005-1011.

146. Wilkinson IB, Cockcroft JR, Webb DJ. Pulse wave analysis and arterial stiffness. *J Cardiovascular Pharmacology*. 1998;32-suppl.3:S33-S37.

147. Wilkinson IB, Fuchs SA, Jansen IM et al. Reproducibility of pulse wave velocity and augmentation index measured by pulse wave analysis. *Journal of Hypertension*. 1998;16:2079-2084.

148. Wilkinson IB, MacCallum H, Flint L et al. The influence of heart rate on augmentation index and central arterial pressure in humans. *Journal of Physiology*. 2000;525:263-270.

149. Wilkinson IB, MacCallum H, Hupperetz PC et al. Changes in the derived central pressure waveform and pulse pressure in response to angiotensin II and noradrenaline in man. *Journal of Physiology*. 2001;530:541-550.

150. Wilkinson IB, MacCallum H, Rooijmans DF et al. Increase augmentation index and systolic stress in type 1 diabetes mellitus. *QJM*. 2000;93:441-448.

151. Wolzt M, Schmetterer L, Rheinberger A et al. Comparison of non-invasive methods for the assessment of haemodynamic drug effects in healthy male and female volunteers: sex differences in cardiovascular responsiveness. *Br J Clin Pharma*. 1995;39:347-359.

152. Womersley JR. Oscillatory flow in arteries: the constrained elastic tube as a model of arterial flow and pulse transmission. *Phys Med Biol*. 1957;2:178-187.

153. Yasmin, Brown MJ. Similarities and differences between augmentation index and pulse wave velocity in the assessment of arterial stiffness. *QJM*. 1999;92:595-600.

154. Zobel LR, Finkelstein SM, Carlye PF et al. Pressure pulse contour analysis in determining the effect of vasodilator drugs on vascular hemodynamic impedance characteristics in dogs. *Am Heart J*. 1980;100:81-88.